

INFORMATION TO USERS

This manuscript has been reproduced from the microfilm master. UMI films the text directly from the original or copy submitted. Thus, some thesis and dissertation copies are in typewriter face, while others may be from any type of computer printer.

The quality of this reproduction is dependent upon the quality of the copy submitted. Broken or indistinct print, colored or poor quality illustrations and photographs, print bleedthrough, substandard margins, and improper alignment can adversely affect reproduction.

In the unlikely event that the author did not send UMI a complete manuscript and there are missing pages, these will be noted. Also, if unauthorized copyright material had to be removed, a note will indicate the deletion.

Oversize materials (e.g., maps, drawings, charts) are reproduced by sectioning the original, beginning at the upper left-hand corner and continuing from left to right in equal sections with small overlaps. Each original is also photographed in one exposure and is included in reduced form at the back of the book.

Photographs included in the original manuscript have been reproduced xerographically in this copy. Higher quality 6" x 9" black and white photographic prints are available for any photographs or illustrations appearing in this copy for an additional charge. Contact UMI directly to order.

UMI

A Bell & Howell Information Company
300 North Zeeb Road, Ann Arbor MI 48106-1346 USA
313/761-4700 800/521-0600

Synthesis and NMR Properties of Dihydrogen-Hydride
Complexes of Rhodium and Iridium

by

Warren James Oldham, Jr.

A dissertation submitted in partial fulfillment
of the requirements for the degree of

Doctor of Philosophy

University of Washington

1996

Approved by *D. M. Heinekey*
(Chairperson of Supervisory Committee)

Program Authorized
to Offer Degree Chemistry

Date *July 18/96*

UMI Number: 9716890

**UMI Microform 9716890
Copyright 1997, by UMI Company. All rights reserved.**

**This microform edition is protected against unauthorized
copying under Title 17, United States Code.**

UMI
300 North Zeeb Road
Ann Arbor, MI 48103

Doctoral Dissertation

In presenting this dissertation in partial fulfillment of the requirements for the Doctoral degree at the University of Washington, I agree that the Library shall make its copies freely available for inspection. I further agree that extensive copying of this dissertation is allowable only for scholarly purposes, consistent with "fair use" as prescribed in the U. S. Copyright Law. Requests for copying or reproduction of this dissertation may be referred to University Microfilms, 1490 Eisenhower Place, P. O. Box 975, Ann Arbor, MI 48106, to whom the author has granted "the right to reproduce and sell (a) copies of the manuscript in microform and/or (b) printed copies of the manuscript made from microform."

Signature Warren J. Oldham Jr.

Date July 18, 1996

University of Washington

Abstract

Synthesis and NMR Properties of Dihydrogen-Hydride
Complexes of Rhodium and Iridium

by Warren James Oldham, Jr.

Chairperson of the Supervisory Committee: Professor Dennis Michael Heinekey
Department of Chemistry

Addition of one equiv. of a tertiary phosphine ligand to toluene solutions of $\text{TpM}(\text{C}_2\text{H}_4)_2$ (Tp = hydridotris(1-pyrazolyl)borate; $\text{M} = \text{Rh}, \text{Ir}$) yields trigonal bipyramidal $\text{TpM}(\text{PR}_3)(\text{C}_2\text{H}_4)$ complexes in which the phosphine ligand occupies the axial site and the ethylene ligand lies in the equatorial plane. Hydrogen readily displaces the respective ethylene ligands through thermally accessible square planar (sp) $(\eta^2\text{-Tp})\text{M}(\text{PR}_3)(\text{C}_2\text{H}_4)$ intermediates to form $\text{TpM}(\text{PR}_3)\text{H}_2$ complexes and free ethylene. Chemical evidence for the unobserved sp intermediate is obtained upon reaction of $\text{TpIr}(\text{PPh}_3)(\text{C}_2\text{H}_4)$ with excess PPh_3 , which gives an equilibrium mixture of starting material and $(\text{N}, \text{C}^5, \text{N-Tp})\text{Ir}(\text{PPh}_3)_2\text{H}$, formed *via* cyclometallation of a pyrazolyl arm of the Tp ligand ($K_{\text{eq}} = 0.1$). Protonation of $\text{TpM}(\text{PR}_3)\text{H}_2$ complexes affords fluxional dihydrogen-hydride complexes, which reveal only a single hydride resonance at all accessible temperatures in the ^1H NMR spectrum. Short T_1 (min) values of 21-22 ms (Ir) and 7 ms (Rh) indicate an H-H bond length of 0.88-1.11 Å in the iridium complexes and 0.73-0.92 Å in the rhodium complex depending on the relative rate of H_2 rotation. In the case of the iridium complexes, partial substitution of the hydride positions with deuterium or tritium results in large temperature dependent isotope shifts and resolvable $J_{\text{H-D}}$ or $J_{\text{H-T}}$ coupling. Analysis of the chemical shift and coupling data as a function of temperature is consistent with a preference for the heavy hydrogen isotopes to occupy the hydride rather than the dihydrogen site.

TABLE OF CONTENTS

	<u>page</u>
List of Figures	ii
List of Tables	iii
<u>Chapter 1</u> : Introduction to Transition Metal Dihydrogen Complexes	1
Notes to Chapter 1	12
<u>Chapter 2</u> : Ethylene(hydridotris(1-pyrazolyl)borato)(triphenylphosphine) Complexes of Rhodium and Iridium	15
Results	17
Discussion	29
Conclusion	35
Experimental	35
Notes to Chapter 2	48
<u>Chapter 3</u> : Synthesis and NMR Properties of Dihydrogen Hydride Complexes of Rhodium and Iridium Stabilized by Hydridotris(1-pyrazolyl)borate Coligands	52
Results	53
Discussion	67
Conclusion	84
Experimental	85
Notes to Chapter 3	93
<u>Chapter 4</u> : Cyclometallation of a Pyrazolyl Arm in Hyridotris(1-pyrazolyl)borate and Tris(1-pyrazolyl)methane Complexes of Iridium	98
Results	99
Discussion	104
Conclusion	105
Experimental	105
Notes to Chapter 4	112
<u>Bibliography</u> :	114

LIST OF FIGURES

Number		page
<u>Chapter 2</u>		
2.1	Observed and simulated ^1H NMR spectra of the ethylene resonances of $\text{TpRh}(\text{PPh}_3)(\text{C}_2\text{H}_4)$.	20
2.2	Observed and simulated ^1H NMR spectra of the ethylene resonances of $\text{TpIr}(\text{PPh}_3)(\text{C}_2\text{H}_4)$.	21
2.3	Plot of $-\ln[2\mathbf{b}]$ (a. u.) versus time (s) for reaction of $2\mathbf{b}$ with H_2 and D_2 .	25
2.4	Plot of $\ln(k_{\text{obs}})$ versus $\ln[\text{H}_2]$ for the reaction of $2\mathbf{b}$ with H_2	25
<u>Chapter 3</u>		
3.1	High field region of the $^1\text{H}\{^31\text{P}\}$ NMR spectrum (CD_2Cl_2 , 500 MHz, 240 K) of a partially deuterated sample of $[\text{TpIr}(\text{PMe}_3)(\text{H}_2)\text{H}]\text{BF}_4$.	59
3.2	Plot of chemical shift of the hydride resonance in 6 , $6-d_1$ and $6-d_2$ as a function of observation temperature.	60
3.3	Plot of H-D coupling in $6-d_1$ and $6-d_2$ as a function of observation temperature	60
3.4	^1H (500 MHz) and ^3H (533 MHz) NMR spectra (CD_2Cl_2 , 240 K) of a partially tritiated sample of $[\text{TpIr}(\text{PMe}_3)(\text{H}_2)\text{H}]\text{BF}_4$.	63
3.5	ORTEP drawing (50% probability ellipsoids) for $[\text{TpIr}(\text{PMe}_3)(\text{H}_2)\text{H}]\text{BF}_4 \cdot \text{CH}_2\text{Cl}_2$.	66
3.6	Plot of H-H bond length in angstroms versus $J_{\text{H-D}}$ in hertz. The range of H-H bond lengths calculated as a function of dihydrogen rotational motion is shown for $[\text{TpIr}(\text{PMe}_3)(\text{H}_2)\text{H}]\text{BF}_4$	77
<u>Chapter 4</u>		
4.1	^1H NMR spectrum of $(\text{N}, \text{C}^5, \text{N-Tp})\text{Ir}(\text{PPh}_3)_2\text{H}$ in CD_2Cl_2 .	101

LIST OF TABLES

<u>Number</u>		<u>page</u>
<u>Chapter 2</u>		
2.1	¹ H NMR Chemical Shift and Coupling Parameters for Coordinated Ethylene of TpM(PPh ₃)(C ₂ H ₄).	22
2.2	Rate Data for the Reaction of TpIr(PPh ₃)(C ₂ H ₄) with H ₂ in CD ₂ Cl ₂ at 296 K.	26
<u>Chapter 3</u>		
3.1	Selected Spectroscopic Data for New Hydride Complexes.	56
3.2	Chemical Shifts of Hydride Resonances and <i>J</i> _{H-D} Coupling Constants for Partially Deuterated Isotopomers of 6-9 .	61
3.3	Hydride Chemical Shifts, <i>J</i> _{P-H} , <i>J</i> _{P-T} , and <i>J</i> _{H-T} Coupling Constants for Partially Tritiated Isotopomers of 6-8 Observed by ¹ H and ³ H NMR Spectroscopy at 240 K.	64
3.4	Significant Bond Distances and Angles for 6 •CH ₂ Cl ₂ .	65
3.5	Calculated H-H Bond Lengths from T ₁ (min) Data in the Limit of Slow and Fast Rotational Motion.	69
3.6	Calculated Parameters via IPR Analysis of ¹ H and ³ H NMR Spectra of 6-8 Acquired at 240 K.	75
3.7	Crystal Data and Parameters for 6 •CH ₂ Cl ₂ .	90
3.8	Atomic Coordinates and Equivalent Isotropic Displacement Coefficients.	91
3.9	Anisotropic Displacement Coefficients.	92

ACKNOWLEDGMENTS

I would like to thank Professor D. Michael Heinekey for his guidance and encouragement during my study at the University of Washington. Special thanks to David Fine, Mark Voges and Cathy Radzewich for their many contributions to this dissertation. Thanks to the entire Heinekey Research Group and to the Inorganic Division for making my stay in Seattle particularly enjoyable. I especially thank Susan Millar for her love and support and valuable input during the final hectic time leading up to this dissertation.

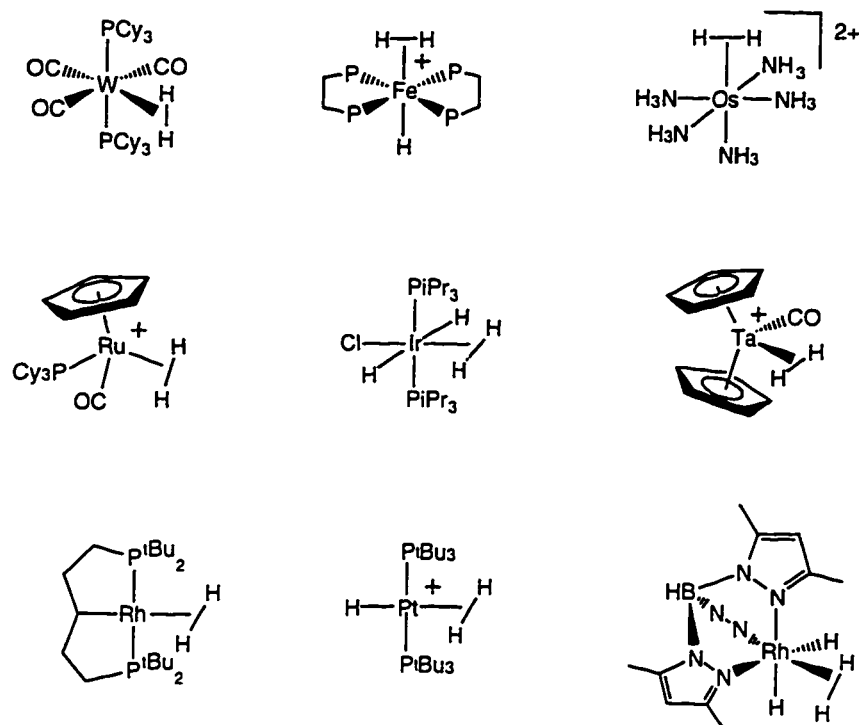
To my Mom and Dad

CHAPTER 1

INTRODUCTION TO TRANSITION METAL DIHYDROGEN COMPLEXES

The discovery of the first stable dihydrogen complexes by Kubas in 1984¹ has sparked a flurry of research activity in several laboratories around the world, including our own at the University of Washington. As a result of this work the number of dihydrogen complexes reported in the literature now totals in the hundreds. Examples from every metal in the vanadium, chromium, manganese, iron and cobalt triads are now known.² Recently a dihydrogen complex of platinum has been reported.³ Generally the dihydrogen ligand is supported by a soft ligand environment composed of CO, PR₃, Cp and/or hydride co-ligands. More recently workers have investigated the possibility of isolating nitrogen supported dihydrogen complexes.⁴⁻⁷ By far the most common electronic configuration of stable dihydrogen complexes is d⁶.² Examples of d², d⁴, and d⁸ complexes have been reported since the field was last reviewed in 1993.^{3,8-12} Some representative examples are shown in scheme 1.1.

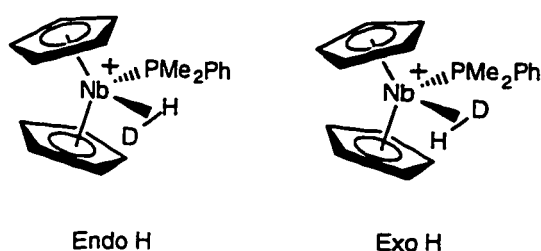
Bonding Model. The bonding in these complexes has been described using a model that is reminiscent of the familiar concepts developed to describe binding of ethylene and other related ligands.¹³⁻¹⁵ The H-H σ orbital donates electron density to an empty metal d orbital of σ symmetry. This interaction is augmented by back-donation from filled metal d orbitals to the σ^* orbital of H₂. Generally the back bonding component has been viewed to be weak, but it has been difficult to separate the σ and π components of the metal-dihydrogen bond. Both σ -donation and π -back bonding serve to weaken the H-H bonding interaction. If back bonding is efficient then complete oxidative addition to afford a metal dihydride complex is expected. Heinekey has argued that the π contribution to the overall metal-dihydrogen bond strength is relatively unimportant.



Scheme 1.1

This argument is based in part on a direct comparison between $W(PR_3)_2(CO)_3(H_2)$ and $[Re(PR_3)_2(CO)_3(H_2)][B(Ar)_4]$ ($R = Cy$ or iPr).¹⁶ Consistent with Heinekey's interpretation, the positive charge in the rhenium case does not seem to compromise the binding affinity of the rhenium center for dihydrogen. The presumably greater electrophilicity of the rhenium complex may result in a stronger metal-dihydrogen bond relative to the neutral tungsten complex. However, quantitative hydrogen affinity studies have been hampered by the lack of a suitable solvent which is compatible with both the tungsten and rhenium systems.¹⁷ Eckert has employed inelastic neutron scattering to measure the barrier to hydrogen rotation for a number of d^6 dihydrogen complexes.¹⁸ In all cases the barrier to hydrogen rotation is between 0.5 and 2.4 kcal/mol. It is difficult to determine the overall stabilization provided by π -back bonding from this measurement because some degree of back bonding is expected in all rotational orientations in d^6 complexes. Very recently Chaudret and coworkers have successfully prepared the first d^2

dihydrogen complexes in which the hydrogen rotational barrier may be directly related to the stabilization resulting from π back bonding.^{8,9} Two separate resonances for the two rotamers of the dihydrogen ligand in $[\text{Cp}_2\text{Nb}(\text{HD})(\text{PMe}_2\text{Ph})]^+$ were observed at low



Scheme 1.2

temperature (203 K) by ^1H NMR spectroscopy. A rotational barrier of 11.0 kcal/mol was estimated at the coalescence temperature from the low temperature limiting chemical shifts ($\Delta\delta = 0.8$ ppm). The Nb-H₂ bond strength is unknown in this system. If the W-H₂ bond strength in $\text{W}(\text{PiPr}_3)_2(\text{CO})_3(\text{H}_2)$ (25 kcal/mol)¹⁹ is comparable then π -back bonding can be estimated to account for about one-half to one-third of the total metal-dihydrogen binding energy. The back bonding observed in the niobium complex can be taken as an upper limit since this complex is very close in energy to the corresponding dihydride complex.

Characterization. Definitive characterization of dihydrogen complexes is a challenging problem. Reliable metrical data for transition metal hydride ligands can only be obtained from single crystal neutron diffraction data. This experiment is, however, limited by the requirement for large high quality crystals and by the very small number of neutron diffraction facilities which operate around the world. To compensate for this deficiency a number of spectroscopic methods have been employed to distinguish between classical and nonclassical hydride complexes. The most common and routinely applied techniques are derived from NMR spectroscopy. Vibrational spectroscopy (IR and Raman) has figured less prominently because vibrations expected for a dihydrogen

ligand are often too weak for detection. In contrast rotational transitions associated with a spinning dihydrogen ligand are readily identified by inelastic neutron scattering.¹⁸ Structural information can also be obtained by solid state NMR spectroscopy, however most labs are not equipped with the required instrumentation and expertise to routinely employ this tool.²⁰ In general, two solution phase ¹H NMR measurements have been carried out to characterize dihydrogen complexes. These are (1) determination of the spin lattice relaxation time (T_1) of the dihydrogen resonance and (2) observation of J_{H-D} coupling for the partially labeled H-D complex. In our own lab, we have relied heavily on these two measurements to infer hydride structure. In order to appreciate the results presented in chapter 3, an introduction to these techniques is included here.

¹H NMR Spin Lattice Relaxation Time (T_1). The T_1 method first proposed by Crabtree has been developed into a powerful characterization tool in the study of dihydrogen complexes.²¹ The short H-H bond length of the dihydrogen ligand results in rapid dipole-dipole relaxation (short T_1). Because dipole-dipole relaxation is proportional to the inverse sixth power of the internuclear distance, the measurement of T_1 values can in principle allow the definitive detection of dihydrogen complexes by a simple solution NMR method. To a first approximation, the relaxation behavior of the dihydrogen ligand is described by eq 1.1, where γ_H is the magnetogyric ratio of hydrogen, ω is the larmor frequency, r is the internuclear H-H bond length, and τ_c is the rotational

$$R_{H-H} = 1/T_1 = \frac{3\gamma_H^4 \hbar^2}{10r^6} \left\{ \frac{\tau_c}{1 + \tau_c^2 \omega^2} + \frac{4\tau_c}{1 + 4\tau_c^2 \omega^2} \right\} \quad (1.1)$$

correlation time of the molecule. Because τ_c is temperature dependent, following the Arrhenius expression, $\tau_c^{-1} = Ae^{-Ea/RT}$, T_1 also depends upon temperature. At a certain rotational correlation time, relaxation will be most efficient leading to a minimum T_1 value. Crabtree and Hamilton first demonstrated that at $T_1(\text{min})$, τ_c is uniquely defined

so that equation 1.1 can be solved to calculate the H-H bond length. At $T_1(\text{min})$, $\tau_c = 0.6158/\omega$ or $0.6158/(2\pi\nu)$, where ν is the spectrometer frequency. Discrepancies between H-H bond lengths determined by ^1H NMR relaxation experiments and those obtained by neutron diffraction or solid state NMR data has been attributed to rapid spinning of the dihydrogen ligand about the M-H₂ bond axis. When hydrogen is spinning much faster than the molecule is tumbling, the rotational correlation time of the molecule no longer reflects the motion of the dihydrogen ligand. In treating the rotational motion of the dihydrogen ligand, Morris has adapted Woessner's equations, which describe the relaxation of a spinning methyl group.²² Eq 1.1 should be expanded as shown in eq 1.2

$$R_{H-H} = \frac{3\gamma_H^4 \hbar^2}{10r^6} \left\{ \left(\frac{0.25\tau_c}{1 + \tau_c^2\omega^2} + \frac{0.75\tau_B}{1 + \tau_B^2\omega^2} \right) + 4 \left(\frac{0.25\tau_c}{1 + 4\tau_c^2\omega^2} + \frac{0.75\tau_B}{1 + 4\tau_B^2\omega^2} \right) \right\} \quad (1.2)$$

to account for the spinning dihydrogen ligand. The new rotational correlation time, $1/\tau_B = (2/\tau_{H_2} + 1/\tau_c)$ where τ_{H_2} and τ_c are the rotational correlation times of the dihydrogen ligand and of the complex, respectively. If τ_c/τ_{H_2} is defined as α , then $\tau_B = \tau_c/(1 + 2\alpha)$ and the bracketed terms of eq 1.2 can be rewritten as shown in eq 1.3. In the limit of fast

$$\left\{ \left(\frac{0.25\tau_c}{1 + \tau_c^2\omega^2} + \frac{0.75(\tau_c / (1 + 2\alpha))}{1 + (\tau_c / (1 + 2\alpha))^2\omega^2} \right) + 4 \left(\frac{0.25\tau_c}{1 + 4\tau_c^2\omega^2} + \frac{0.75(\tau_c / (1 + 2\alpha))}{1 + 4(\tau_c / (1 + 2\alpha))^2\omega^2} \right) \right\} \quad (1.3)$$

$$R_{H-H} = \frac{3\gamma_H^4 \hbar^2 (0.25)}{10r^6} \left\{ \frac{\tau_c}{1 + \tau_c^2\omega^2} + \frac{4\tau_c}{1 + 4\tau_c^2\omega^2} \right\} \quad (1.4)$$

rotational motion of the dihydrogen ligand, eq 1.3 is simplified to eq 1.4. At $T_1(\text{min})$, eqs 1.1 and 1.4 may be rearranged to solve for the H-H bond length in the limit of no hydrogen rotation and in the limit of rapid hydrogen rotation (with respect to molecular tumbling). These are shown in eqs 1.5 and 1.6, respectively.²³

$$r_{H-H} = 5.815 \left(\frac{1}{R_{H-H} \nu} \right)^{1/6} \quad (\text{slow rotation}) \quad (1.5)$$

$$r_{H-H} = 4.611 \left(\frac{1}{R_{H-H} \nu} \right)^{1/6} \quad (\text{fast rotation}) \quad (1.6)$$

The observed rate of relaxation of the dihydrogen ligand is actually the sum of the mutual dipolar relaxation within the dihydrogen ligand (R_{d-d}) and the contributions resulting from interactions with other dipoles in the molecule (R_o) (i.e. $R_{H_2} = R_{d-d} + R_o$). Halpern has shown that quantitative treatment of eqs 1.5 and 1.6 requires that the relaxation due to the H-H dipole interaction be known explicitly.²⁴ Additionally for a fluxional polyhydride complex suspected to contain a dihydrogen ligand, the observed dipolar relaxation rate is the population weighted average of all the hydride sites. The contribution to the total relaxation from sources other than the adjacent hydrogen atom of the dihydrogen ligand can be estimated in some cases. For example by measuring the T_1 (min) of a related complex which contains only terminal hydride ligands. In some situations, a unique structural assignment is not defined by the experimental T_1 (min) values. Halpern's study has shown that there is overlap between the range of T_1 (min) values found for classical and nonclassical polyhydride complexes if many hydride coligands are present or if the metal center contributes to rapid relaxation (e.g. Mn, Co and Re). Some ambiguity may also result if the H-H bond length of the dihydrogen ligand is greater than 1.3 Å. These factors have been particularly troubling for a family of rhenium complexes of the form $ReH_7(PR_3)_2$, for which conflicting classical and nonclassical formulations have been proposed.^{21,24-28} In one case a classical heptahydride structure was confirmed by single crystal neutron diffraction experiments (e.g. $ReH_7(dppe)$)²⁹, but a similar experiment carried out for $Re(H_2)H_5(Ptol_3)_2$ revealed a

dihydrogen ligand with a long H-H bond of *ca.* 1.36 Å.³⁰ These observations point out the subtle energy differences between the two structural isomers. The rhodium and iridium dihydrogen-hydride complexes which will be described in this work can, however, be accurately characterized by this method.

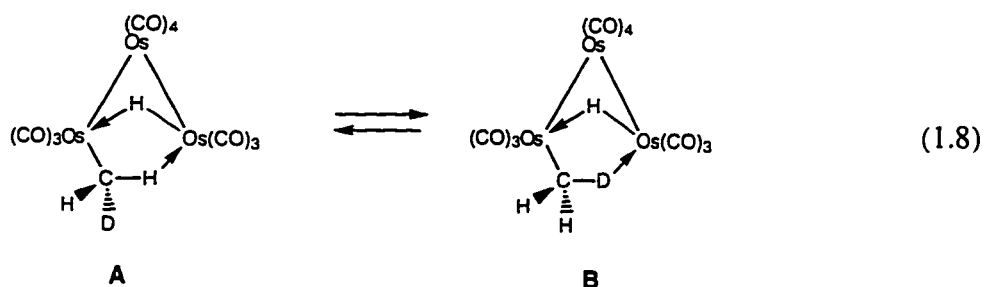
$J_{\text{H-D}}$ Coupling. In general, the most definitive solution-state indicator for the presence of a dihydrogen ligand is the observation of $J_{\text{H-D}}$ coupling in the ^1H NMR spectrum of the corresponding H-D complex. In most cases, the reported $J_{\text{H-D}}$ coupling constants for simple dihydrogen complexes are 20 to 35 Hz, reduced from a value of 43 Hz for H-D gas. In comparison, two-bond $^2J_{\text{H-D}}$ couplings in dihydride complexes are usually less than 2-3 Hz. Within the last few years, so called “stretched” dihydrogen complexes have been characterized by neutron diffraction experiments.³¹ The observed $J_{\text{H-D}}$ coupling for these complexes can be as low as 4 Hz. In this situation the $J_{\text{H-D}}$ coupling constant cannot uniquely define the hydride structure. This observation implies that the observed $J_{\text{H-D}}$ coupling constant for a dihydrogen ligand should be inversely proportional to the H-H bond length ($r_{\text{H-H}}$). Consistent with this expectation, plots of $J_{\text{H-D}}$ versus $r_{\text{H-H}}$ yield a reasonably straight line defined approximately by eq 1.7.^{32,33} In a timely publication by Hush and coworkers the observed inverse relationship between

$$r_{\text{H-H}} = -0.0163J_{\text{H-D}} + 1.41 \quad (1.7)$$

$J_{\text{H-D}}$ and $r_{\text{H-H}}$ for dihydrogen complexes has been reproduced by computational methods.³⁴ Curiously, the opposite trend is found for free dihydrogen, i.e. $J_{\text{H-H}}$ initially *increases* as the H-H bond is lengthed, then rapidly falls off in the limit of very long H-H bond lengths.³⁵ Fluxional polyhydride complexes, $L_m\text{M}(\text{H}_2)\text{H}_n$ ($n \geq 1$), suspected to contain a dihydrogen ligand should also display H-D couplings in the ^1H NMR spectrum upon partial deuteration, albeit reduced in magnitude due to statistical averaging.

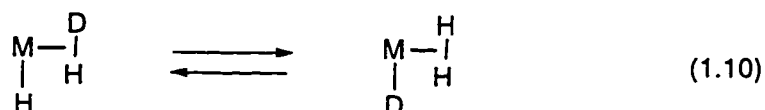
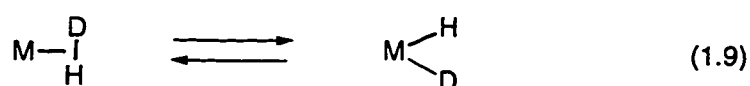
Surprisingly, retention of H-D coupling in the high-temperature limiting spectrum of transition metal polyhydrides has rarely been observed.

Isotopic Perturbation of Resonance. Partial isotopic substitution of the hydride positions of a fluxional polyhydride complex may result in large (> 100 ppb) temperature dependent isotope effects on the chemical shift of the hydride resonance due to isotopic perturbation of resonance (IPR). IPR was first developed by Saunders as a tool in the study of fluxional carbocations.³⁶ Calvert and Shapley subsequently applied this method in an organometallic system to characterize an osmium cluster containing a fluxional agostic methyl $C\cdots H\cdots Os$ bond.³⁷ In this particular case, partial substitution of deuterium in the agostic methyl group of $Os_3(CO)_{10}(\mu-H)(\mu-CH_3)$ results in distinct resonances for the $-CH_3$, $-CH_2D$, and $-CHD_2$ isotopomers in the 1H NMR spectrum. The isotope shifts, $\Delta_1 = \delta(CH_2D) - \delta(CH_3)$ and $\Delta_2 = \delta(CHD_2) - \delta(CH_2D)$ vary from -340 and -390 ppb at 35 °C to -550 and -680 ppb at -76 °C. These observations were proposed to result from isotopic perturbation of equilibria of the type shown in eq 1.8. Analysis of the isotope shifts allowed calculation of the limiting chemical shifts of the terminal methyl hydrogen atoms and the bridging agostic hydrogen atom, as well as the energy difference between **A** and **B**. Structure **A** was found to be 130 cal/mol lower in energy

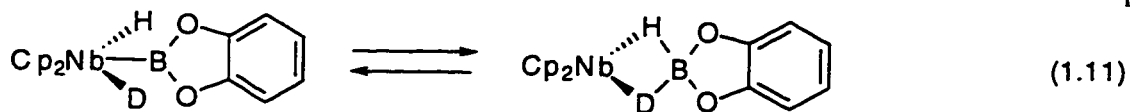


than **B**, which was rationalized by the greater zero point energy difference between C-H and C-D in the terminal site. A number of agostic complexes have now been characterized by this method.³⁸ The isotope shifts resulting from IPR should be

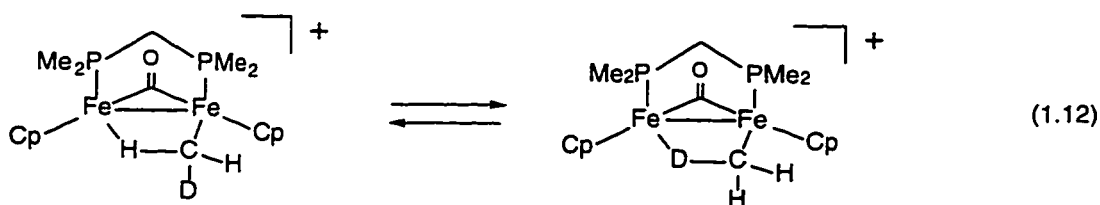
distinguished from the small (0 to -50 ppb) temperature independent shifts which are commonly observed for static molecules.³⁹ For example, the proton resonance of free HD (g) is shifted only 36 ppb upfield of H₂ (g).⁴⁰ In the case of dihydrogen complexes, IPR may result from two different causes. Substitution of the hydride positions with deuterium may perturb a rapid equilibrium between two different structural forms, for example an equilibrium between a dihydrogen and a dihydride complex (eq 1.9).



Alternatively, within one polyhydride structure, this effect may result from nonstatistical isotopic substitution of two chemically distinct proton sites which are in rapid equilibrium (eq 1.10). The underlying cause of this perturbation is a change in the energy difference between equilibrating species upon substitution with deuterium. Differences in zero point energy between hydrogen and deuterium causes deuterium to favor a particular structure or hydride site of an equilibrium mixture, thereby altering the original equilibrium population. In practice eqs 1.9 and 1.10 can be distinguished by comparing the isotope shifts in the ¹H and ²H NMR spectra. In the first type of equilibrium (eq 1.9), identical isotopomers will be observed at the same chemical shift in both the ¹H and ²H NMR spectra. But the fully protio and fully deuterio isotopomers will be observed at different chemical shifts. An example of an equilibrium between two different structures has been characterized using this method by Hartwig in the case of an equilibrium between a hydridoborate and a boryl complex (eq 1.11).⁴¹ In the second equilibrium situation (eq 1.10), the hydride resonance of the fully protio and fully deuterio complexes will resonate at the same frequency in the ¹H and ²H NMR spectrum, respectively. The



isotope shifts relative to these species will be in the opposite direction as observed by ^1H and ^2H NMR spectroscopy. That is if partial deuteration results in an *upfield* isotope shift in the ^1H NMR spectrum, then the isotope shift in the ^2H NMR spectrum will be *downfield*. A literature example of an equilibrium between two different proton sites in the same structure which has been characterized using both ^1H and ^2H NMR spectroscopy is provided by Stone's investigation of $[\text{Fe}_2(\mu\text{-CH}_3)(\mu\text{-CO})(\mu\text{-dppm})\text{Cp}_2]\text{PF}_6$ (eq 1.12).⁴² A similar analysis is valid if partial incorporation of tritium



in the hydride positions is studied by ^1H and ^3H NMR spectroscopy. A few scattered reports have invoked IPR to explain unusual isotope effects on the hydride resonance of polyhydride complexes, however a definitive study of this phenomenon has not been reported.

Organization of the Thesis. The oxidative addition of hydrogen to a transition metal complex is a fundamental step in many important catalytic reactions.⁴³⁻⁴⁵ Because dihydrogen complexes may be viewed as models of the transition state of H_2 oxidative addition, the study of isolable dihydrogen complexes allows for the first time a detailed examination of species which have only previously been accessible using computational methods.⁴⁶ In this thesis the relationship between structure and solution state properties of rhodium and iridium dihydrogen complexes is investigated. We build on previous

studies in our group of cyclopentadienyl complexes of the form $[\text{CpIr}(\text{L})\text{H}_3]\text{BF}_4$ (L = tertiary phosphine) which are characterized as classical trihydride complexes.^{47,48} The goal of this work has been to stabilize a dihydrogen-hydride ground state structure by altering the non hydride coligands of the original Cp complexes. Our approach has been to substitute the Cp ligand with the related hydridotris(1-pyrazolyl)borate (Tp) ligand. The details of this work are outlined in three chapters. Chapter 2 covers the synthesis, structure and reactions of $\text{TpM}(\text{PPh}_3)(\text{C}_2\text{H}_4)$ (M = Rh and Ir). The utility of these new complexes as intermediates in the synthesis of $\text{TpM}(\text{PPh}_3)\text{H}_2$ complexes is demonstrated. Chapter 3 describes the preparation and properties of $[\text{TpM}(\text{L})(\text{H}_2)\text{H}]\text{BF}_4$ (M = Rh and Ir). In all cases, a facile fluxional process renders the hydride ligands equivalent on the NMR time scale to the lowest accessible temperature. The presence of a bound dihydrogen ligand is indicated by short $T_1(\text{min})$ values of 7 ms (Rh) or 21-22 ms (Ir). Partial substitution of the hydride positions with deuterium or tritium results in large temperature dependent isotope shifts. These observations are novel in polyhydride complexes and have been interpreted as a manifestation of isotopic perturbation of equilibria. Chapter 4 relates observations of the first example of cyclometallation of the Tp ligand. The $\text{TpIr}(\text{PPh}_3)(\text{C}_2\text{H}_4)$ complex is found to react reversibly with excess PPh_3 to afford (N, C⁵, N-Tp)Ir(PPh₃)₂H and free ethylene. A similar reaction involving a closely related tris(1-pyrazolyl)methane complex is also described.

Notes to Chapter 1.

- (1) Kubas, G. J.; Ryan, R. R.; Swanson, B. I.; Vergamini, P. J.; Wasserman, H. J. *J. Am. Chem. Soc.* **1984**, *106*, 451-452.
- (2) Heinekey, D. M.; Oldham, W. J., Jr. *Chem. Rev.* **1993**, *93*, 913-926.
- (3) Gusev, D. G.; Notheis, J. U.; Rambo, J. R.; Hauger, B. E.; Eisenstein, O.; Caulton, K. G. *J. Am. Chem. Soc.* **1994**, *116*, 7409-7410.
- (4) Bucher, U. E.; Lengweiler, T.; Nanz, D.; Philipsborn, W. v.; Venanzi, L. M. *Angew. Chem. Int. Ed. Engl.* **1990**, *29*, 548-549.
- (5) Hamilton, D. G.; Luo, X. L.; Crabtree, R. H. *Inorg. Chem.* **1989**, *28*, 3198-3203.
- (6) Moreno, B.; Sabo-Etienne, S.; Chaudret, B.; Rodriguez, A.; Jalon, F.; Trofimenko, S. *J. Am. Chem. Soc.* **1995**, *117*, 7441-7451.
- (7) Paneque, M.; Poveda, M. L.; Toboada, S. *J. Am. Chem. Soc.* **1994**, *116*, 4519-4520.
- (8) Sabo-Etienne, S.; Chaudret, B.; el Makarim, H. A.; Barthelat, J.; Daudey, J.; Ulrich, S.; Limbach, H.; Moïse, C. *J. Am. Chem. Soc.* **1995**, *117*, 11602-11603.
- (9) Jalón, F. A.; Otero, A.; Manzano, B. R.; Villaseñor, E.; Chaudret, B. *J. Am. Chem. Soc.* **1995**, *117*, 10123-10124.
- (10) Gusev, D. G.; Kuznetsov, V. F.; Eremenko, I. L.; Berke, H. *J. Am. Chem. Soc.* **1993**, *115*, 5831-5832.
- (11) Neuner, B.; Schrock, R. R. *Organometallics* **1996**, *15*, 5-6.
- (12) Vigalok, A.; Ben-David, Y.; Milstein, D. *Organometallics* **1996**, *15*, 1839-1844.
- (13) Hay, P. J. *Chem. Phys. Lett.* **1984**, *103*, 466-469.
- (14) Saillard, J.; Hoffmann, R. *J. Am. Chem. Soc.* **1984**, *106*, 2006-2026.
- (15) Jean, Y.; Eisenstein, O.; Volatron, F.; Maouche, B.; Sefta, F. *J. Am. Chem. Soc.* **1986**, *108*, 6587-6592.
- (16) Heinekey, D. M.; Schomber, B. M.; Radzewich, C. E. *J. Am. Chem. Soc.* **1994**, *116*,

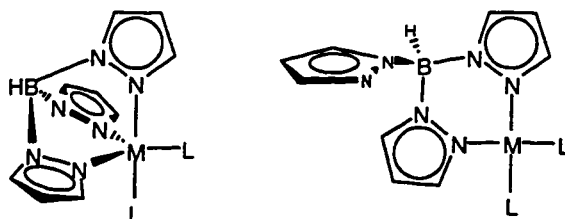
- (17) Radzewich, C. E.; Heinekey, D. M. personal communication, 1995.
- (18) Eckert, J. *Spectrochim. Acta* **1992**, *48A*, 363-378.
- (19) Gonzalez, A. A.; Zhang, K.; Nolan, S. P.; de la Vega, R. L.; Mukerjee, S. L.; Hoff, C. L. *Organometallics* **1988**, *7*, 2429-2435.
- (20) Zilm, K. W.; Millar, J. M. *Adv. Magn. Opt. Reson.* **1990**, *15*, 163-200.
- (21) Hamilton, D. G.; Crabtree, R. H. *J. Am. Chem. Soc* **1988**, *110*, 4126-4133.
- (22) Bautista, M. T.; Earl, K. A.; Maltby, P. A.; Morris, R. H.; Schweitzer, C. T.; Sella, A. *J. Am. Chem. Soc* **1988**, *110*, 7031-7036.
- (23) Bautista, M. T.; Cappellani, E. P.; Drouin, S. D.; Morris, R. H.; Schweitzer, C. T.; Sella, A.; Zubkowski, J. *J. Am. Chem. Soc* **1991**, *113*, 4876-4887.
- (24) Desrosiers, P. J.; Cai, L.; Lin, Z.; Richards, R.; Halpern, J. *J. Am. Chem. Soc* **1991**, *113*, 4173-4184.
- (25) Costello, M. T.; Walton, R. A. *Inorg. Chem.* **1988**, *27*, 2563-2564.
- (26) Luo, X. L.; Crabtree, R. H. *J. Am. Chem. Soc* **1990**, *112*, 4813-4821.
- (27) Haynes, G. R.; Martin, R. L.; Hay, P. J. *J. Am. Chem. Soc* **1992**, *114*, 28-36.
- (28) Michos, D.; Luo, X.; Howard, J. A. K.; Crabtree, R. H. *Inorg. Chem.* **1992**, *31*, 3914-3916.
- (29) Howard, J. A. K.; Mason, S. A.; Johnson, O.; Diamond, I. C.; Crennell, S.; Keller, P. A.; Spencer, J. L. *J. Chem. Soc., Chem. Commun.* **1988**, 1502-1503.
- (30) Brammer, L.; Howard, J. A. K.; Johnson, O.; Koetzle, T. F.; Spencer, J. L.; Stringer, A. M. *J. Chem. Soc., Chem. Commun.* **1991**, 241-243.
- (31) Hasegawa, T.; Li, Z.; Parkin, S.; Hope, H.; McMullan, R. K.; Koetzle, T. F.; Taube, H. *J. Am. Chem. Soc* **1994**, *116*, 4352-4356.
- (32) Heinekey, D. M.; Luther, T. A. *Inorg. Chem.* **1996**, *35*, in press.
- (33) Maltby, P. A.; Schlaf, M.; Steinbeck, M.; Lough, A. J.; Morris, R. H.; Klooster, W. T.; Koetzle, T. F.; Srivastava, R. C. *J. Am. Chem. Soc* **1996**, *118*, 5396-5407.

- (34) Bacskay, G. B.; Bytheway, I.; Hush, N. S. *J. Am. Chem. Soc* **1996**, *118*, 3753-3756.
- (35) Bacskay, G. B. *Chem. Phys. Lett.* **1996**, *242*, 507.
- (36) Saunders, M.; Kates, M. R. *J. Am. Chem. Soc* **1977**, *99*, 8070-8071.
- (37) Calvert, R. B.; Shapley, J. R. *J. Am. Chem. Soc* **1978**, *100*, 7726-7727.
- (38) Brookhart, M.; Green, M. L. H.; Wong, L. *Prog. Inorg. Chem.* **1988**, *36*, 1-124.
- (39) Hansen, P. E. *Annu. Rep. NMR Spectrosc.* **1983**, *15*, 105-234.
- (40) Evans, D. F. *Chem. Ind. (London)* **1961**, 1960.
- (41) Hartwig, J. F.; De Gala, S. R. *J. Am. Chem. Soc* **1994**, *116*, 3661-3662.
- (42) Dawkins, G. M.; Green, M.; Orpen, A. G.; Stone, F. G. A. *J. Chem. Soc., Chem. Comm.* **1982**, 41-43.
- (43) Collman, J. P.; Hegedus, L. S.; Norton, J. R.; Finke, R. G. *Principles and Application of Organotransition Metal Chemistry*; University Science Books: Mill Valley, CA, 1987.
- (44) Crabtree, R. H. *The Organometallic Chemistry of the Transition Metals*; 2nd ed.; John Wiley & Sons: New York, 1994.
- (45) Parshall, G. W.; Ittel, S. D. *Homogeneous Catalysis*; 2nd ed.; John Wiley & Sons, Inc.: New York, 1992.
- (46) Hay, P. J. In *Transition Metal Hydrides*; A. Dedieu, Ed.; VCH Publishers, Inc: New York, 1992.
- (47) Heinekey, D. M.; Millar, J. M.; Koetzle, T. F.; Payne, N. G.; Zilm, K. W. *J. Am. Chem. Soc* **1990**, *112*, 909-919.
- (48) Heinekey, D. M.; Hinkle, A. S.; Close, J. D. *J. Am. Chem. Soc* **1996**, *118*, 5353-5361.

CHAPTER 2

ETHYLENE(HYDRIDOTRIS(1-PYRAZOLYL)BORATO) (TRIPHENYLPHOSPHINE) COMPLEXES OF RHODIUM AND IRIIDIUM

The hydridotris(1-pyrazolyl)borate (Tp) class of ligands generally forms stable metal complexes containing either a bidentate or tridentate array of nitrogen-ligated pyrazolyl arms.¹ The subtle interplay between steric and electronic factors which favors one structure over another is clearly evident in the series of low valent rhodium and iridium complexes of the form $\text{Tp}^{\text{R2}}\text{ML}_2$ ($\text{L} = \text{CO}$, CNR , or olefin).²⁻⁹ The solution phase, ground state coordination geometry in these species has been shown to be either trigonal bipyramidal (tbp) or square planar (sp) or a mixture of both, depending on the

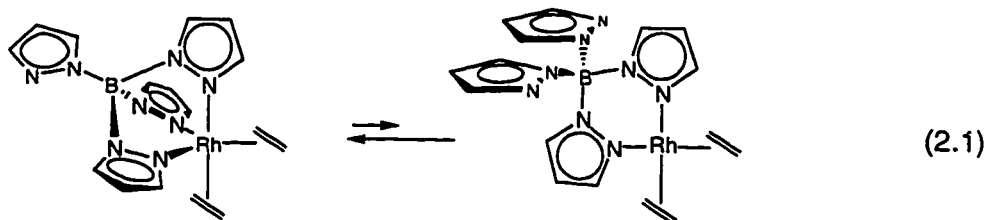


Scheme 2.1

metal center, the substituents of the Tp ligand, and the donor ligands (scheme 2.1). The tbp structure is related to the sp form by simple dissociation of an equatorial pyrazolyl arm. Since little additional ligand rearrangement is required, this dynamic process is often observed with only small activation barriers. In fact, a dynamic equilibrium between tbp and sp structures has recently been carefully examined by Venanzi and coworkers for an extensive series of rhodium complexes, $\text{Tp}^{3\text{R},4\text{R},5\text{R}}\text{Rh}(\text{LL})$ ($\text{LL} = 2\text{CO}$, NBD , COD).^{9,10} Solution phase IR spectroscopy of the bis-CO complexes showed that in certain cases, both tbp and sp forms were present in solution. By altering the

16

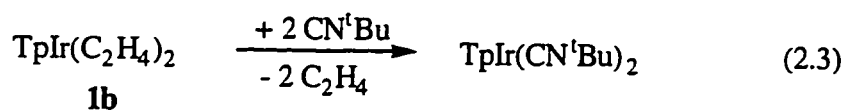
substituents of the Tp ligand and/or the solvent, it was possible to shift the equilibrium to favor either five-coordinate *tbp* complexes or four-coordinate *sp* complexes. Similar isomeric mixtures have been observed by Trofimenko and coworkers in more elaborately substituted $\text{Tp}^{3R,4R,5R}\text{Rh}(\text{CO})_2$ complexes.¹¹ In most cases the solution phase structure mirrors that determined in the solid state by single crystal x-ray diffraction. However, small crystal packing forces can favor selective crystallization of the minor isomer, thereby providing evidence for its existence in solution.¹² The ground state structure of $\text{TpM}(\text{C}_2\text{H}_4)_2$ ($\text{M} = \text{Rh}$ (**1a**)¹³ and Ir (**1b**)^{14,15}) is not known with certainty. A static *sp* or *tbp* structure is expected to show a 2:1 pattern of pyrazolyl resonances by ^1H or ^{13}C NMR analysis. Instead, a fluxional process renders the pyrazolyl arms equivalent at all accessible temperatures. A *tbp* structure is suggested by low temperature ^1H NMR studies of terakis(pyrazolyl)borate analogs, $(\text{Bpz}_4)\text{Rh}(\text{LL})$, which reveal two pyrazolyl environments in a 3:1 ratio when $\text{LL} = \text{COD}$ or duroquinone.⁴ These are assigned to the dynamically averaged pyrazolyl ligands coordinated to the metal center and to the uncoordinated pyrazolyl arm, respectively. Likewise, a *tbp* structure was assigned to $\text{TpRh}(\text{COD})$ based on comparison of its ^{103}Rh NMR chemical shift to a number of related complexes.⁹ Square planar intermediates have been shown to be thermally accessible, indicated by exchange of free and bound pyrazolyl groups in $(\text{Bpz}_4)\text{M}(\text{LL})$ complexes (eq 2.1).^{3,4,16} Even when this exchange is



slow on the NMR timescale, separate resonances for the *sp* form were not detected. We estimate that K_{eq} for equilibria of the type shown in eq 2.1 must therefore be less than

(200 K) were complete in less time than it was possible to acquire an NMR spectrum (less than 2 min). Separate experiments carried out in the same fashion except for addition of excess ethylene to each NMR tube gave identical results. Solutions of **2a** or **2b** protected from air and light are stable at room temperature for weeks in common solvents, although **2a** rapidly decomposes in chlorinated solvents. **1a** was previously reported to decompose to a mixture of uncharacterized products upon reaction with PPh₃ in CH₂Cl₂.^{2,3} We find that reaction in any nonhalogenated solvent such as THF, benzene or toluene results in clean and quantitative conversion to **2a**. Concentration of these solutions and addition of pentane affords yellow or very pale yellow microcrystalline samples of **2a** and **2b** respectively. Carmona and coworkers have also recently reported that Tp^{Me2}Rh(C₂H₄)₂ reacts at 20 °C with CO, PMe₃, or CN^tBu to yield stable Tp^{Me2}Rh(L)(C₂H₄) complexes in benzene.^{19,20} Tp^{Me2}Ir(C₂H₄)₂ reacts at 60 °C in neat thiophene to yield Tp^{Me2}Ir(SC₄H₄)(2-thienyl)₂.²¹

The parent bis-ethylene complex, **1b** also reacts cleanly with PMe₃, PCy₃ or PiPr₃ to yield the corresponding TpIr(PR₃)(C₂H₄) complexes. Special care is necessary in the reaction of **1b** with PMe₃ because addition of excess ligand apparently results in products containing more than one PMe₃ ligand (see chapter 4). Nitrogen donor ligands such as pyridine or NCMe did not react with **1b** at room temperature. CN^tBu reacts with **1b** to yield a bright yellow solution of TpIr(CN^tBu)₂, characterized by analogy to



the known TpIr(CO)₂ complex (eq 2.3).¹⁴ The bis-CN^tBu complex slowly decomposes in solution over 24 hours and was not isolated.

Variable temperature ¹H and ¹³C{¹H} NMR and selected NOE experiments have been undertaken to establish the solution state structures of **2a** and **2b**. These data

indicate that a common t_{bp} geometry is obtained in solution with PPh₃ coordinated in the axial site and ethylene positioned in the equatorial plane. Broad ill defined resonances for the Tp and PPh₃ ligands are observed at room temperature in the ¹H NMR spectrum of **2a**. Exchange of axial and equatorial pyrazolyl ligands and rotation about the Rh–P bond in the intermediate exchange region accounts for these broad lines. Dissociation of the PPh₃ ligand from the metal center was ruled out as a possible explanation for the broad aromatic resonances because addition of excess PPh₃ yields identical lineshapes attributed to the metal complex and sharp multiplets for free PPh₃. Upon cooling, the Tp resonances decoalesce and sharpen into a 2:1 pattern characteristic of C_s symmetry. Analysis of the temperature dependence of the exchange between axial and equatorial pyrazolyl ligands using the method of Shanan-Atidi and Bar-Eli²² gives an activation barrier for this process of 14.3 kcal/mol at the coalescence temperature of 279 K. Sharp resonances for the PPh₃ ligand are observed in a 2:1 ratio below 230 K indicating slow rotation about the Rh–P bond. Hindered rotation about the Ir–P bond in the intermediate exchange region is also observed for **2b**, although no evidence for axial/equatorial pyrazolyl arm exchange is detected to 353 K. The activation barrier for pyrazolyl site exchange in **2b** must therefore be greater than 18.4 kcal/mol. The coupling patterns observed for the respective ethylene ligands in ¹H NMR spectra are characteristic of static AA'BB'XY or AA'BB'X spin systems (X = ³¹P and Y = ¹⁰³Rh) centered at 1.68 and 0.96 ppm respectively. No change in these patterns is observed from 193 to 353 K. Computer simulation of the complex ethylene multiplets (fig 2.1 and 2.2) provide the chemical shift and coupling parameters summarized in Table 2.1. Similar analyses have been reported for related cyclopentadienyl complexes.^{23,24} The coupling constants for the ethylene ligand of **2b** are only slightly reduced from those calculated for **1b** (see experimental section). Results from selective ¹H NMR NOE experiments confirm that the ethylene ligand of **2** occupies an equatorial position of the

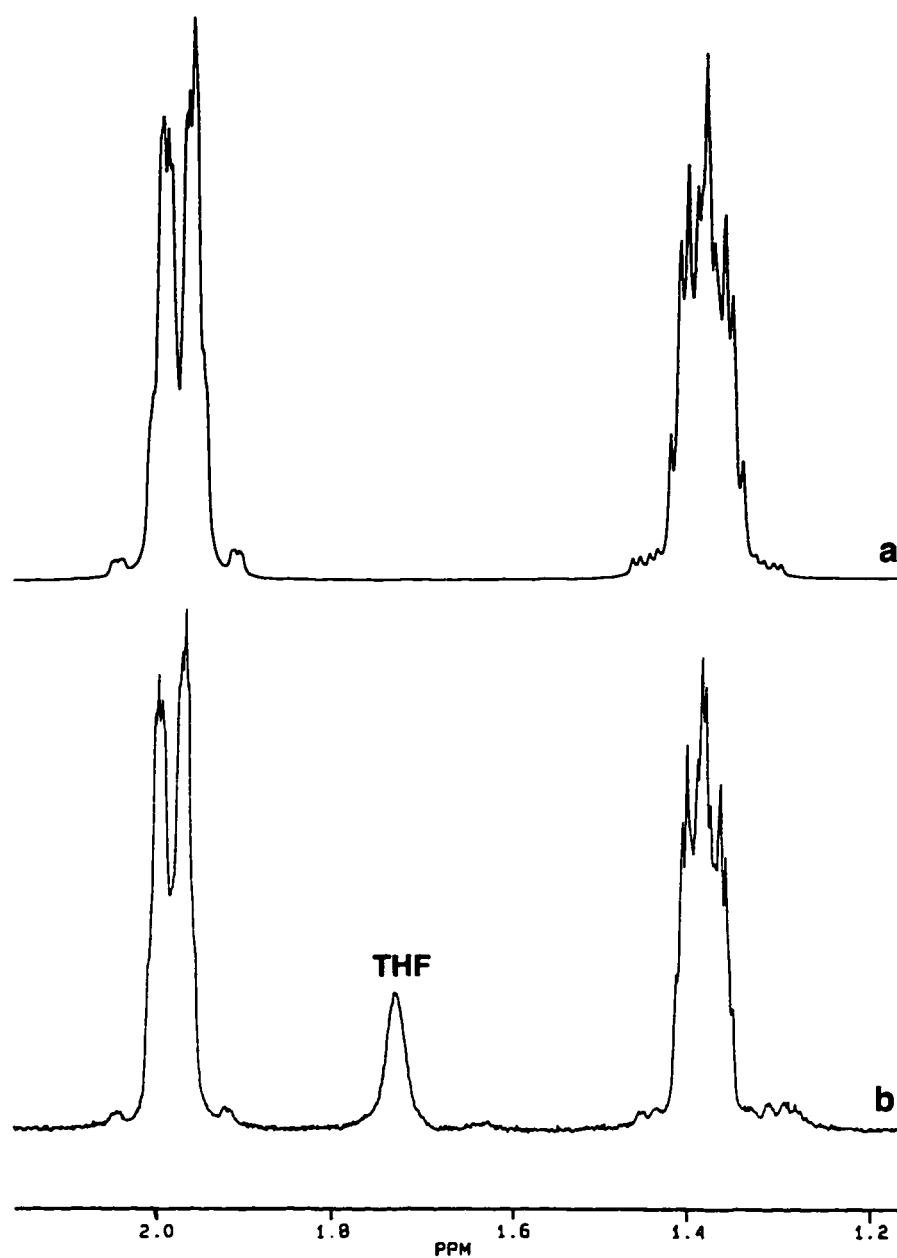


Figure 2.1 Observed and simulated ^1H NMR spectra of the ethylene resonances of $\text{TpRh}(\text{PPh}_3)(\text{C}_2\text{H}_4)$.

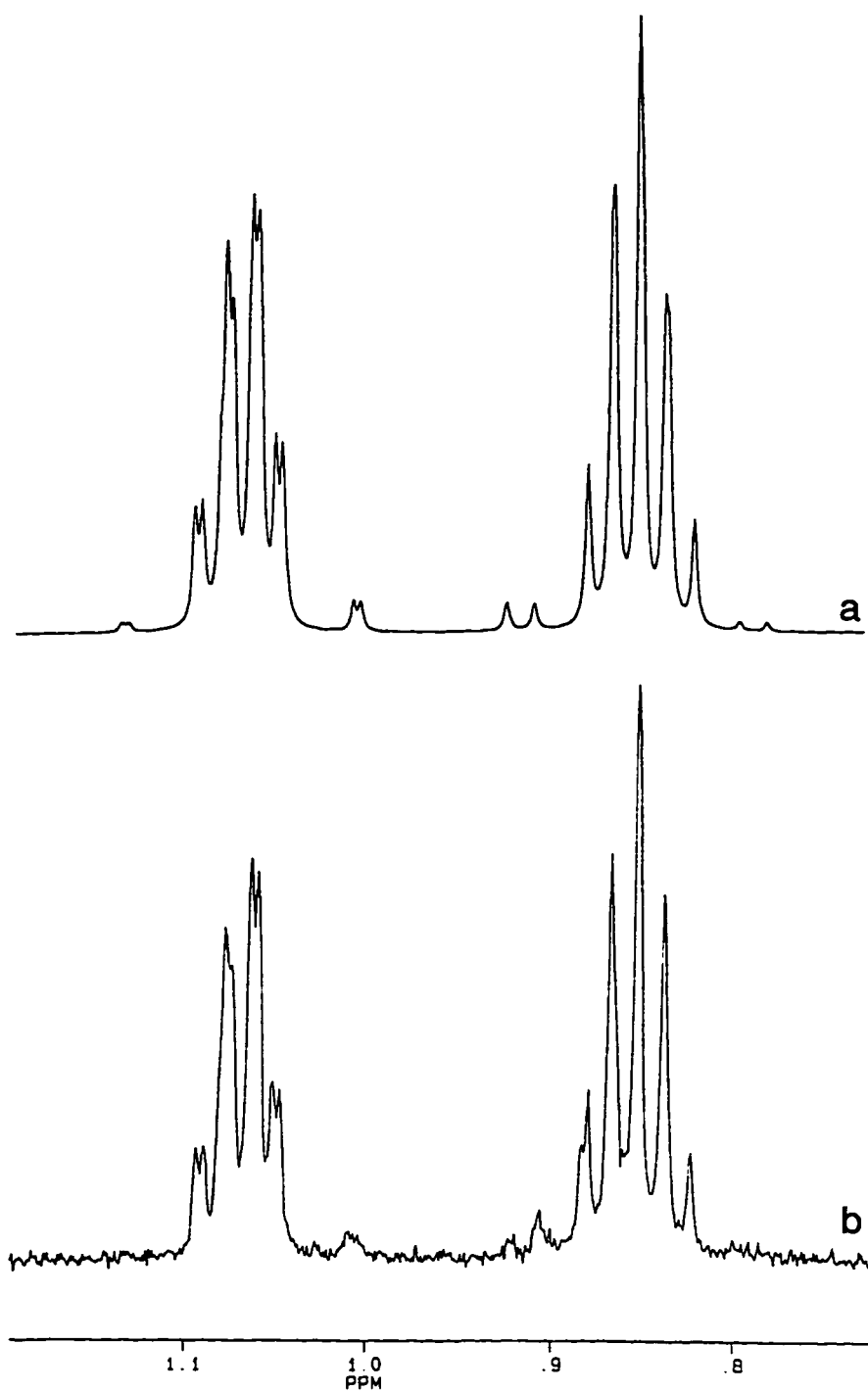
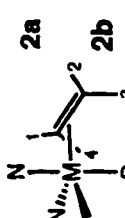
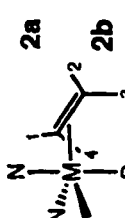


Figure 2.2 Observed and simulated ^1H NMR spectra of the ethylene resonances of $\text{TpIr}(\text{PPh}_3)(\text{C}_2\text{H}_4)$.

Table 2.1. ¹H NMR Chemical Shift and Coupling Parameters for Coordinated Ethylene for TpM(PPh₃)(C₂H₄)

Compound	Chemical Shift (ppm)				Coupling Constants (Hz)							
	δ _{AA'} (1, 2)	δ _{BB'} (3, 4)	J ₁₂	J ₃₄	J ₁₃	J ₁₄	J ₁₅ ^a	J ₃₅ ^a	J ₁₆ ^b	J ₃₆ ^b		
 2a	1.98 ^c	1.38 ^c	8.8	8.8	12.1	-3.5	1.2	5.8	2.8	2.6		
 2b	1.06 ^d	0.85 ^d	8.8	8.6	8.8	-4.5	1.2	4.5	—	—		
Ethylene ^e	5.4		11.6		19.1	2.5						

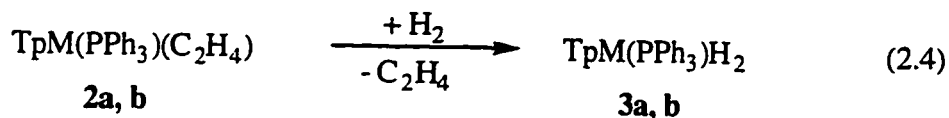
^aPhosphorous-hydrogen coupling. ^bRhodium-hydrogen coupling. ^cTHF-d₈. ^dCD₂Cl₂.

^eValues from Sheppard, N.; Lynden-Bell, R. M. *Proc. Roy. Soc. (London)* 1962, A269, 385-403.

tbp geometry. Irradiation of the AA' resonance (1.96 or 1.06 ppm) of the ethylene ligand gives a strong NOE enhancement of H³ of the axial pyrazolyl arm and to the BB' (1.38 or 0.85 ppm) ethylene resonance. Irradiation of the BB' resonance gives an NOE enhancement of the AA' resonance exclusively. Since only a single resonance at high field is observed for the respective ethylene ligands in the ¹³C{¹H} NMR spectra, the ethylene ligand must lie in the equatorial plane with a mirror plane bisecting the C=C. The ¹³C{¹H} NMR chemical shifts of the ethylene ligand in **2a, b** are shifted significantly upfield to 26.0 and 2.0 ppm respectively. A similar value of 4.1 ppm has been reported for CpIr(PMe₃)(C₂H₄).²⁵ The chemical shift of free ethylene, for comparison, is *ca.* 123 ppm.

Oro and coworkers have also assigned a tbp structure to TpIr(CO)(C₂H₄). For this complex, ¹H NMR NOE experiments verify that the CO and C₂H₄ ligands occupy axial and equatorial sites, respectively. The lower limit for ethylene rotation in **2** was calculated by computer simulation of the experimental spectra to be greater than 19.8 (**2a**) and 20.8 (**2b**) kcal/mol. The general observation of hindered ethylene rotation in d⁸-ML₄(C₂H₄) complexes arises from the large decrease in metal(π) to C₂H₄(π*) back bonding when C₂H₄ is rotated 90° out of the trigonal plane.²⁶⁻²⁸ In our case the facially constrained Tp ligand also prevents Berry pseudorotation-coupled ethylene rotation.²⁶ Eisenstein, Caulton and coworkers have postulated that apical CO ligands should decrease the ethylene rotational barrier by overlap of the CO(π*) and the C₂H₄(π*) in the transition state.²⁹ However, the ethylene ligand of TpIr(CO)(C₂H₄) has also been reported to be static on the NMR timescale to 373 K,⁸ which suggests that the ethylene rotational barriers of **2** are significantly greater than 20 kcal/mol.

Reactions with Hydrogen. Solutions of **2a** or **2b** react with 1-2 atm of hydrogen to yield TpM(PPh₃)H₂ (**3a, b**) (eq 2.4). Reactions carried out in sealed NMR tubes and monitored by ¹H NMR spectroscopy indicate quantitative conversion to **3a, b**



with displacement of ethylene. Even after complete conversion to **3**, no ethane was observed by ^1H NMR analysis. The rates of these reactions as a function of metal center were found to be essentially identical in THF- d_8 ($t_{1/2} = ca. 30$ min). **3** is conveniently prepared in one pot by sequentially reacting **1** with phosphine then repressurizing a degassed solution with 1-2 atmospheres of H_2 . Pale yellow (**3a**) or colorless (**3b**) microcrystals are obtained upon addition of pentane to concentrated benzene or toluene solutions. A similar ethylene displacement reaction has been identified for reaction of $\text{Pt(PR}_3\text{)}_2\text{(C}_2\text{H}_4)$ ($\text{R} = \text{Me}$ or Et) with H_2 .³⁰ The hydride ligands of **3a, b** are identified in solution by ^1H NMR (CD_2Cl_2) spectroscopy by their characteristic upfield shifts at -16.42 (dd, $J_{\text{P-H}} = 28.4$ Hz, $J_{\text{Rh-H}} = 18.9$ Hz) and -20.47 ppm (d, $J_{\text{P-H}} = 22.1$ Hz) respectively. IR data for these complexes obtained as Nujol mulls show two M-H bands each at 2092, 2069 cm^{-1} (**3a**) and 2179, 2139 cm^{-1} (**3b**). Appropriate resonances for the Tp and PPh_3 ligands were observed in the ^1H and $^{13}\text{C}\{^1\text{H}\}$ NMR spectra. Interestingly, the protons of the pyrazolyl arm positioned trans to the phosphine ligand weakly couple to the phosphorus nucleus ($J_{\text{P-H}} = ca. 1\text{-}2$ Hz). $^1\text{H}\{^{31}\text{P}\}$ NMR experiments confirm that the origin of the small coupling results from the *trans*- PPh_3 ligand. The effect is most pronounced at the H^4 -pyrazolyl position, which is five bonds removed from the phosphorus atom and is general for the $\text{TpM(PR}_3\text{)}$ fragment described in this work. A number of Tp complexes are known which also contain phosphine donor ligands, however long range P-H coupling to the pyrazolyl protons has not been previously reported.

Determination of the Rate Law for Reaction of 2b with H_2 . The rate law for reaction of **2b** with H_2 was determined under pseudo first order conditions at constant

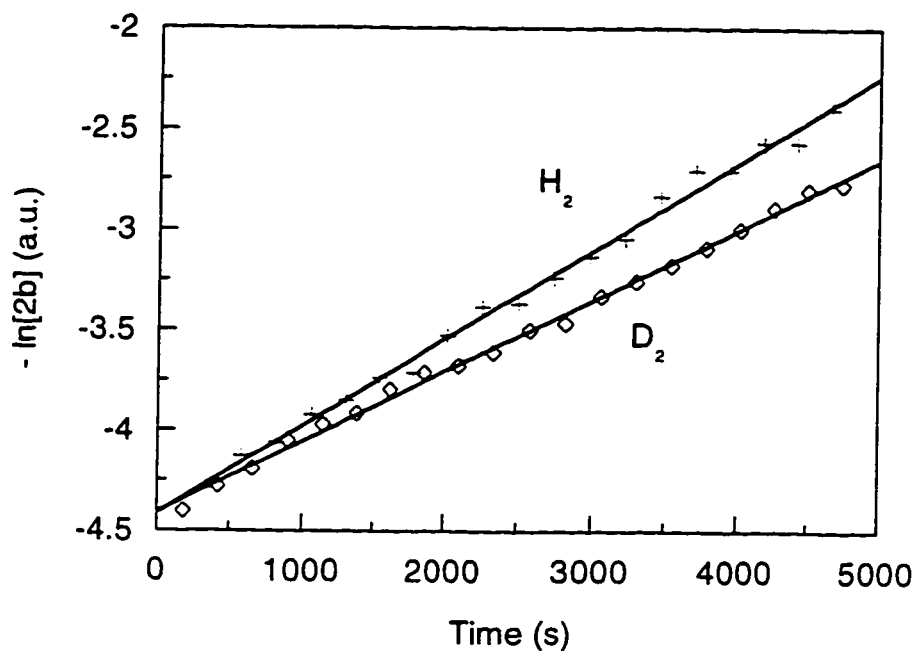


Figure 2.3. Plot of $-\ln[2b]$ (a.u.) vs. time (s) for reaction of **2b** with H_2 (+) and D_2 (\diamond) in CD_2Cl_2 at 296 K. $[2b]_i = 3.51 \times 10^{-3}$ M; $P_{H_2} = P_{D_2} = 750$ torr; $[H_2] = 2.3 \times 10^{-3}$ M ($k_{obs}(H_2) = 4.4 \times 10^{-4} s^{-1}$; $k_{obs}(D_2) = 3.5 \times 10^{-4} s^{-1}$; $k_H/k_D = 1.26 \pm 0.18$).

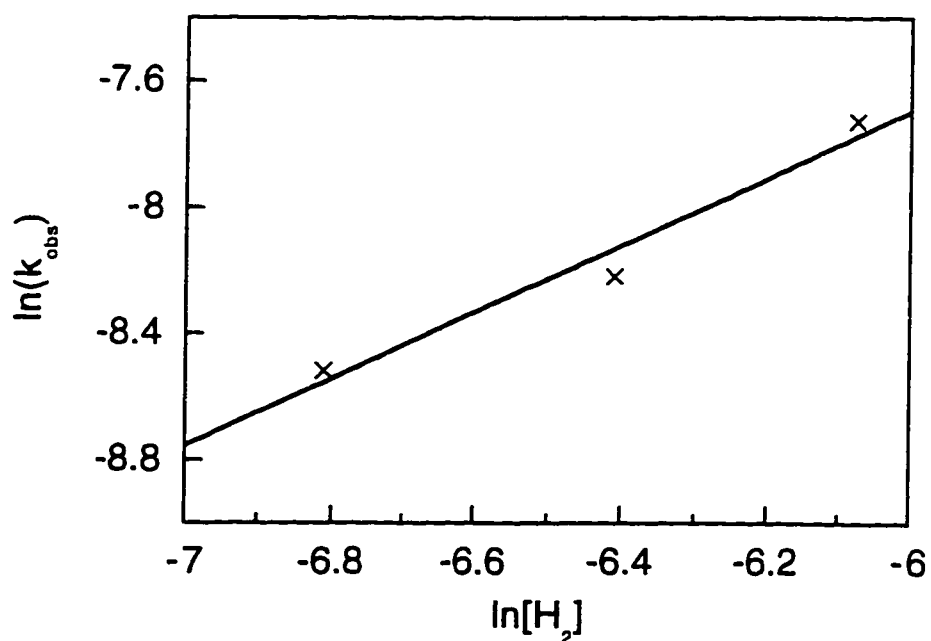


Figure 2.4. Plot of $\ln(k_{obs})$ vs. $\ln[H_2]$ ($r^2 = 0.98$) for the reaction of **2b** with H_2 in CD_2Cl_2 at 296 K. The slope of the line (order in $[H_2]$) is 1.1 ± 0.2 .

H₂ concentration in the dark. Dilute CD₂Cl₂ solutions of **2b** react cleanly with H₂ to form **3b** and ethylene. A first order plot of -ln[**2b**] vs. time is nicely linear through three half lives (fig 2.3). A small isotope effect was observed when the reaction was carried out with D₂ ($k_{H_2}/k_{D_2} = 1.26 \pm 0.18$). Variation of the H₂ pressure from 359 to 750 torr demonstrates a first order dependence on H₂ concentration (fig 2.4). No apparent effect on the rate of this reaction was observed when an excess of ethylene was added to the reaction mixture. A slight acceleration was noted when the reaction was run with a ten-fold excess of PPh₃. A side reaction between **2b** and PPh₃ accounts for this observation (see chapter 4). These results, summarized in Table 2.2, indicate an associative rate law for reaction of H₂ with **2b** (eq 2.5). The observed rate constant (k_{obs}) under pseudo first order conditions is equal to $k''[H_2]$, where k'' is the second order rate constant.

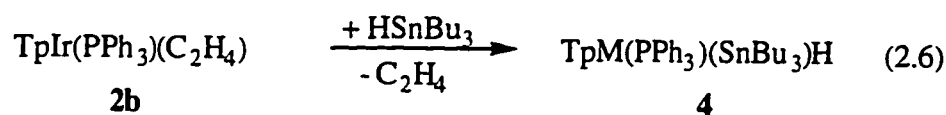
$$\text{rate} = k''[H_2][\mathbf{2b}] \quad (2.5)$$

Table 2.2 Rate data for the reaction of **2b** with H₂ in CD₂Cl₂ at 296K.^a

[2b] _i x 10 ³ (M)	[H ₂] x 10 ³ (M)	[other] x 10 ³ (M)	k_{obs} x 10 ⁴ (s ⁻¹)
3.51	2.3	—	4.4
3.51	1.6	—	2.7
3.51	1.1	—	2.0
3.51	2.3	35 (C ₂ H ₄)	4.1
3.51	2.3	36 (PPh ₃)	5.3
3.51	2.3 (D ₂)	—	3.5

^aSee the Experimental Section for details of the procedure and estimated uncertainties.

General Reactivity. A few reactions of **2b** with common laboratory reagents have been characterized. Addition of one equiv. of HSnBu_3 to a benzene or CH_2Cl_2 solution of **2b** immediately yields $\text{TpIr}(\text{PPh}_3)(\text{SnBu}_3)\text{H}$ (**4**) and free ethylene (eq 2.6).



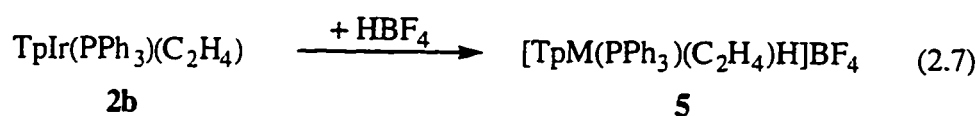
A total of nine pyrazolyl resonances are observed for **4** by ^1H NMR spectroscopy, characteristic of a complex with C_1 symmetry. Appropriate resonances for the PPh_3 and SnBu_3 ligands are also noted as well as a distinctive hydride resonance at -19.97 ppm. The hydride resonance exhibits coupling to the PPh_3 ligand ($J_{\text{P-H}} = 21.6$ Hz) and to the $^{117}/^{119}$ isotopes of tin (7.7 and 8.6 % abundance, each spin = 1/2). Because the magnetogyric ratios are nearly equivalent for the two tin isotopes,³¹ a single set of tin satellites ($J_{\text{Sn-H}} = 87$ Hz) is observed which accounts for *ca.* 16 % of the hydride intensity. A large Sn-P coupling constant ($J_{\text{Sn-P}} = 141$ Hz) is also observed by ^{31}P NMR analysis. Complex **4** may find utility as a convenient precursor to a family of $\text{TpIr}(\text{PPh}_3)(\text{R})\text{H}$ complexes by substitution of the Ir-SnBu₃ bond. However, **4** does not react with MeI under mild conditions to form the anticipated methyl hydride complex.

Addition of HSiEt_3 to a C_6D_6 solution of **2b** gives no reaction and addition of HSiCl_3 yields a complex mixture of products which were not characterized. Iodine reacts cleanly with **2b** to form $\text{TpIr}(\text{PPh}_3)\text{I}_2$ and ethylene. No reaction was observed with MeI, di-^tbutylperoxide or hydrazine under mild conditions and upon heating these reaction mixtures to 60 °C for several hours, only decomposition products were observed. The oxidative ethylene substitution reactions observed for the PPh_3 substituted complex **2b**, contrasts with the reactivity of the bis-ethylene parent, **1b**. For example, **1b** reacts with H_2 or I_2 to yield $\text{TpIr}(\text{C}_2\text{H}_4)(\text{C}_2\text{H}_5)\text{H}$ and $[\text{TpIr}(\text{C}_2\text{H}_4)_2\text{I}]$.

respectively. $[\text{TpIr}(\text{C}_2\text{H}_4)_2\text{I}]\text{I}$ reacts in turn with PPh_3 to yield $[\text{TpIr}(\text{PPh}_3)(\text{C}_2\text{H}_4)\text{I}]\text{I}$.

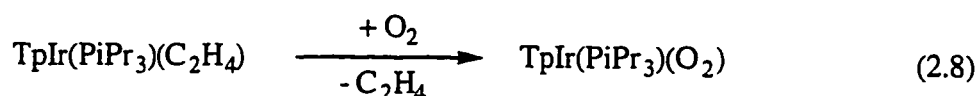
No reaction was observed between **1b** and HSnBu_3 .

Methylene chloride solutions of **2b** react with $\text{HBF}_4 \cdot \text{Et}_2\text{O}$ to yield $[\text{TpIr}(\text{PPh}_3)(\text{C}_2\text{H}_4)\text{H}]\text{BF}_4$ (**5**) (eq 2.7), which can be isolated as colorless crystals upon addition of Et_2O and cooling to $-30\text{ }^\circ\text{C}$. Spectroscopic data confirm that protonation has occurred at the metal center rather than at a pendant pyrazolyl nitrogen.⁶ The characteristic hydride resonance was observed in solution by ^1H NMR spectroscopy at



-14.64 ppm (d, $J_{\text{P-H}} = 15.6\text{ Hz}$) and in the solid state by IR spectroscopy as a sharp band at 2226 cm^{-1} .

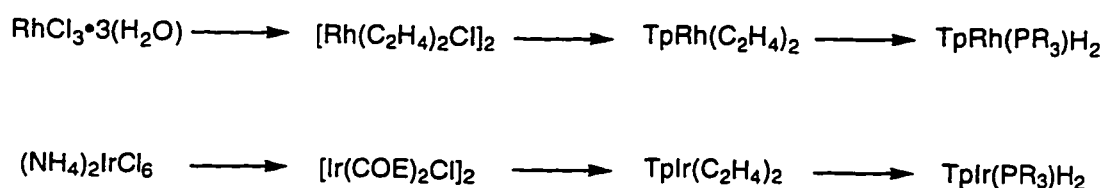
We have observed that benzene- d_6 solutions of $\text{TpIr}(\text{PR}_3)(\text{C}_2\text{H}_4)$ complexes react when exposed to air to give a new complex with C_s symmetry and free ethylene. Under controlled conditions, nitrogen and oxygen were added to separate NMR tubes containing degassed benzene- d_6 solutions of $\text{TpIr}(\text{PiPr}_3)(\text{C}_2\text{H}_4)$. No reaction was observed with N_2 , however the reaction with O_2 gave the same product which was observed upon exposure to air. These products are tentatively assigned as dioxygen complexes (eq 2.8), although this has not been confirmed with supporting spectroscopic



and analytical data. Reactions carried out in CD_2Cl_2 solutions under otherwise identical conditions gave a complex mixture of products.

Discussion

As part of our work in the study of hydride structure and dynamics, we required a convenient method to prepare $\text{TpM}(\text{PR}_3)\text{H}_2$ ($\text{M} = \text{Rh}$ and Ir) complexes.³² The synthetic methods outlined in this chapter provide these species in excellent yield in only three steps from the noble metal salts (scheme 2.2). Preliminary results indicate that this synthetic method is general for a range of phosphine ligands, including bulky phosphines such as PCy_3 . Previous syntheses of complexes related to **3** have been

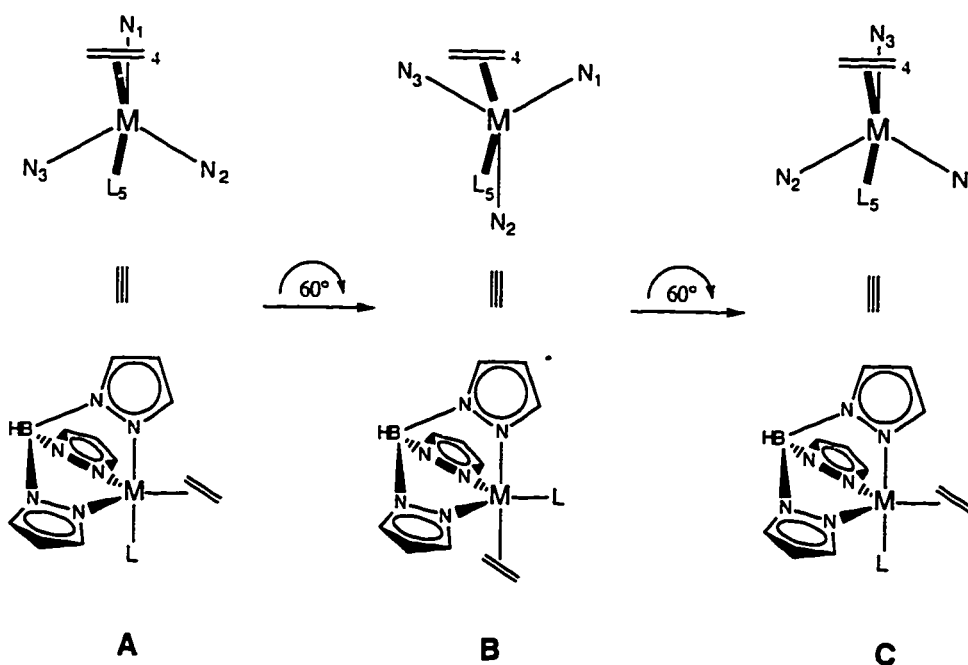


Scheme 2.2

reported,³²⁻³⁵ however these procedures are much less convenient and are unlikely to become of general use. The ease with which reactions 2.2 and 2.4 occur are in marked contrast to the analogous reactions of the cyclopentadienyl systems. Thermal substitution of ethylene by phosphine ligands occurs only with difficulty,³⁶⁻³⁸ if at all³⁹ in $(\text{C}_5\text{R}_5)\text{M}(\text{C}_2\text{H}_4)_2$ ($\text{R} = \text{H}$ and Me ; $\text{M} = \text{Rh}$ and Ir) complexes. Thermal reactions of $(\text{C}_5\text{R}_5)\text{M}(\text{PR}_3)(\text{C}_2\text{H}_4)$ complexes with H_2 are unknown to our knowledge. The difference in reactivity lies in the facile interconversion between 18 electron *tbp* and 16 electron *sp* structures in the *Tp* system. Solution state structure and dynamics, and kinetic data are discussed in the following sections to clarify the proposed reaction mechanisms.

Hydridotris(1-Pyrazolyl)borate Dynamics. A facile dynamic process serves to exchange the axial and equatorial pyrazolyl ligands of **1** at all accessible temperatures. We have obtained ^1H NMR spectra in the fast exchange limit to 130 K in

CDCl₂F solutions, indicating a free energy of activation for this process of less than 6 kcal/mol assuming a chemical shift difference of *ca.* 10 Hz. A number of mechanistic studies of Tp fluxionality have concluded that pyrazolyl site exchange occurs within the coordination sphere of the metal without metal-nitrogen bond cleavage.^{4,40-43} Berry pseudorotation (BPR) is commonly proposed to account for dynamic ligand rearrangements in five coordinate complexes.⁴⁴ However, the steric restraints imposed by the bridgehead boron atom prevents the Tp ligand from spanning *trans*-axial sites, which is required for BPR. A more likely mechanism in this case is turnstile rotation (TR).⁴⁵ The result of TR is rotation of the Tp ligand around the M•••B-H axis by 60°. This mechanism effectively exchanges two axial and equatorial ligands, but leaves one of the equatorial ligands unchanged. Considering scheme 2.3, conformation **A** depicts axial ligands, N(1) and L(5) and equatorial ligands, N(2), N(3), and C₂H₄(4). Rotation about the M•••B-H axis of 60° produces conformation **B** with axial sites now occupied by N(2) and C₂H₄(4) and equatorial sites occupied by N(1), N(3) and L(5). Only N(3)

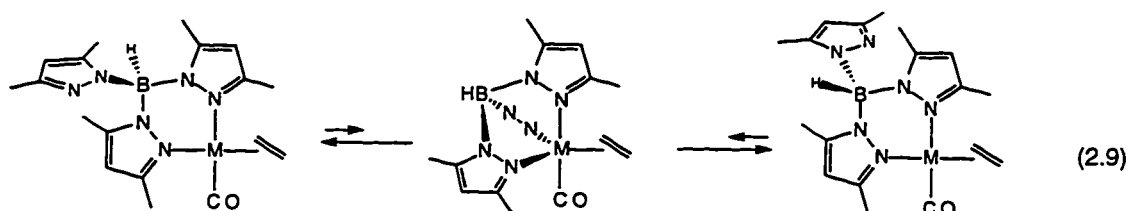


Scheme 2.3

remains in a chemically equivalent site following TR. When L(5) is C₂H₄, **A** and **B** are identical. However when L(5) is any other donor ligand, **B** represents the highest energy intermediate or transition state along the exchange pathway. A second turnstile iteration results in the final structure, **C** in which axial and equatorial pyrazolyl sites have exchanged, and the positions of C₂H₄ and L are unchanged from the initial structure **A**. The nature of L has a dramatic effect on the activation barrier of the pyrazolyl exchange process. The activation barriers for the series of complexes, TpIr(L)(C₂H₄) (L = C₂H₄, CO,⁸ PPh₃) are < 6, 14, and > 18.4 kcal/mol respectively. The barrier of pyrazolyl site exchange for L other than C₂H₄ is a direct measure of the difference in energy between **A** and **B** and increases as the σ -donor ability of L increases. On changing the metal from Rh to Ir in **2**, the barrier increases by more than 4.1 kcal/mol. For this problem the most important difference between Rh and Ir is expected to be the difference in π -back bonding ability. Back bonding to the ethylene ligand is a stabilizing interaction, in both an axial or equatorial site. However, a much larger stabilization results when ethylene occupies the equatorial site. The metal orbital of local π -symmetry in the trigonal plane is hybridized to offer the greatest spatial and energy overlap with the π^* ethylene orbital. The absolute stabilization is smaller for Rh than for Ir as evidenced by the ¹³C NMR chemical shifts of the C₂H₄ ligands at 26.0 and 2.0 ppm, respectively. In contrast, π -back bonding to an axial coordinated ethylene ligand (which occurs in **B**) is expected to be similar between the two metals because the filled metal orbital of local π symmetry is mostly unhybridized d_{yz}.²⁷

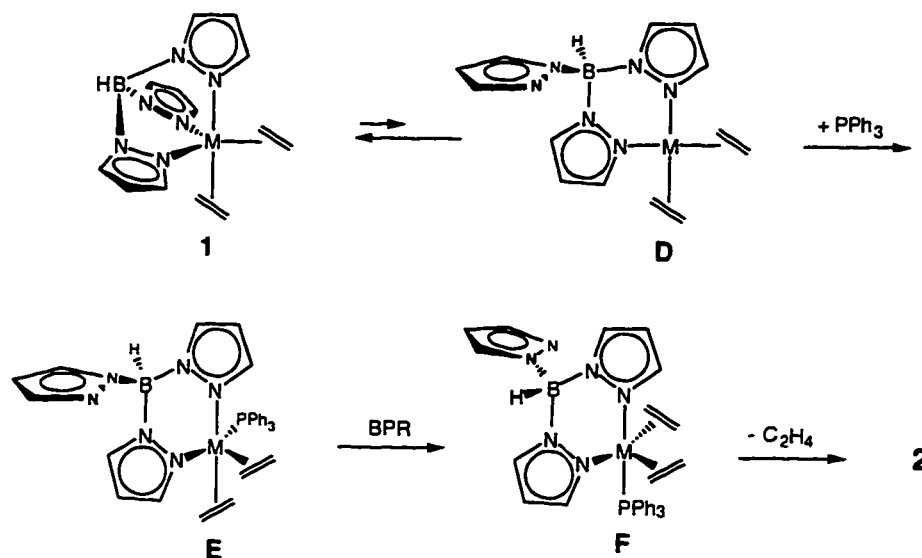
A second dynamic process, distinct from TR, is equilibrium between tbp and sp structures. It is important to point out that axial and equatorial pyrazolyl arms of a tbp structure are not exchanged by this mechanism. The research groups of Cocivera and Oro have previously demonstrated that equilibria of this type are rapid in complexes that also display rapid TR. Thus complexes of the type, (Bpz₄)M(LL) display only one set

of pyrazolyl peaks at ambient temperature. Data reported by Graham and coworkers supports the notion that equilibria between *sp* and *tbp* structures can also be fast when TR is slow. Both $\text{Tp}^{\text{Me}_2}\text{Rh}(\text{CO})(\text{C}_2\text{H}_4)$ and $\text{Tp}^{\text{CF}_3, \text{Me}}\text{Ir}(\text{CO})(\text{C}_2\text{H}_4)$ are assigned *sp* structures by a systematic comparison of carbonyl stretching bands of related complexes.^{5,46} A static *sp* structure is expected to show a 1:1:1 pattern of pyrazolyl resonances by ^1H and ^{13}C NMR analysis. Instead, a 2:1 pattern is observed, which is invariant to $-80\text{ }^\circ\text{C}$. A dynamic equilibrium with a *tbp* intermediate effectively exchanges the uncoordinated pyrazolyl group with only one of the bound ligands (eq 2.9). TR should be slow in the $(\eta^3\text{-Tp}^{\text{R,R'}})\text{M}(\text{CO})(\text{C}_2\text{H}_4)$ intermediate for the reasons



discussed above. We propose that a similar equilibrium is obtained for both **1** and **2**, although the *tbp* form is the more stable isomer. The concentration of the *sp* form must be very small because the ^1H and ^{13}C NMR chemical shifts show no significant temperature dependence, which might signal a shift in equilibrium concentrations.

Reaction Mechanisms. Complex **1** reacts too rapidly with PPh_3 , even at 200 K, to study by conventional NMR methods. In comparison the reported halflives for reaction of $(\text{C}_5\text{H}_5)\text{M}(\text{C}_2\text{H}_4)_2$ with excess PPh_3 are 67 (Rh)³⁶ and 635 (Ir)³⁸ minutes at 393K. These complexes react via high energy intermediates by either a dissociative or associative mechanism.³⁷ The latter pathway appears to be more general and may be accommodated if ring slip from $\eta^5\text{-}$ to $\eta^3\text{-C}_5\text{H}_5$ coordination is invoked.⁴⁷ We propose that a related process operates in the Tp system. However, in this case 16 electron *sp*



Scheme 2.4

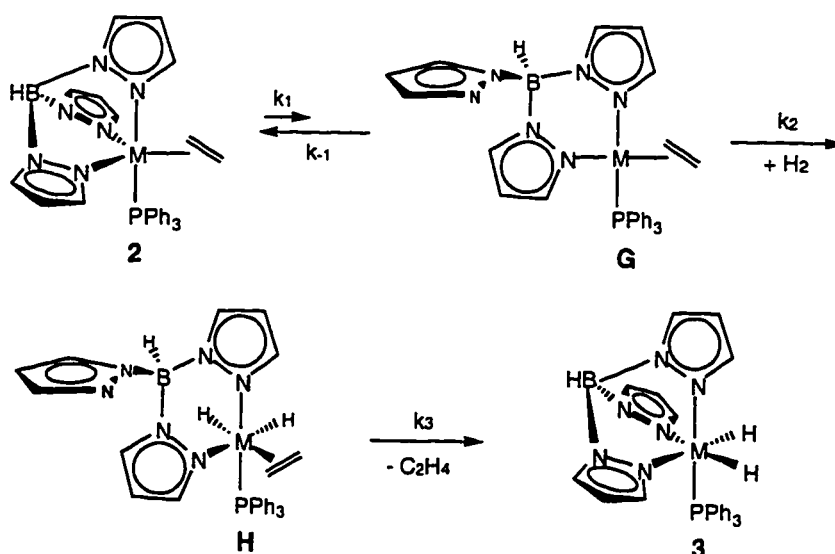
intermediates are close in energy. A reasonable mechanism for reaction of **1** with PPh_3 is outlined in scheme 2.4. Nucleophilic attack of the sp intermediate, **D** forms an unstable tbp complex, **E**. According to a computational study of $[\text{Ir}(\text{PH}_3)_3(\text{C}_2\text{H}_4)_2]^+$, rearrangement to **F** via Berry pseudorotation is at least 30 kcal/mol downhill.²⁹ Subsequent loss of an ethylene ligand and coordination of the free pyrazolyl arm yields **2**. An alternative pathway in which an ethylene ligand is displaced directly from **E** is considered less likely because the resulting structure (see **B** in scheme 2.3) is known to be particularly unstable.

Solutions of **2** react cleanly with H_2 to give **3** and ethylene. No inhibition of the reaction is observed in the presence of a large excess of ethylene or PPh_3 . Dissociation of these ligands prior to the rate determining step is thus ruled out. The first order dependence on $[\text{H}_2]$ and the small isotope effect (1.26 ± 0.18) for reactions with D_2 are consistent with oxidative addition of H_2 in the rate determining step. Oxidative addition of H_2 is well known in 16-electron sp complexes of rhodium and iridium and typically shows a small $k_{\text{H}_2}/k_{\text{D}_2}$.⁴⁸ A structure of this type is obtained if an equilibrium between

tbp and sp structures is invoked for **2**. A mechanism consistent with the experimental observations is outlined in scheme 2.5. The rate equation derived for this sequence of steps is shown in eq 2.10. Assuming that $k_{-1} \gg k_2[H_2]$, then this equation reduces to the observed rate law (eq 2.5), where $k'' = k_1k_2/k_{-1}$. This assumption is reasonable

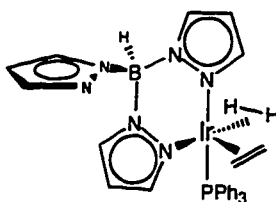
$$\text{rate} = \frac{k_1k_2[2b][H_2]}{k_{-1} + k_2[H_2]} \quad (2.10)$$

because k_1/k_{-1} is small. If H_2 approaches the face opposite the pendant pyrazolyl arm, and parallel with the pz-Ir-C₂H₄ axis, the resulting oxidative addition product, **H** is obtained. The ethylene ligand in **H** is positioned trans to the labilizing hydride ligand and is also properly situated for rapid displacement by the pendant pyrazolyl arm. Intermediates related to **H** have been implicated in the reaction of NaTp with [(NCMe)₃Ir(PMe₃)H₂]SO₃CF₃. Sequential displacement of the three acetonitrile ligands via (η^1 -Tp)Ir(PMe₃)(MeCN)₂H₂⁴⁹ and (η^2 -Tp)Ir(PMe₃)(MeCN)H₂ intermediates, ultimately yields TpIr(PMe₃)H₂.³² Eisenberg and coworkers have shown



Scheme 2.5

that oxidative addition of H_2 to sp iridium complexes occurs stereoselectively along the axis containing a π -acceptor ligand (in this case, ethylene).⁵⁰ As H_2 approaches the metal center, the trans pair of ligands will bend back, forming a *tbp* intermediate or transition state which is stabilized by the π -acid ligand in the equatorial plane (scheme 2.6). For reaction of **2** with H_2 , oxidative addition is a favorable reaction. Closely



Scheme 2.6

related H_2 complexes which have been stabilized against oxidative addition are described in the following chapter.

Conclusion

The synthesis and characterization of $TpM(PPh_3)(C_2H_4)$ has been described. These complexes provide a convenient entry into hydridotris(pyrazolyl)borate phosphine chemistry of rhodium and iridium. Hydrogen readily displaces the respective ethylene ligands through thermally accessible sp (η^2 - Tp) $M(PPh_3)(C_2H_4)$ intermediates to form $TpM(PPh_3)H_2$ and free ethylene.

Experimental Section

General Methods. All manipulations were conducted under a dry argon or nitrogen atmosphere using standard Schlenk and drybox techniques. Argon and nitrogen were deoxygenated and dried by passage through Chemical Dynamics Corp. R3-11 CuO catalyst followed by Mallinckrodt Aquasorb containing P_2O_5 . Air-sensitive compounds

were manipulated in an MBraun labmaster 130 glove box equipped with integrated dry train loaded with copper catalyst and molecular sieves. Solvents were purified by distillation from Na-K-benzophenone (except CH_2Cl_2 from P_2O_5) under a nitrogen atmosphere. Deuterated NMR solvents (purchased from Cambridge Isotope Laboratories) were degassed, and stored over CaH (CD_2Cl_2) or Na-K-benzophenone (C_6D_6 , toluene- d_8 , THF- d_8). Hydrogen (99.999%) and ethylene (99.7%) were purchased from Airco. Unless stated otherwise all other reagents were obtained from Aldrich and used as received.

Potassium hydridotris(1-pyrazolyl)borate (KTp) was prepared by the procedure of Trofimenko.⁵¹ $\text{RhCl}_3 \cdot 3\text{H}_2\text{O}$ was obtained as a gift from the laboratory of Prof. Martin Gouterman. $(\text{NH}_4)_2\text{IrCl}_6$ was recovered from laboratory iridium residues following published procedures.⁵²

^1H NMR spectra were recorded on Bruker AC200, AF300, or WM500 spectrometers and referenced internally to the residual proton resonance of the deuterated solvent with respect to tetramethylsilane (TMS). ^{13}C NMR spectra were collected on the AC200, AF300, and WM500 spectrometers operating at a frequency of 50.32, 75.46 and 125.76 MHz, respectively, and referenced internally to the solvent. ^{31}P NMR spectra were collected on the AC200 and WM500 spectrometers at frequencies of 81.02 and 202.45 MHz, respectively, and referenced externally to 85% H_3PO_4 . Variable temperature NMR measurements were performed using the Bruker B-VT1000 temperature control module with a copper-constantan thermocouple. Temperature calibration was obtained by measurement of the chemical shift difference between the $-\text{CH}_3$ and $-\text{OH}$ peaks of a standard methanol sample using the method of Van Geet.⁵³ Line shape analysis of NMR spectra was performed using a modified version of the DYNAMAR program. The $J_{\text{H-H}}$ coupling constants observed for the pyrazolyl

resonances are typically *ca.* 2 Hz and are not explicitly reported in the characterization data which follows.

Infrared spectra were recorded as Nujol mulls between NaCl plates on a Perkin-Elmer model 1600 Fourier transform spectrophotometer (2.0 cm⁻¹ resolution).

Elemental analyses were performed by Canadian Microanalytical Services, Ltd., Vancouver, BC.

Synthesis of Complexes.

TpRh(C₂H₄)₂ (1a). This compound was prepared following the procedure of Trofimenko¹³ from [Rh(C₂H₄)₂Cl]₂.⁵⁴ Yield 60%. ¹H NMR (C₆D₆): 7.59, 7.41 (d, 3 H each, 3,5-pz); 5.90 (t, 3 H, 4-pz); 2.52 (d, J_{Rh-H} = 1.6 Hz, 8 H, C₂H₄). ¹³C{¹H} NMR (C₆D₆): 139.5, 134.8 (s, 3,5-pz); 105.2 (s, 4-pz); 49.0 (d, J_{Rh-C} = 13 Hz, C₂H₄). IR 2461 (ν_{B-H}).

TpIr(C₂H₄)₂ (1b). This compound was prepared following the procedure of Tanke and Crabtree¹⁴ from [Ir(COE)₂Cl]₂.⁵⁵ Yield 88%. ¹H NMR (C₆D₆): 7.64, 7.35 (d, 3 H each, 3,5-pz); 5.80 (t, 3 H, 4-pz); 2.25 (br s, 8 H, C₂H₄). ¹³C{¹H} NMR (C₆H₆): 139.4, 134.7 (s, 3,5-pz); 105.6 (s, 4-pz); 29.6 (s, C₂H₄); ¹H NMR (CDCl₂F, 210 K): 7.81, 7.70 (d, 3 H each, 3,5-pz); 6.25 (t, 3 H, 4-pz); 2.44, 1.70 (m, AA'XX' spin system, J_{cis} = 9.0, J_{trans} = 11.3, J_{gem} = -2.1 Hz, 2 H each, C₂H₂). IR: 2474 (ν_{B-H}).

TpRh(PPh₃)(C₂H₄) (2a). To a 100 mL schlenk flask containing TpRh(C₂H₄)₂ (0.1124 g, 0.302 mmol), PPh₃ (0.0825 g, 0.315 mmol) and a teflon coated stir bar was added benzene (10 mL) by cannula. Vigorous bubbling was observed as the solid reagents dissolved, producing a bright yellow solution. This was allowed to stir at room temperature for 60 min upon which time the volume of the solution was reduced under vacuum and pentane was added to afford a yellow microcrystalline precipitate, which was filtered off and dried under vacuum. Yield 160 mg (87%). ¹H NMR (toluene-*d*₈): 7.63 (br s, 3 H, 5-pz); 7.40 (br s, 3 H, 3-pz), 7.63-7.18, 6.98 (br m, 15 H, PPh₃); 5.82 (t,

3 H, 4-pz); 2.39, 1.77 (m, 2 H each, C₂H₄). ¹H NMR (toluene-*d*₈, 223 K): 7.81 (m, 4 H, *o*-C₆H₅); 7.66 (d, 2 H, 5-pz_{eq}); 7.48 (d, 2 H, 3-pz_{eq}); 7.44 (br d, 1 H, 5-pz_{ax}); 7.12 (br d, 1 H, 3-pz_{ax}); 7.03 (m, 6 H, *m* and *p*-C₆H₅); 6.94, 6.68 (t, *J* = 8.8 and 7.6 Hz respectively, 2 H each, *o* and *m*-C₆H₅); 6.78 (t, *J* = 6.5 Hz, 1 H, *p*-C₆H₅); 5.83 (t, 2 H, 4-pz_{eq}); 5.77 (m, 1 H, 4-pz_{ax}); 2.45, 1.83 (m, 2 H each, C₂H₄). ¹H NMR (THF-*d*₈, 219 K) 7.77 (d, 2 H, 5-pz_{eq}); 7.70 (br s, 1 H, 5-pz_{ax}); 7.62 (m, 4 H, *o*-C₆H₅); 7.48 (m, 6 H, *m*, *p*-C₆H₅); 7.19 (partially obscured, 1 H, 3-pz_{ax}); 7.18 (d, 2 H, 3-pz_{eq}); 7.14 (t, *J* = 7.4 Hz, 1 H, *p*-C₆H₅); 6.87, 6.68 (t, *J* = 7.6, 8.6 Hz respectively, 2 H each, *o* and *m*-C₆H₅); 6.13 (m, 1 H, 4-pz_{ax}); 5.92 (t, 2 H, 4-pz_{eq}); 1.89, 1.28 (m, 2 H each, C₂H₄). ¹³C{¹H} NMR (THF-*d*₈): 143.8 (s, 3-pz); 135.5 (d, *J*_{P-C} = 9.8 Hz, *o*- or *m*-PPh₃); 134.9 (s, 5-pz); 133.1 (d, *J*_{P-C} = 45 Hz, *i*-PPh₃); 130.5 (s, *p*-PPh₃); 128.5 (d, *J*_{P-C} = 9.6 Hz, *o* or *m*-PPh₃); 104.8 (s, 4-pz); 26.0 (d of d, *J*_{Rh-C} = 17 Hz, *J*_{P-C} = 4 Hz, C₂H₄). ¹³C{¹H} NMR (THF-*d*₈, 213 K): 143.8 (s, 3 C, 3-pz_{ax} + eq); 135.7 (d, *J*_{P-C} = 9.8 Hz, 4 C, *o* or *m*-PPh₃); 135.0 (s, 2 C, 5-pz_{eq}); 134.9 (s, 1 C, 5-pz_{ax}); 132.8 (d, *J*_{P-C} = 43.5 Hz, 1 C, *i*-PPh₃); 132.6 (d, *J*_{P-C} = 46.5 Hz, 2 C, *i*-PPh₃); 130.9 (s, 2 C, *p*-PPh₃); 130.2 (s, 1 C, *p*-PPh₃); 128.9 (d, *J*_{P-C} = 9.6 Hz, 4 C, *o* or *m*-PPh₃); 128.1 (d, *J*_{P-C} = 8.6 Hz, 2 C, *o* or *m*-PPh₃); 105.2 (s, 1 C, 4-pz_{ax}); 104.9 (s, 2 C, 4-pz_{eq}). ³¹P{aromatic ¹H} NMR (THF-*d*₈): 57.9 (d of t, *J*_{Rh-P} = 156 Hz, *J*_{H-P} = 2.8 Hz). IR: 2468 (ν_{B-H}). Anal. Calcd for C₂₉H₂₉BN₆PRh: C, 57.45; H, 4.82; N, 13.86. Found: C, 56.42; H, 4.67; N, 13.73.

TpIr(PPh₃)(C₂H₄) (2b). To a schlenk flask containing TpIr(C₂H₄)₂ (100 mg, 0.22 mmol), PPh₃ (61 mg, 0.23 mmol) and a teflon coated stir bar was added THF via cannula. The pale yellow solution was stirred at room temperature for 60 min, then the volume was reduced under vacuum. A light yellow precipitate was obtained upon addition of pentane and cooling to -30 °C overnight. This was filtered off and washed with additional pentane then dried under vacuum. Yield 131 mg (86%). ¹H NMR

(CD₂Cl₂, rt): 7.76, 7.21 (d, 2 H each, 3,5-pz_{eq}); 7.69, 7.28 (m and d respectively, 1 H each, 3,5-pz_{ax}); 7.39 (v br, 15 H, PPh₃); 6.18 (m, 1 H, 4-pz_{ax}); 5.93 (t, 2 H, 4-pz_{eq}); 1.07, 0.85 (m, 2 H each, C₂H₄). ¹H NMR (CD₂Cl₂, 220 K): 7.76, 7.19 (d, 2 H each, 3,5-pz_{eq}); 7.70, 7.23 (br s, 1 H each, 3,5-pz_{ax}); 7.51-7.39 (m, 10 H, PPh₃); 7.14 (t, J = 7 Hz, 1 H, p-C₆H₅); 6.88, 6.58 (t, J = 7 Hz, 2 H each, o- and m-C₆H₅); 6.18 (m, 1 H, 4-pz_{ax}); 5.93 (t, 2 H 4-pz_{eq}); 0.95, 0.75 (m, 2 H each, C₂H₄). ¹³C{¹H} NMR (CD₂Cl₂, rt): 143.5, 134.9 (s, 2 C each, 3,5-pz_{eq}); 135.6, 133.5 (s, 1 C each, 3,5-pz_{ax}); 135, 130, 128 (br, PPh₃); 105.2 (s, 2 C, 4-pz_{eq}); 104.9 (s, 1 C, 4-pz_{ax}); 2.0 (s, C₂H₄). ³¹P{¹H} NMR (CD₂Cl₂): 9.64 (s). ¹H NMR (toluene-*d*₈): 7.75, 7.00 (extremely br, 15 H, PPh₃); 7.58, 7.42 (d, 2 H each, 3,5-pz_{eq}); 7.41, 7.26 (d, 1 H, 3,5-pz_{ax}); 5.79 (m, 1 H, 4-pz_{ax}); 5.72 (t, 2 H, 4-pz_{eq}); 1.59, 1.35 (apparent q and p respectively, 2 H each, C₂H₄). IR: 2474 (ν_{B-H}). Anal. Calcd for C₂₉H₂₉BIrN₆P: C, 50.08; H, 4.20; N, 12.08. Found: C, 50.71; H, 4.43; N, 11.58.

TpIr(PMe₃)(C₂H₄). This complex was prepared on a small scale by addition of PMe₃ (1.1 μL, 0.01 mmol) via syringe to an NMR tube containing a C₆D₆ solution of TpIr(C₂H₄)₂ (4.7 mg, 0.01 mmol). ¹H NMR (C₆D₆): 7.63, 7.59 (d, 2 H each, 3,5-pz_{eq}); 7.38, 7.28 (m and d respectively, 1 H each, 3,5-pz_{ax}); 5.95 (t, 2 H, 4-pz_{eq}); 5.74 (m, 1 H, 4-pz_{ax}); 1.64, 1.55 (m, 2 H each, C₂H₄); 0.99 (d, J_{P-H} = 9.5 Hz, PMe₃). ³¹P{¹H} NMR (C₆D₆): -42.5 (s).

TpIr(PCy₃)(C₂H₄). Prepared as described for **2b**. ¹H NMR (C₆D₆): 7.99, 7.67 (d, 2 H each, 3,5-pz_{eq}); 7.35, 7.32 (m and d respectively, 1 H, 3,5-pz_{ax}); 6.04 (t, 2 H, 4-pz_{eq}); 5.73 (m, 1 H, 4-pz_{ax}); 2.55 (p, J = 4 Hz, 2 H, C₂H₄); 1.74 (q, J = 4 Hz, 2 H, C₂H₄); 2.23 (br q, J = 11 Hz, PCy₃); 2.5-0.8 (extremely broad envelope of PCy₃ resonances). ³¹P{¹H} (C₆D₆): -11.04 (s). IR: 2476 (ν_{B-H}). Anal. Calcd for C₂₉H₄₇BIrN₆P: C, 48.81; H, 6.64; N, 11.78. Found: C, 48.19; H, 6.46; N, 11.32.

TpIr(PiPr₃)(C₂H₄). Prepared as described for **2b**. ¹H NMR (C₆D₆): 7.95, 7.65 (d, 2 H each, 3,5-pz_{eq}); 7.33, 7.26 (in and d respectively, 1 H each, 3,5-pz_{ax}); 5.98 (t, 2 H, 4-pz_{eq}); 5.70 (m, 1 H, 4-pz_{ax}); 2.40, 1.70 (m, 2 H each, C₂H₄); 2.31 (m, 3 H, PCHMe₂); 1.04 (v br, 18 H, PCHMe₂). ³¹P{¹H} NMR (C₆D₆): -3.95 (s). IR: 2455 (ν_{B-H}).

TpIr(CN^tBu)₂. This complex was prepared on a small scale in a sealed NMR tube. Against a counterflow of Ar, CN^tBu (1.5 μL, 0.013 mmol) was added via syringe to an NMR tube containing a C₆D₆ solution of TpIr(C₂H₄)₂ (3.0 mg, 0.0065 mmol). The originally colorless solution was observed to become reddish, then orange, then bright yellow within a minute. Extensive decomposition was observed if the reaction was carried out in CD₂Cl₂. ¹H NMR (C₆D₆): 7.91, 7.70 (d, 3 H each, 3,5-pz); 6.06 (t, 3 H, 4-pz); 0.98 (s, 18 H, CN^tBu).

TpRh(PPh₃)H₂ (3a). To a 70-mL glass bomb containing TpRh(PPh₃)(C₂H₄) (51.9 mg, 0.086 mmol) and a teflon coated stir bar was vacuum transferred benzene (10 mL). The head space was backfilled with hydrogen (1220 torr) and the flask was warmed to room temperature and allowed to stir, protected from light for 16 h. The resulting pale yellow solution was transferred to a schlenk tube and the volume was reduced under vacuum. Addition of pentane affords off white crystals which were filtered off, washed with pentane, then dried under vacuum. Yield 45 mg (91%). A similar procedure, carried out using toluene as solvent and substituting D₂ in place of H₂ provided TpRh(PPh₃)D₂. ¹H NMR (C₆D₆): 7.92, 7.44 (br and m respectively, 1 H each, 3,5-pz_{ax}); 7.69-7.59 (m, 6 H, PPh₃); 7.56, 6.78 (d, 2 H each, 3,5-pz_{eq}); 6.99-6.93 (m, 9 H, PPh₃); 5.84 (m, 1 H, 4-pz_{ax}); 5.76 (t, 2 H, 4-pz_{eq}); -15.68 (dd, J_{Rh-H} = 18.3 Hz, J_{P-H} = 28.7 Hz, 2 H, Rh-H). ¹³C{¹H} NMR (C₆D₆): 145.8, 133.8 (s, 1 C, 3,5-pz_{ax}); 142.9, 134.5 (s, 2 C, 3,5-pz_{eq}); 135.7 (d, J_{P-C} = 48 Hz, i-C₆H₅); 134.5 (d, J_{P-C} = 11 Hz, o- or m-C₆H₅); 129.9 (d, J = 2 Hz, p-C₆H₅); 128.2 (partially obscured by C₆D₆, o- or

m-C₆H₅); 105.1 (s, 1 C, 4-pz_{ax}); 104.6 (s, 2 C, 4-pz_{eq}). ³¹P{aromatic ¹H} NMR (C₆D₆): 63.8 (dt, J_{Rh-P} = 149 Hz, J_{H-P} = 28 Hz). ¹H NMR (CD₂Cl₂): 7.70, 7.62 (br s and m respectively, 1 H each, 3,5-pz_{ax}); 7.65, 6.50 (d, 2 H each, 3,5-pz_{eq}); 7.44-7.25 (m, 15 H, PPh₃); 6.14 (m, 1 H, 4-pz_{ax}); 5.88 (t, 2 H, 4-pz_{eq}); -16.42 (dd, J_{Rh-H} = 18.9 Hz, J_{P-H} = 28.4 Hz, Rh-H). ¹³C{¹H} NMR (CD₂Cl₂): 145.7, 135.4 (s, 1 C each, 3,5-pz_{ax}); 142.9, 134.8 (s, 2 C each, 3,5-pz_{eq}); 135.1 (dd, J_{Rh-C} = 9.8 Hz, J_{P-C} = 47.7 Hz, i-C₆H₅); 134.4, 128.4 (d, J_{P-C} = 11 and 10 Hz respectively, o-, m-C₆H₅); 130.3 (s, p-C₆H₅); 105.3 (s, 1 C, 4-pz_{ax}); 104.7 (s, 2 C, 4-pz_{eq}). ³¹P{aromatic ¹H} (CD₂Cl₂): 62.3 (dt, J_{Rh-P} = 147 Hz, J_{P-H} = 28 Hz). IR: 2475 (ν_{B-H}); 2092, 2069 (ν_{Rh-H}). Anal. Calcd for C₂₇H₂₇BN₆PRh: C, 55.89; H, 4.69; N, 14.48. Found: C, 55.59; H, 4.83; N, 14.12.

TpIr(PPh₃)H₂ (3b). Prepared in toluene solution by a procedure identical to that employed for the Rh analog. Yield 95%. ¹H NMR (C₆D₆): 8.04, 7.35 (br s and m respectively, 1 H each, 3,5-pz_{ax}); 7.66-7.59 (m, 6 H, PPh₃); 7.49, 6.85 (d, 2 H each, 3,5-pz_{eq}); 6.99-6.95 (m, 9 H, PPh₃); 5.75 (m, 1 H, 4-pz_{ax}); 5.67 (t, 2 H, 4-pz_{eq}); -19.70 (d, 2 H, J_{P-H} = 23.1 Hz, Ir-H). ³¹P{aromatic ¹H} NMR (C₆D₆): 18.8 (t, J_{P-H} = 22.3 Hz). ¹H NMR (CD₂Cl₂): 7.83, 7.63 (br s and m respectively, 1 H each, 3,5-pz_{ax}); 7.66, 6.61 (d, 2 H each, 3,5-pz_{eq}); 7.39-7.24 (m, 15 H, PPh₃); 6.13 (m, 1 H, 4-pz_{ax}); 5.86 (t, 2 H, 4-pz_{eq}); -20.47 (d, J_{P-H} = 22.1 Hz, 2 H, Ir-H). ¹³C{¹H} NMR (CD₂Cl₂): 146.4, 134.8 (s, 1 C, 3,5-pz_{ax}); 143.3, 134.7 (s, 2 C, 3,5-pz_{eq}); 135.3 (d, J_{P-C} = 56 Hz, i-C₆H₅); 134.2, 128.2 (d, J_{P-C} = 10 Hz, o- and m-C₆H₅); 130.1 (s, p-C₆H₅); 106.0 (s, 1 C, 4-pz_{ax}); 105.2 (s, 2 C, 4-pz_{eq}). ¹³P{aromatic ¹H} (CD₂Cl₂): 16.9 (t, J_{P-H} = 22.0 Hz). IR: 2481 (ν_{B-H}); 2179, 2139 (ν_{Ir-H}). Anal. Calcd for C₂₇H₂₇BIrN₆P: C, 48.44; H, 4.07; N, 12.55. Found: C, 48.20; H, 4.01; N, 12.24.

TpIr(PiPr₃)H₂. This complex was prepared on a small scale in a sealed NMR tube upon addition of 1 atm of H₂ to a C₆D₆ solution of TpIr(PiPr₃)(C₂H₄). ¹H NMR

(C₆D₆): 7.94, 7.36 (br and m respectively, 1 H each, 3,5-pz_{ax}); 7.66, 7.57 (d, 2 H each, 3,5-pz_{eq}); 5.93 (t, 2 H, 4-pz_{eq}); 5.70 (t, 1 H, 4-pz_{ax}); 2.06 (sextet, J = 7.1 Hz, 3 H, CHMe₂); 1.06 (dd, J = 13.1 and 7.1 Hz, 18 H, CHMe₂); -21.67 (d, J_{P-H} = 22 Hz, Ir-H).

TpIr(PPh₃)(SnBu₃)H (4). Addition of SnBu₃H (19 μL, 0.071 mmol) to a pale yellow toluene (5 mL) solution of TpIr(PPh₃)(C₂H₄) (47.7 mg, 0.069 mmol) was observed to result in immediate bleaching to provide a clear colorless solution. The volatiles were then stripped under vacuum, leaving a colorless oil which was dissolved in pentane. Reducing the volume of the pentane solution and cooling to -30 °C failed to yield crystalline material. The pentane was subsequently stripped to give a sticky solid which was characterized by ¹H and ³¹P NMR and IR spectroscopy. ¹H NMR (C₆D₆): 8.18, 7.33 (br s, 1 H each, 3,5-pz trans to PPh₃); 7.51, 7.36, 7.04, 6.51 (d, 1 H each, 3,5-pz); 7.07-7.64 (m, 6 H, PPh₃); 7.02-6.96 (m, 9 H, PPh₃); 5.83 (m, 1 H, 4-pz trans to PPh₃); 5.79, 5.52 (t, 1 H each, 4-pz); 1.7-0.8 (complex m, SnBu₃); -19.97 (d with ^{117/119}Sn satellites, J_{P-H} = 21.6 Hz, J_{Sn-H} = 87 Hz, Ir-H). ³¹P{aromatic ¹H} (C₆D₆): 9.07 (d with ^{117/119}Sn satellites, J_{P-H} = 21 Hz, J_{Sn-P} = 143 Hz). IR: 2477 (ν_{B-H}); 2131 (ν_{Ir-H}).

TpIr(PPh₃)I₂. This complex was prepared on a small scale in an NMR tube by addition of I₂ to a CD₂Cl₂ solution of **2b**. ¹H NMR (CD₂Cl₂): 8.53, 7.62 (d and m respectively, 1 H each, 3,5-pz_{ax}); 7.72, 6.77 (d, 2 H each, 3,5-pz_{eq}); 7.54-7.39, 7.33-7.25 (m, 15 H, PPh₃); 6.29 (m, 1 H, 4-pz_{ax}); 5.88 (t, 2 H, 4-pz_{eq}). ³¹P{¹H} NMR (CD₂Cl₂): -30.8 (s).

TpIr(PMe₃)I₂. To a CH₂Cl₂ (15 mL) solution of TpIr(PMe₃)H₂ (192 mg, 0.397 mmol) was added N-iodosuccinimide (203 mg, 0.902 mmol) to form a bright yellow solution. This was allowed to stir under air overnight. The solution was concentrated under vacuum and methanol added to give bright yellow crystals, which were filtered off and washed with cold methanol (2 x 5 mL). Yield 214 mg (73%). ¹H NMR (CD₂Cl₂):

8.42, 7.63 (d and m respectively, 1 H each, 3,5-pz_{ax}); 8.10, 7.75 (d, 2 H each, 3,5-pz_{eq}); 6.29 (t, 2 H, 4-pz_{eq}); 6.26 (m, 1 H, 4-pz_{ax}); 1.79 (d, $J_{P-H} = 10.7$ Hz, PMe₃). ¹³C{¹H} NMR (CD₂Cl₂): 146.6, 135.5 (s, 3, 5-pz_{ax}); 145.4, 136.8 (s, 3,5-pz_{eq}); 106.6 (s, 4-pz_{eq}); 106.4 (s, 4-pz_{ax}); 17.9 (d, $J_{C-P} = 43$ Hz, PMe₃). ³¹P{¹H} NMR (CD₂Cl₂): -59.3 (s). IR: 2506 (ν_{B-H}). Anal Calcd. for C₁₂H₁₉BIrI₂N₆P: C, 19.61; H, 2.61; N, 11.43. Found: C, 19.77; H, 2.53; N, 11.35.

[TpIr(PPh₃)(C₂H₄)H]BF₄ (5). Against a flow of Ar, HBF₄•Et₂O (4 μL, 0.03 mmol) was syringed into a pale yellow CH₂Cl₂ (5 mL) solution of TpIr(PPh₃)(C₂H₄) (13.5 mg, 0.019 mmol). The resulting colorless solution was allowed to stir at room temperature for 10 min, then the volume was reduced under vacuum. Upon addition of Et₂O and cooling, a colorless flocculent precipitate was obtained, which was filtered off and dried under vacuum. Yield 8 mg (53 %). ¹H NMR (CD₂Cl₂): 8.02, 7.77, 7.73 (m), 7.38, 7.22, 6.79 (d, 1 H each, 3,5-pz); 7.62-7.54, 7.43, 7.12 (br m, 15 H, PPh₃); 6.39, 5.92 (t, 1 H each, 4-pz); 6.28 (m, 1 H, 4-pz trans to PPh₃); 3.78, 3.39 (m, 2 H each, C₂H₄); -14.64 (d, $J_{P-H} = 15.6$ Hz, 1 H, Ir-H). ³¹P{aromatic ¹H} NMR (CD₂Cl₂): -3.76 (d, $J_{P-H} = 15$ Hz). IR: 2508 (ν_{B-H}); 2226 (ν_{Ir-H}). Anal. Calcd for C₂₉H₃₀B₂F₄IrN₆P: C, 44.47; H, 3.86; N, 10.73. Found: C, 43.46; H, 3.77; N, 10.38.

TpIr(PCy₃)(O₂). This complex was prepared on a small scale in an NMR tube upon addition of 648 torr of O₂ to a C₆D₆ solution of TpIr(PCy₃)(C₂H₄) (t_{1/2} = 30 min). ¹H NMR (C₆D₆): 8.35, 7.32 (br, 1 H each, 3,5-pz_{ax}); 7.83, 7.41 (d, 2 H each, 3,5-pz_{eq}); 5.85 (m, 1 H, 4-pz_{ax}); 5.81 (t, 2 H, 4-pz_{eq}); 2.29-0.86 (complex m, PCy₃).

TpIr(PiPr₃)(O₂). This complex was prepared on a small scale in an NMR tube upon addition of 300 torr of O₂ to a C₆D₆ solution of TpIr(PiPr₃)(C₂H₄) (t_{1/2} = 50 min). Reactions conducted in CD₂Cl₂ were observed to yield decomposition products. ¹H NMR (C₆D₆): 8.29, 7.29 (m, 1 H each, 3,5-pz_{ax}); 7.78, 7.41 (d, 2 H each, 3,5-pz_{eq});

5.80 (m, 1 H, 4-pz_{ax}); 5.78 (t, 2 H, 4-pz_{eq}); 2.27 (m, 3 H, PCHMe₂); 1.20 (dd, J = 7.1 and 13.1 Hz, 18 H, PCHMe₂).

TpIr(C₂H₅)(C₂H₄)H. This complex was prepared on a small scale in C₆D₆ or methylcyclohexane-*d*₁₄ or CD₂Cl₂ solutions and observed by ¹H NMR spectroscopy. The cleanest reactions were observed in methylcyclohexane-*d*₁₄. Extensive H-D exchange was observed in C₆D₆. The head space of an NMR tube containing a frozen solution of TpIr(C₂H₄)₂ was back filled with 780 torr of H₂, then cooled with a dewar of N₂(l) and flame sealed. Samples were carefully warmed to room temperature and shaken. The insertion product was observed to form over *ca.* 20 h. Further reaction times gave increasing amounts of unidentified decomposition products. ¹H NMR (methylcyclohexane-*d*₁₄, referenced to H₂ at 4.6 ppm): 7.89, 7.69, 7.59, 7.55, 7.48, 7.05 (d, 1 H each, 3,5-pz); 6.17, 6.13, 5.99 (t, 1 H each, 4-pz); 2.96, 2.85 (m, 2 H each, C₂H₄); 1.10, 0.86 (m, 1 H each CH₂CH₃); 0.90 (t, 3 H, CH₂CH₃); -16.46 (s, 1 H, Ir-H).

[TpIr(C₂H₄)₂I]I. This complex was prepared on a small scale in an NMR tube upon addition of I₂ to a CD₂Cl₂ solution of TpIr(C₂H₄)₂. ¹H NMR (CD₂Cl₂): 8.18 (d, 2 H, 3,5-pz); 7.75 (d, 3 H, overlapping 3,5pz); 7.22 (d, 1 H, 3,5-pz); 6.38 (t, 2 H, 4-pz); 6.31 (t, 1 H, 4-pz); 4.11, 3.99 (br, 4 H each, C₂H₄).

Fluxionality. The activation barrier for the exchange of axial and equatorial pyrazolyl ligands in **2a** was determined by monitoring the resonances of 4-pz as a function of temperature. At room temperature a single sharp triplet integrating to three protons is observed at 5.82 ppm. This peak decoalesces at 279 K (300 MHz) into two separate resonances at 5.83 (t, 2 H) and 5.77 ppm (m, 1 H). Using the method of Shanan-Atidi and Bar-Eli²² for analysis of exchange between unequal populations, an activation energy of exchange was calculated using eq 2.11, where k_B = Boltzmann's

constant, h = Planck's constant, T_c = temperature of coalescence (K), δ_v = chemical shift difference in the static spectrum (Hz), $X = 2\pi\delta_v\tau$ (note $1/\tau = (1/\tau_{eq}) + (1/\tau_{ax})$ where τ_{eq} and τ_{ax} are the lifetimes of the equatorial and axial sites, respectively), and ΔP = difference in mole fractions of the exchanging nuclei. For this problem the ratio of

$$\Delta G^\ddagger = RT \ln \left[\frac{k_B}{h\pi} \left(\frac{T_c}{\delta_v} \right) \left(\frac{X}{1 + \Delta P} \right) \right] \quad (2.11)$$

equatorial to axial protons is always 2:1, so that ΔP equals 1/3 (i.e. 2/3 - 1/3). X is evaluated as 2.0823 from Table 6.1 of Sandström's text.⁵⁶ The lower limit of pyrazolyl site exchange for **2b** was calculated using the same equation and the limiting chemical shifts at the highest temperature of 353 K.

The lower limit for the barrier to ethylene rotation was calculated using eqn 2.12.

$$\Delta G^\ddagger = -RT \ln \left(\frac{kh}{k_B T} \right) \quad (2.12)$$

The upper limit for the rotational rate constant (k) used in this equation was determined by simulation of the experimental spectra at the highest temperature of 353 K, using a modified version of the DYNAMAR program. For **2a** and **2b**, k is less than 4 and 1 s⁻¹, respectively.

Kinetic Studies Kinetic experiments were carried out by monitoring the ¹H NMR spectrum of **2b** under H₂(D₂) in CD₂Cl₂ on an Bruker AF-300 spectrometer. For a given set of experimental conditions a spectrum was acquired every four minutes under computer control for a total of 20 data points (> 3 half lives). Each FID is the sum of 24 scans collected in 60 s (AQ + D1 = 2.5 s). Following data collection, an FID was then written to disk and a delay of 180 s followed, before the next acquisition. The first

FID of each data set was fourier transformed (FT) and phased. The rest of the files in the data set were then transformed using an AUTOFT routine using the phasing and intensity parameters from the first spectrum. This method allowed an absolute comparison of integral intensities from spectrum to spectrum within one kinetic run. The disappearance of **2b** was followed by monitoring the 4-pz_{eq} resonance at 5.93 ppm. The formation of **3b** was followed by monitoring the 4-pz_{eq} resonance at 5.86 ppm. A standard solution of **2b** (3.51×10^{-3} M) was prepared in the glove box. Aliquots (0.5 ml) were then transferred to NMR tubes equipped with Kontes valve vacuum line adaptors. Using a high vacuum line, the samples were degassed with three freeze-pump-thaw cycles before adding H₂ (or ethylene). The samples remained frozen in liquid nitrogen during H₂ addition. The pressure of H₂ above the sample was measured using an Omega series 136 mV transducer equipped with an Omega model DP2000 digital indicator. The Kontes valve was then closed and the tube immersed in liquid nitrogen one inch below the point where the sample was flame sealed. Samples containing ethylene were prepared by first condensing 0.04 mmol of ethylene (calculated from known pressures and volumes) into a frozen degassed sample at 77 K. H₂ was then added and flame sealed as described above. A side reaction between **2b** and PPh₃ (see chapter 4) required that samples with PPh₃ be prepared in a slightly different fashion. These were prepared by addition of solid **2b** and PPh₃ (10 equiv.) to an NMR tube equipped with a Kontes valve vacuum line adapter. CD₂Cl₂ (0.45 mL) was vacuum transferred to the NMR tube and the head space backfilled with 750 torr H₂. All samples were stored at 77 K until immediately before each kinetic run. The samples were run sequentially by thawing to room temperature (time zero), shaking vigorously for 60 s, then inserting into the NMR probe. Acquisition of the first FID commenced within 3-5 minutes of time zero. The concentration of H₂ was measured for a standard CD₂Cl₂ sample under 750 torr H₂. The concentration of H₂ at lower pressures was

calculated assuming Henry's law. Integration of the H₂ resonance against a ferrocene standard indicated an H₂ (750 torr) concentration of 1.7×10^{-3} M. Correcting for the fact that *ca.* 25% of H₂ at room temperature is composed of an NMR silent spin isomer, i.e. para H₂,⁵⁷ the true concentration is 2.3×10^{-3} M. The solubility of D₂ was assumed to be identical. This is close to the literature value published for CHCl₃ (2.7×10^{-3} M).⁵⁸ Pignolet has previously noted that the concentration of H₂ determined by solution NMR methods⁵⁹ is significantly smaller than published values.^{58,60} ¹H NMR determinations of H₂ concentration will systematically underestimate the true H₂ concentration as a function of the ortho/para H₂ ratio, which is temperature dependent.⁶¹ Even under the lowest H₂ pressures employed in this study, the total number of moles of H₂ was always at least 20 fold excess. If diffusion of H₂ from the head space into the solution is faster than reaction with **2b**, then pseudo first order kinetics are expected. When $[\mathbf{2b}]_i = 3.51 \times 10^{-3}$ M and the H₂ pressure is 750 torr these conditions were satisfied (fig 2.3). At lower H₂ pressures significant curvature was observed, indicating a diffusion limited reaction.⁶² For these data runs, k_{obs} was calculated from the initial rate using the first 4 to 5 data points. The error in k_{obs} is estimated to be $\pm 10\%$ based on reproducibility of the values.

Notes to Chapter 2.

- (1) Substitution of the Tp ligand is represented by superscripts as suggested by Trofimenko. For example, methyl substituents in the 3, 5-positions are indicated as, $\text{Tp}^{\text{Me}2}$. For a comprehensive review of this class of complexes see: Trofimenko, S. *Chem. Rev.* **1993**, *93*, 943-980.
- (2) O'Sullivan, D. J.; Lalor, F. J. *J. Organometal. Chem.* **1974**, *65*, 47-C49.
- (3) Cocivera, M.; Desmond, T. J.; Ferguson, G.; Kaitner, B.; Lalor, F. J.; O'Sullivan, D. J. *Organometallics* **1982**, *1*, 1125-1132.
- (4) Cocivera, M.; Ferguson, G.; Lalor, F. J.; Szczecinski, P. *Organometallics* **1982**, *1*, 1139-1142.
- (5) Ghosh, C. K.; Rodgers, D. P. S.; Graham, W. A. G. *J. Chem. Soc., Chem. Commun.* **1988**, 1511-1512.
- (6) Ball, R. G.; Ghosh, C. K.; Hoyano, J. K.; McMaster, A. D.; Graham, W. A. G. *J. Chem. Soc., Chem. Commun.* **1989**, 341-342.
- (7) Jones, W. D.; Hessel, E. T. *Inorg. Chem.* **1991**, *30*, 778-783.
- (8) Ciriano, M. A.; Fernández, M. J.; Modrego, J.; Rodríguez, M. J.; Oro, L. A. *J. Organometal. Chem.* **1993**, *443*, 249-252.
- (9) Bucher, U. E.; Currao, A.; Nesper, R.; Rüegger, H.; Venanzi, L. M.; Younger, E. *Inorg. Chem.* **1995**, *34*, 66-74.
- (10) Bucher, U. E.; Fässler, T. F.; Hunziker, M.; Nesper, R.; Rüegger, H.; Venanzi, L. M. *Gazz. Chim. Ital.* **1995**, *125*, 181-188.
- (11) Rheingold, A. L.; Ostrander, R. L.; Haggerty, B. S.; Trofimenko, S. *Inorg. Chem.* **1994**, *33*, 3666-3676.
- (12) Cocivera, M.; Ferguson, G.; Kaitner, B.; Lalor, F. J.; O'Sullivan, D. J.; Parvez, M.; Ruhl, B. *Organometallics* **1982**, *1*, 1132-1139.
- (13) Trofimenko, S. *J. Am. Chem. Soc.* **1969**, *91*, 588-595.

- (14) Tanke, R. S.; Crabtree, R. H. *Inorg. Chem.* **1989**, *28*, 3444-3447.
- (15) Fernández, M. J.; Rodríguez, M. J.; Oro, L. A.; Lahoz, F. J. *J. Chem. Soc., Dalton Trans.* **1989**, 2073-2079.
- (16) Fernandez, M. J.; Rodríguez, M. J.; Oro, L. A. *Polyhedron* **1991**, *10*, 1595-1598.
- (17) Collman, J. P.; Hegedus, L. S.; Norton, J. R.; Finke, R. G. *Principles and Application of Organotransition Metal Chemistry*; University Science Books: Mill Valley, CA, 1987.
- (18) Crabtree, R. H. *The Organometallic Chemistry of the Transition Metals*; 2nd ed.; John Wiley & Sons: New York, 1994.
- (19) Pérez, P. J.; Poveda, M. L.; Carmona, E. *Angew. Chem. Int. Ed. Engl.* **1995**, *34*, 231-233.
- (20) Paneque, M.; Taboada, S.; Carmona, E. *Organometallics* **1996**, *15*, 2678-2679.
- (21) Paneque, M.; Poveda, M. L.; Rey, L.; Taboada, S.; Carmona, E.; Ruiz, C. *J. Organometal. Chem.* **1995**, *504*, 147-149.
- (22) Shanan-Atidi, H.; Bar-Eli, K. H. *J. Phys. Chem.* **1970**, *74*, 961-963.
- (23) Cramer, R.; Kline, J. B.; Roberts, J. D. *J. Am. Chem. Soc.* **1969**, *91*, 2519-2524.
- (24) Szajek, L. P.; Lawson, R. J.; Shapley, J. R. *Organometallics* **1991**, *10*, 357-361.
- (25) Bell, T. W.; Huddleton, D. M.; McCamley, A.; Partridge, M. G.; Perutz, R. N.; Willner, H. *J. Am. Chem. Soc.* **1990**, *112*, 9212-9226.
- (26) Albright, T. A.; Hoffmann, R.; Thibeault, J. C.; Thorn, D. L. *J. Am. Chem. Soc.* **1979**, *101*, 3801-3812.
- (27) Rossi, A. R.; Hoffmann, R. *Inorg. Chem.* **1975**, *14*, 365-374.
- (28) Segal, J. A.; Johnson, B. F. G. *J. Chem. Soc., Dalton Trans.* **1975**, 677-681.
- (29) Lundquist, E. G.; Folting, K.; Streib, W. E.; Huffman, J. C.; Eisenstein, O.; Caulton, K. G. *J. Am. Chem. Soc.* **1990**, *112*, 855-863.
- (30) Paonessa, R. S.; Trogler, W. C. *J. Am. Chem. Soc.* **1982**, *104*, 1138-1140.

- (31) Emsley, J. *The Elements*; Oxford University Press: New York, 1989.
- (32) Heinekey, D. M.; Oldham, W. J., Jr. *J. Am. Chem. Soc.* **1994**, *116*, 3137-3138.
- (33) Paneque, M.; Poveda, M. L.; Toboada, S. *J. Am. Chem. Soc.* **1994**, *116*, 4519-4520.
- (34) Bovens, M.; Gerfin, T.; Gramlich, V.; Petter, W.; Venanzi, L. M.; Haward, M. T.; Jackson, S. A.; Eisenstein, O. *New. J. Chem.* **1992**, *16*, 337-345.
- (35) Ferrari, A.; Polo, E.; Rügger, H.; Sostero, S.; Venanzi, L. M. *Inorg. Chem.* **1996**, *35*, 1602-1608.
- (36) Cramer, R. *J. Am. Chem. Soc.* **1972**, *94*, 5681-5685.
- (37) Cramer, R.; Seiwel, L. P. *J. Organometal. Chem.* **1975**, *92*, 245-252.
- (38) Lawson, R. J. Thesis, University of Illinois, 1978.
- (39) Batchelor, R. J.; Einstein, F. W. B.; Lowe, N. D.; Palm, B. A.; Yan, X.; Sutton, D. *Organometallics* **1994**, *13*, 2041-2052.
- (40) Meakin, P.; Trofimenko, S.; Jesson, J. P. *J. Am. Chem. Soc.* **1972**, *94*, 5677-5681.
- (41) Manzer, L. E.; Meakin, P. Z. *Inorg. Chem.* **1976**, *15*, 3117-3120.
- (42) Reger, D. L.; Tarquini, M. E. *Inorg. Chem.* **1983**, *22*, 1064-1068.
- (43) Steyn, M. M. d. V.; Singleton, E.; Hietkamp, S.; Liles, D. C. *J. Chem. Soc., Dalton Trans.* **1990**, 2991-2997.
- (44) Berry, R. S. *J. Chem. Phys.* **1960**, *32*, 933-938.
- (45) Ugi, I.; Marquarding, D.; Klusacek, H.; Gillespie, P. *Acc. Chem. Res.* **1971**, *4*, 288-296.
- (46) Ghosh, C. K.; Hoyano, J. K.; Krentz, R.; Graham, W. A. G. *J. Am. Chem. Soc.* **1989**, *111*, 5480-5481.
- (47) Schuster-Woldan, H. G.; Basolo, F. *J. Am. Chem. Soc.* **1966**, *88*, 1657-1663.

- (48) James, B. R. *Homogeneous Hydrogenation*; John Wiley & Sons: New York, 1973.
- (49) A monodentate Tp^{t-butyl} complex has recently been structurally characterized: Gutiérrez, E.; Hudson, S. A.; Monge, A.; Nicasio, M. C.; Paneque, M.; Carmona, E. *J. Chem. Soc., Dalton Trans.* **1992**, 2651-2653.
- (50) Johnson, C. E.; Eisenberg, R. *J. Am. Chem. Soc.* **1985**, *107*, 3148-3160.
- (51) Trofimenko, S. *Inorg. Synth.* **1979**, *12*, 99.
- (52) Kauffman, G. B.; Myers, R. D. *Inorg. Synth* **1978**, *18*, 131-133.
- (53) Gordon, A. J.; Ford, R. A. *The Chemist's Companion*; John Wiley & Sons: New York, 1972, pp 303.
- (54) Cramer, R. *Inorg. Synth.* **1973**, *15*, 14-16.
- (55) Onderdelinden, A. L. *Inorg. Synth* **1974**, *15*, 18.
- (56) Sandström, J. *Dynamic NMR Spectroscopy*; Academic Press: London, 1982.
- (57) Abragam, A. *Principles of Nuclear Magnetism*; Oxford University Press: Oxford, 1983.
- (58) *Solubility Data Series, Hydrogen and Deuterium*; Young, C. L., Ed.; Pergamon Press: New York, 1981; Vol. 5/6.
- (59) Aubart, M. A.; Chandler, B. D.; Gould, R. A. T.; Krogstad, D. A.; Schoondergang, M. F. J.; Pignolet, L. H. *Inorg. Chem.* **1994**, *33*, 3724-3734.
- (60) Fogg, P. G. T.; Gerrand, W. *Solubility of Gases in Liquids*; John Wiley & Sons: New York, 1991.
- (61) An interesting and mechanistically useful consequence of hydrogen spin state isomerism has been recognized by Eisenberg. Eisenberg, R. *Acc. Chem. Res.* **1991**, *24*, 110-116.
- (62) Sun, Y.; Landau, R. N.; Wang, J.; Le Blonde, C.; Blackmond, D. G. *J. Am. Chem. Soc.* **1996**, *118*, 1348-1353.

CHAPTER 3

SYNTHESIS AND NMR PROPERTIES OF DIHYDROGEN-HYDRIDE COMPLEXES OF RHODIUM AND IRIDIUM STABILIZED BY HYDRIDOTRIS(1-PYRAZOLYL)BORATE COLIGANDS

Since the first report of a stable molecular hydrogen complex by Kubas¹, the possibility that a fluxional polyhydride complex might also contain a dihydrogen ligand has been actively investigated.² For example, Crabtree and coworkers have employed ¹H NMR T₁ measurements to detect short H-H contacts in complexes such as [Ir(PCy₃)₂H₆]⁺.³ In this case a very short T₁(193 K) value of *ca.* 50 ms (250 MHz) was interpreted as evidence for the presence of at least one and possibly two dihydrogen ligands in the polyhydride coordination sphere. In contrast, a long T₁(193 K) value of 820 ms was obtained for the neutral pentahydride complex, Ir(PCy₃)₂H₅, consistent with a pentagonal bipyramidal structure which is also observed in the solid state by single crystal neutron diffraction analysis. In fluxional polyhydride complexes, it is often found that only one hydride resonance can be observed in the ¹H NMR spectrum, even at very low temperatures. When this situation occurs, structural characterization in solution depends upon indirect methods, in which the observed NMR parameters are a population weighted average of all the hydride environments. Important publications from the research groups of Crabtree,³ Halpern⁴ and Morris⁵ have described a quantitative treatment of hydride relaxation in polyhydride complexes which allows useful structural information to be obtained from T₁ (min) data. An introduction to this treatment is found in chapter 1.

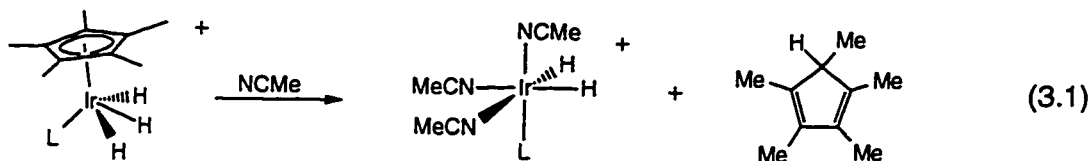
Heinekey and coworkers have previously reported the structure and properties of cationic iridium complexes of the form [CpIr(L)H₃]BF₄ (L = various PR₃), which have been shown to adopt iridium (V) trihydride structures in the solid state.^{6,7} These

complexes undergo a rapid hydride rearrangement which leads to a single hydride resonance in the ^1H NMR spectrum above *ca.* 220 K. At very low temperatures, spectra consistent with the solid state structure are obtained.

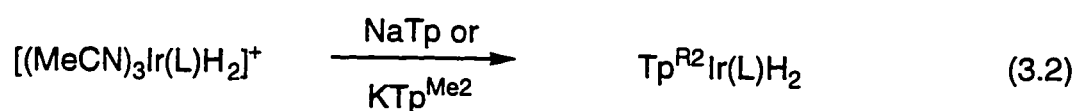
In this chapter we investigate the effect of substituting the Cp ligand of $[\text{CpIr}(\text{L})\text{H}_3]\text{BF}_4$ complexes with the hydridotris(1-pyrazolyl)borate (Tp) ligand.⁸ The new Tp complexes, $[\text{TpIr}(\text{L})(\text{H}_2)\text{H}]\text{BF}_4$ ($\text{L} = \text{PMe}_3$ and PPh_3) are formulated as dihydrogen-hydride complexes, although only a single hydride resonance is observed in the ^1H NMR spectrum at all accessible temperatures. We have also obtained spectroscopic evidence for the thermally labile rhodium complex $[\text{TpRh}(\text{PPh}_3)(\text{H}_2)\text{H}]\text{B}(\text{Ar})_4$ ($\text{Ar} = 3,5\text{-(CF}_3)_2\text{C}_6\text{H}_3$). The dihydrogen-hydride formulation for the rhodium and iridium complexes is supported by short T_1 (min) values of 7 ms (Rh) and 21-22 ms (Ir). Incorporation of deuterium or tritium in the hydride positions of the iridium complexes results in large temperature dependent isotope shifts in the ^1H and ^3H NMR spectra, which are attributed to isotopic perturbation of equilibria. A similar isotope effect is not observed for the rhodium complex. In this chapter, we show that these isotope effects arise from non-statistical occupation of different hydride sites and can be used to obtain structural information. Some aspects of the iridium chemistry have been previously communicated.⁸

Results

Synthesis. We have prepared complexes of the form $\text{TpIr}(\text{L})\text{H}_2$ ($\text{L} = \text{PMe}_3$ or PPh_3) by two methods. The first approach was developed following a report of an unusual pentamethylcyclopentadienyl (Cp^*) displacement reaction by Pederson and Tilset.⁹ These workers found that $[\text{Cp}^*\text{Ir}(\text{PPh}_3)\text{H}_3]\text{BF}_4$ reacts in acetonitrile to form $[(\text{MeCN})_3\text{Ir}(\text{PPh}_3)\text{H}_2]\text{BF}_4$ and free Cp^*H . We have found that the related PMe_3 complex, $[\text{Cp}^*\text{Ir}(\text{PMe}_3)\text{H}_3]\text{SO}_3\text{CF}_3$ also reacts in acetonitrile to form $[(\text{MeCN})_3\text{Ir}(\text{PMe}_3)\text{H}_2]\text{SO}_3\text{CF}_3$ (eq 3.1). The three MeCN ligands of the new complexes



are easily displaced under mild conditions by the pyrazolyl arms of the Tp ligand to form TpIr(L)H₂ complexes (L = PMe₃ (**1**) and PPh₃(**2**)). These reactions are conveniently carried out in one pot by generating the tris-acetonitrile intermediate *in situ*, then adding one equiv. of NaTp in a second step. The procedure has also been used to prepare Tp^{Me₂}Ir(PMe₃)H₂ (**3**) upon addition of KTp^{Me₂} to an acetonitrile solution of [(MeCN)₃Ir(PMe₃)H₂]⁺ (eq 3.2). Complexes **1** - **3** are observed by ¹H and ³¹P NMR analysis to form in *ca.* 85% yield over several hours when reactions are carried out in sealed NMR tubes in CD₃CN solutions. The yields are reduced by the formation of a second complex which has not yet been identified. The impurity persists even when a CD₂Cl₂ solution of the product mixture was heated to 65° C for several hours. Complexes **1** -**3** are stable to air and water and can be purified by chromatography on alumina, eluting with toluene. Isolated yields are typically 55-70%. The dihydride complexes are colorless, thermally stable, and crystalline and are readily identified by their appropriate analytical and spectroscopic data, which are detailed in the experimental section. Selected spectroscopic data are reported in Table 3.1.

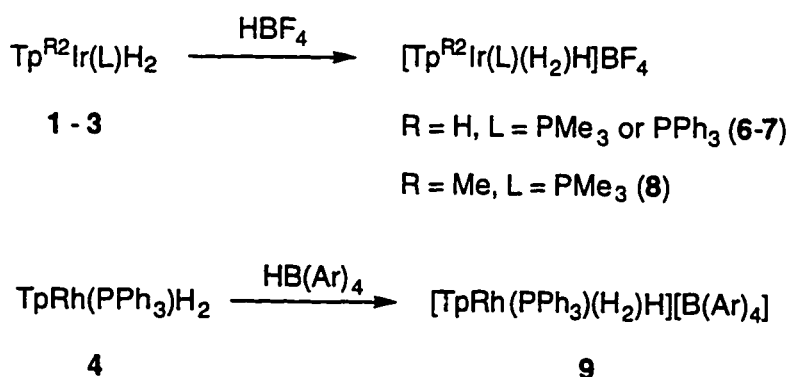


R = H, L = PMe₃ (**1**); R = H, L = PPh₃ (**2**); R = Me, L = PMe₃ (**3**)

We have developed an alternative approach to these dihydride complexes using the reaction of phosphine ligands with TpM(C₂H₄)₂ (M = Rh, Ir) (Chapter 2). The

resulting $\text{TpM}(\text{PR}_3)(\text{C}_2\text{H}_4)$ complexes react with hydrogen to afford the dihydride complexes in very good yield. For example $\text{TpRh}(\text{PPh}_3)\text{H}_2$ (**4**) has been prepared using this method. We have also found that the cationic tris(1-pyrazolyl)methane (tpm) complex, $[(\text{tpm})\text{Ir}(\text{PPh}_3)\text{H}_2]\text{BF}_4$ (**5**) may be prepared in this fashion from the new $[(\text{tpm})\text{Ir}(\text{C}_2\text{H}_4)_2]\text{BF}_4$ complex (Chapter 4).

Addition of one equiv. of $\text{HBF}_4 \cdot \text{Et}_2\text{O}$ to CD_2Cl_2 solutions of **1** - **3** at ambient temperature or below affords new complexes without elimination of H_2 (scheme 3.1). The Tp^{Me_2} complex decomposes at room temperature over the course of several hours, however its lifetime in solution can be extended considerably if the protonation reaction is carried out with $[\text{H}(\text{Et}_2\text{O})_2][\text{B}(\text{Ar})_4]$ ($\text{Ar} = 3,5\text{-(CF}_3)_2\text{C}_6\text{H}_3$). Similarly **4** decomposes immediately at 210 K to a complex mixture of products upon addition of $\text{HBF}_4 \cdot \text{Et}_2\text{O}$. Reactions carried out with $[\text{H}(\text{Et}_2\text{O})_2][\text{B}(\text{Ar})_4]$ yield $[\text{TpRh}(\text{PPh}_3)(\text{H}_2)\text{H}][\text{B}(\text{Ar})_4]$ (**9**), which is stable in solution to 250 K. Complex **5** was not observed to react with excess $\text{HBF}_4 \cdot \text{Et}_2\text{O}$ or HSO_3CF_3 in CD_2Cl_2 . However, significant broadening of the hydride resonance of **5** in the ^1H NMR spectrum may indicate a hydrogen exchange process via a small population of the dicationic $[(\text{tpm})\text{Ir}(\text{PPh}_3)(\text{H}_2)\text{H}](\text{BF}_4)_2$ complex. The iridium complexes $[\text{TpIr}(\text{L})(\text{H}_2)\text{H}]\text{BF}_4$ ($\text{L} = \text{PMe}_3$ (**6**) and PPh_3 (**7**)) were found to be thermally stable and could be isolated as colorless salts upon addition of $\text{HBF}_4 \cdot \text{Et}_2\text{O}$ to Et_2O or $\text{Et}_2\text{O}/\text{CH}_2\text{Cl}_2$ solutions of the parent dihydride complexes.



Scheme 3.1

General Spectroscopic Characterization. Selected data for the new cationic hydride complexes are presented in Table 3.1. Complexes **6-9** exhibit a 2:1 pattern of Tp resonances in the ^1H and ^{13}C NMR spectra which is characteristic of a structure with C_5 symmetry. In all cases this pattern is unchanged upon cooling to 180 K. An appropriate resonance for the respective hydride ligands is observed at high field near -10.4 ppm in the ^1H NMR spectra of **6-8**. A similar resonance at -7.95 ppm is observed for the rhodium complex **9**. Generally these resonances are broad with no distinguishing features. However, in the case of complex **6**, the hydride resonance is a doublet with P-H coupling of 11 Hz. A total of three hydride ligands (no structure implied) is confirmed by the observation of a quartet for the PMe_3 resonance in the $^{31}\text{P}\{\text{Me } ^1\text{H}\}$ NMR spectrum at

Table 3.1 Selected Spectroscopic Data for New Hydride Complexes

Complex	^1H NMR (300 MHz, CD_2Cl_2)			IR (Nujol)	
	$\delta_{\text{M-H}}$ (ppm)	$J_{\text{P-H}}$ (Hz)	$T_1(\text{min})$ (ms)	$\nu_{\text{B-H}}$ (cm^{-1})	$\nu_{\text{I-H}}$ (cm^{-1})
1	-21.30	25.0	542 ^a	2482	2142
2	-20.47	22.1	359 ^b	2481	2179, 2139
3	-22.11	26.7	c	2511	2138
4	-16.42	28.4 ^d	304 ^e	2475	2092, 2069
5	-20.93	23.3	c	c	c
6	-10.40	11	21 ^f	2499	2199
7	-9.77	g	22 ^e	2502	2197
8	-11.0	g	c	c	c
9	-7.95	g	7 ^e	c	c

^a177 K. ^b201 K. ^cnot measured. ^d $J_{\text{Rh-H}} = 18.9$ Hz. ^e195 K. ^f182 K. ^gnot resolved.

-42.7 ppm ($J_{P-H} = 10$ Hz). For complex **6** a sharp IR absorption at 2199 cm^{-1} is attributed to an Ir-H stretch and a band at 2499 cm^{-1} is assigned to the B-H stretch. Similar observations were made for **7**. The minimum of the longitudinal relaxation time (T_1) is found to be 21-22 ms for **6** and **7**, but is 7 ms for **9**. These short T_1 (min) measurements indicate that **6-9** are best formulated as dihydrogen-hydride complexes. A facile fluxional process renders the hydride ligands equivalent on the NMR timescale. This process accounts for the apparent C_s symmetry indicated by the pattern of Tp resonances.

NMR Observations for Partially Deuterated Complexes. Deuteration of the hydride positions is observed over the course of several hours at room temperature upon exposure of solutions of **6-8** to an atmosphere of D_2 . A mixture of well resolved H_3 , H_2D , and HD_2 isotopomers is observed by 1H NMR spectroscopy. Large temperature dependent *downfield* isotope shifts are noted for the hydride resonances of the deuterated complexes. A representative spectrum of the hydride region for complex **6** acquired with ^{31}P decoupling at 240 K is shown in Figure 3.1. The resonances of the Tp and phosphine ligands are unaffected by deuteration of the hydride positions and show no unusual temperature dependence. The isotope shifts for **6**, $\Delta_1 = \delta(H_2D) - \delta(H_3)$ and $\Delta_2 = \delta(HD_2) - \delta(H_2D)$, vary from +228 and +122 ppb at 215 K to +149 and +72 ppb at 280 K, respectively. Over a similar temperature range, the observed H-D coupling of the hydride resonance varies from *ca.* 6.9 to 7.6 Hz for **6- d_1** and from *ca.* 8.8 to 8.7 Hz for **6- d_2** . At the lowest temperatures (< 215 K) the apparent J_{H-D} coupling is reduced due to significant line broadening caused by efficient nuclear relaxation. At 275 K and above line broadening due to intermolecular proton exchange results in unreliable H-D coupling constant measurements. These observations are graphically illustrated in Figures 3.2 and 3.3. Very similar temperature dependent isotope shifts and H-D coupling constants are observed for **7** and **8**. The hydride resonances of the H_2D and HD_2 isotopomers of **7** are significantly broadened compared to **6** and **8**, so that the J_{H-D} coupling constants could

not be accurately measured in this case. However, based on the total width of the hydride peaks, the $J_{\text{H-D}}$ coupling constants of **7** is similar to those measured for **6** and **8**. Data for these complexes acquired at 240 K are summarized in Table 3.2.

The hydride resonance of the H_2D isotopomer appears as a distorted 1:1:1 triplet in which the height of the two outer lines are slightly reduced in intensity (see Figure 3.1). Similarly the HD_2 isotopomer appears as a distorted 1:2:3:2:1 five line pattern, in which the outer lines are also slightly reduced in intensity. This distortion may be due to unusually efficient relaxation of the quadrupolar deuterium nucleus (*vide infra*).^{10,11}

Complex **9** fails to exchange with D_2 under the low temperature conditions at which it is stable. In this case, partial deuteration of the hydride positions was accomplished by reacting $\text{TpRh}(\text{PPh}_3)_2$ with one equiv. of $[\text{H}(\text{Et}_2\text{O})_2][\text{B}(\text{Ar})_4]$ at low temperature. The hydride positions are estimated to contain *ca.* 55% deuterium by integration of the hydride resonance against the Tp resonances in the ^1H NMR spectrum (one scan). A broad featureless hydride resonance at the same chemical shift as the undeuterated complex is observed for the mixture of **9**, **9- d_1** and **9- d_2** . The linewidth of the hydride resonance upon deuteration is slightly reduced from 75 Hz to 63 Hz (300 MHz, 210 K). The chemical shift of this resonance shows no significant temperature dependence.

A CDCl_2F solution composed principally of **6- d_2** was investigated at low temperature by ^1H NMR spectroscopy. As the temperature was lowered the hydride resonance of the HD_2 isotopomer continued to shift downfield, however no evidence for decoalescence of this resonance was observed to 127 K. At this temperature the HD_2 resonance is observed at -9.64 ppm. Although the hydride resonance of the H_3 isotopomer cannot be observed at this temperature due to efficient dipolar relaxation, we estimate its chemical shift to be *ca.* -10.3 ppm. The isotope shift, $\delta(\text{HD}_2) - \delta(\text{H}_3)$ at this temperature is then *ca.* 660 ppb.

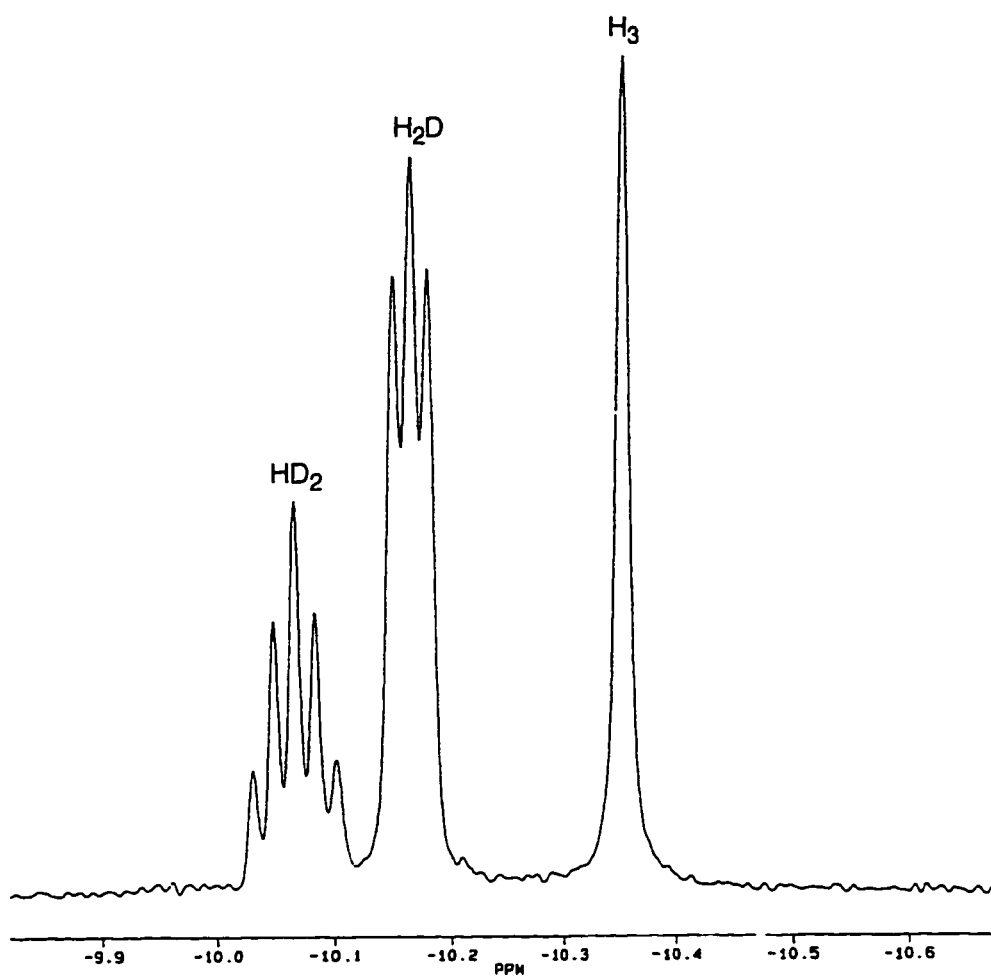


Figure 3.1 High field region of the $^1\text{H}\{^{31}\text{P}\}$ NMR spectrum (CD_2Cl_2 , 500 MHz, 240 K) of a partially deuterated sample of $[\text{TpIr}(\text{PMe}_3)(\text{H}_2)\text{H}]\text{BF}_4$ (**6**). The chemical shifts and $J_{\text{H-D}}$ coupling constants are given in Table 3.2.

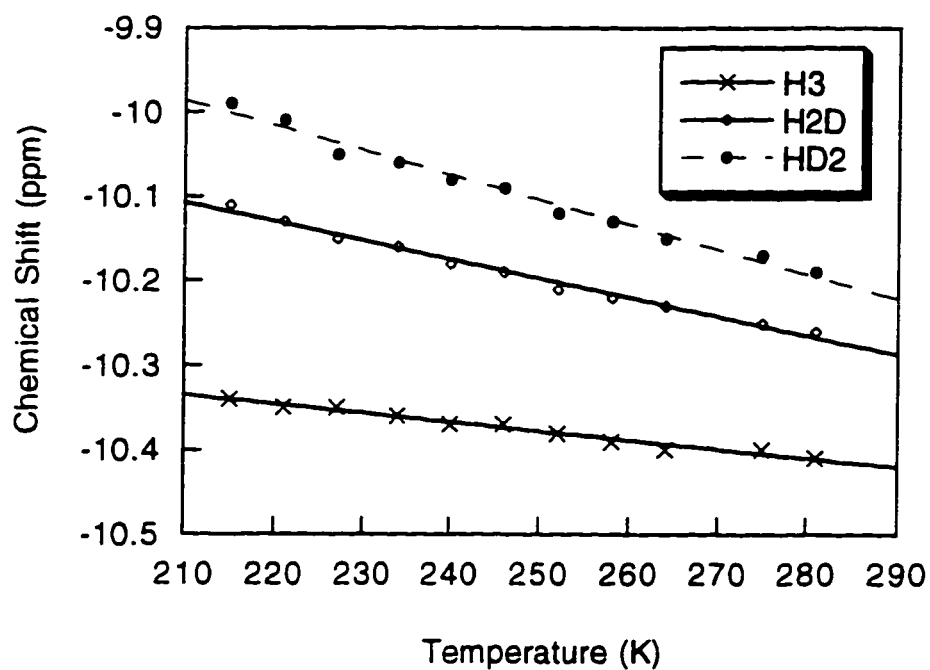


Figure 3.2 Plot of chemical shift of the hydride resonance in **6**, **6-d₁** and **6-d₂** as a function of observation temperature.

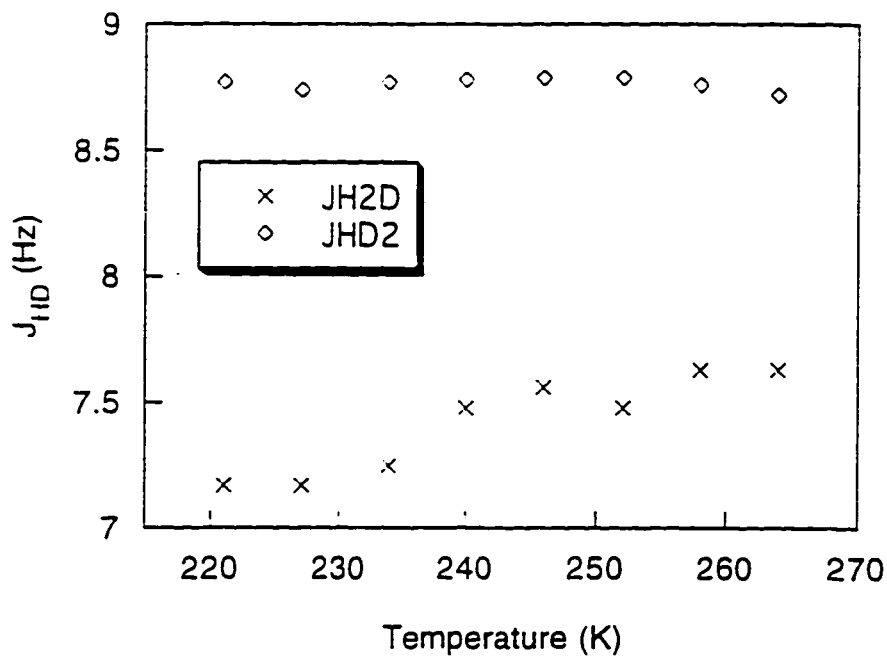


Figure 3.3 Plot of H-D coupling in **6-d₁** and **6-d₂** as a function of observation temperature.

Table 3.2 Chemical Shifts of Hydride Resonances and $J_{\text{H-D}}$ Coupling Constants For Partially Deuterated Isotopomers of Complexes 6-9.

Complex	Isotopomer	Hydride Shift (ppm)	$J_{\text{H-D}}$ (Hz)
6 ^a	H ₃	-10.37	—
	H ₂ D	-10.18	7.48
	HD ₂	-10.08	8.78
7 ^a	H ₃	-9.80	—
	H ₂ D	-9.61	b
	HD ₂	-9.52	b
8 ^a	H ₃	-11.06	—
	H ₂ D	-10.84	7.33
	HD ₂	-10.75	8.90
9 ^c	H ₃	-7.96	d
	H ₃ , H ₂ D, HD ₂	-7.94	e

^a $^1\text{H}\{^{31}\text{P}\}$ NMR (500 MHz, 240 K). ^b not resolved. ^c ^1H NMR (300 MHz, 213 K). ^d broad, linewidth = 75 Hz. ^e broad, linewidth = 63 Hz.

NMR Spectra of Partially Tritiated Complexes. Incorporation of tritium into the hydride positions of **6-8** was observed when CD₂Cl₂ solutions were exposed to T₂ gas (*ca.* 200 torr) for several hours at room temperature. Distinct hydride resonances for the H₃ and H₂T isotopomers were observed in the ^1H NMR spectrum. The central peak of the HT₂ triplet was observed in the case of **7** and **8**, but was not detected for **6** because the concentration of the HT₂ isotopomer was too small. The sample activity in each case is estimated to be less than 10 mCi. For **6** the hydride resonance of the H₂T isotopomer is shifted *downfield* of the H₃ isotopomer by 280 ppb at 240 K (Figure 3.4). The H₂T resonance appears as a broad doublet of doublets due to coupling to phosphorus ($J_{\text{P-H}} =$

9.9 Hz) and tritium ($J_{T-H} = 54.5$ Hz). The hydride resonance of the H_3 isotopomer is a doublet ($J_{P-H} = 11.6$ Hz), due to coupling to phosphorus (see Figure 3.4).

In the 3H NMR spectrum, distinct hydride resonances for the T_3 , T_2H , and TH_2 isotopomers were observed. The T_2H and TH_2 isotopomers are shifted significantly *upfield* of the T_3 isotopomer. The isotope shifts at 240 K, $\Delta_3 = \delta(T_2H) - \delta(T_3)$ and $\Delta_4 = \delta(TH_2) - \delta(T_2H)$ are -150 and -250 ppb, respectively. The T_3 isotopomer was observed at the same chemical shift as the H_3 isotopomer in the 1H NMR spectrum. The T_2H isotopomer appears as a doublet of doublets coupling to phosphorus ($J_{P-T} = 11.5$ Hz) and hydrogen ($J_{T-H} = 63.3$ Hz). The TH_2 isotopomer is a broad triplet with an observed T-H coupling constant of 53.2 Hz, which is identical within experimental error to the H-T coupling constant observed for the H_2T isotopomer in the 1H NMR spectrum. The 1H and 3H NMR data for **7-8** are summarized in Table 3.3.

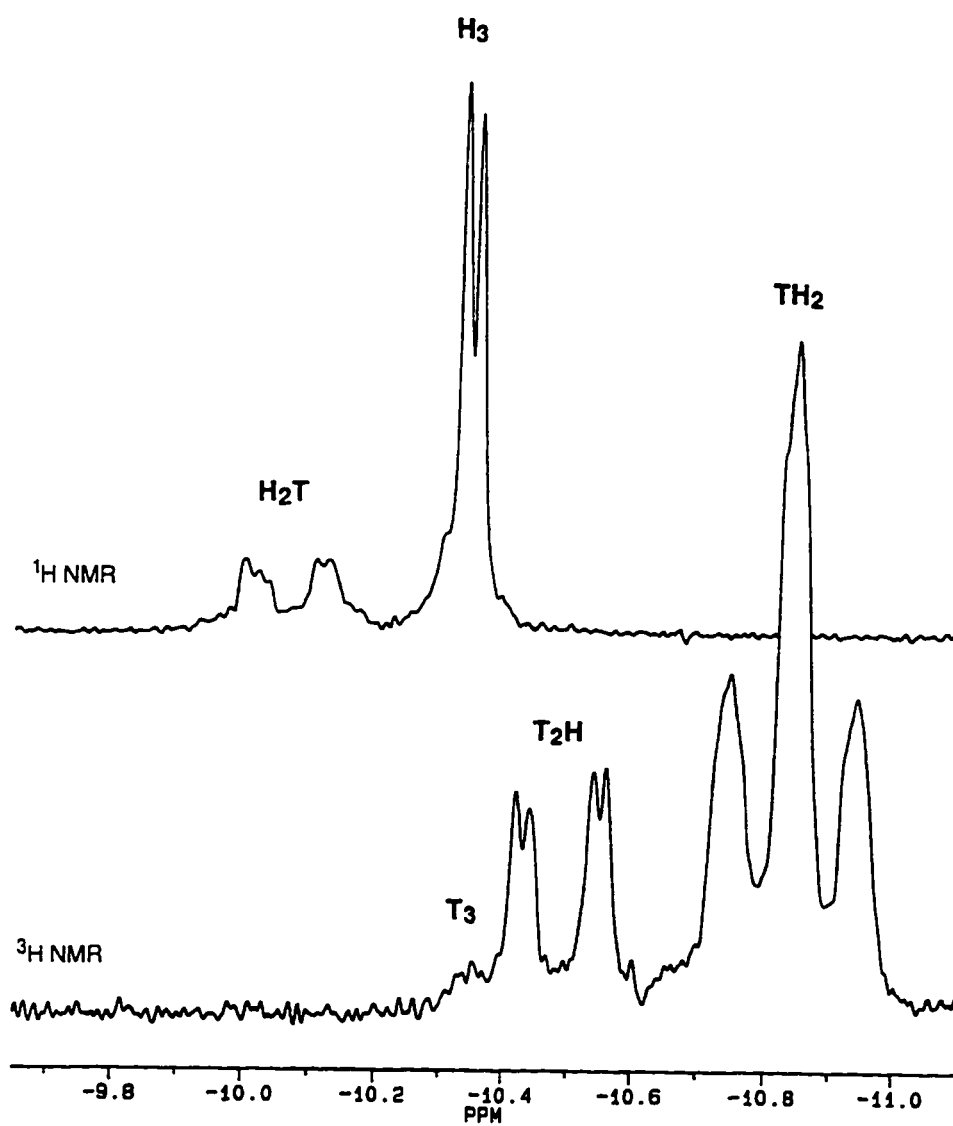


Figure 3.4 Top: ^1H NMR spectrum (CD_2Cl_2 , 500 MHz, 240 K) of a partially tritiated sample of **6**. Bottom: ^3H NMR spectrum (CD_2Cl_2 , 533 MHz, 240 K).

Table 3.3 Hydride Chemical Shifts, J_{P-H} , J_{P-T} , and J_{H-T} Coupling Constants For Partially Tritiated Isotopomers of **6-8** observed by ^1H and ^3H NMR Spectroscopy at 240 K.

Complex	Isotopomer	$\delta_{\text{Ir-H3}}$ (ppm)	J_{P-H} (Hz)	J_{H-T} (Hz)
6 ^1H NMR	H ₃	-10.35	11.6	—
	H ₂ T	-10.07	9.9	54.5
	HT ₂	a	a	a
6 ^3H NMR	T ₃	-10.35	12.9	—
	T ₂ H	-10.50	11.5	63.3
	TH ₂	-10.75	b	53.2
7 ^1H NMR	H ₃	-9.70	9.1	—
	H ₂ T	-9.44	b	52.6
	HT ₂	-9.23	b	b
7 ^3H NMR	T ₃	-9.70	b	—
	T ₂ H	-9.82	9.7	64.3
	TH ₂	-10.16	11.6	52.2
8 ^1H NMR	H ₃	-11.06	11.9	—
	H ₂ T	-10.75	b	51.7
	HT ₂	-10.52	b	b
8 ^3H NMR	T ₃	-11.06	b	—
	T ₂ H	-11.22	b	65.7
	TH ₂	-11.62	b	51.0

^anot observed. ^bnot resolved.

Structural Characterization. Crystals of $6 \cdot \text{CH}_2\text{Cl}_2$ suitable for x-ray diffraction have been obtained by slow diffusion of Et_2O into a concentrated CH_2Cl_2 solution of **6**. An ORTEP drawing of the iridium cation and key structural features are given in Figure 3.5 and Table 3.4. The hydrogen atoms, BF_4^- anion and the CH_2Cl_2 of crystallization have been omitted for clarity. The metal bound dihydrogen ligand and the hydride ligand were not reliably located. No unusual intermolecular interaction between BF_4^- and the iridium metal center is observed. The closest Ir-F contact is 3.541(15) Å. The closest contact between iridium and the CH_2Cl_2 of crystallization is 3.832(15) Å. The bond lengths and bond angles observed for $6 \cdot \text{CH}_2\text{Cl}_2$ are typical of Ir(III) Tp complexes.^{12,13} The Ir-N bond lengths to the equatorial pyrazolyl ligands are significantly different (2.161 (8) vs. 2.070 (8) Å). This observation may reflect the trans relationship of the pyrazolyl ligands to the hydride and the dihydrogen ligand, respectively. Details of the structure solution and refinement are included in the experimental section.

Table 3.4 Significant Bond Distances and Angles for $6 \cdot \text{CH}_2\text{Cl}_2$.

Distances, Å			
Ir-P	2.280(3)	Ir-N(2)	2.161(8)
Ir-N(3)	2.105(7)	Ir-N(6)	2.070(8)
P-C(10)	1.772(12)	P-C(11)	1.805(10)
P-C(12)	1.795(11)		
Angles, deg			
P-Ir-N(2)	96.0(2)	P-Ir-N(3)	177.6(2)
N(2)-Ir-N(3)	86.3(3)	P-Ir-N(6)	94.(2)
N(2)-Ir-N(6)	84.3(3)	N(3)-Ir-N(6)	85.5(3)
Ir-P-C(10)	115.0(4)	Ir-P-C(11)	114.0(4)
Ir-P-C(12)	114.0(4)	B1-Ir-P	128.6 (2)

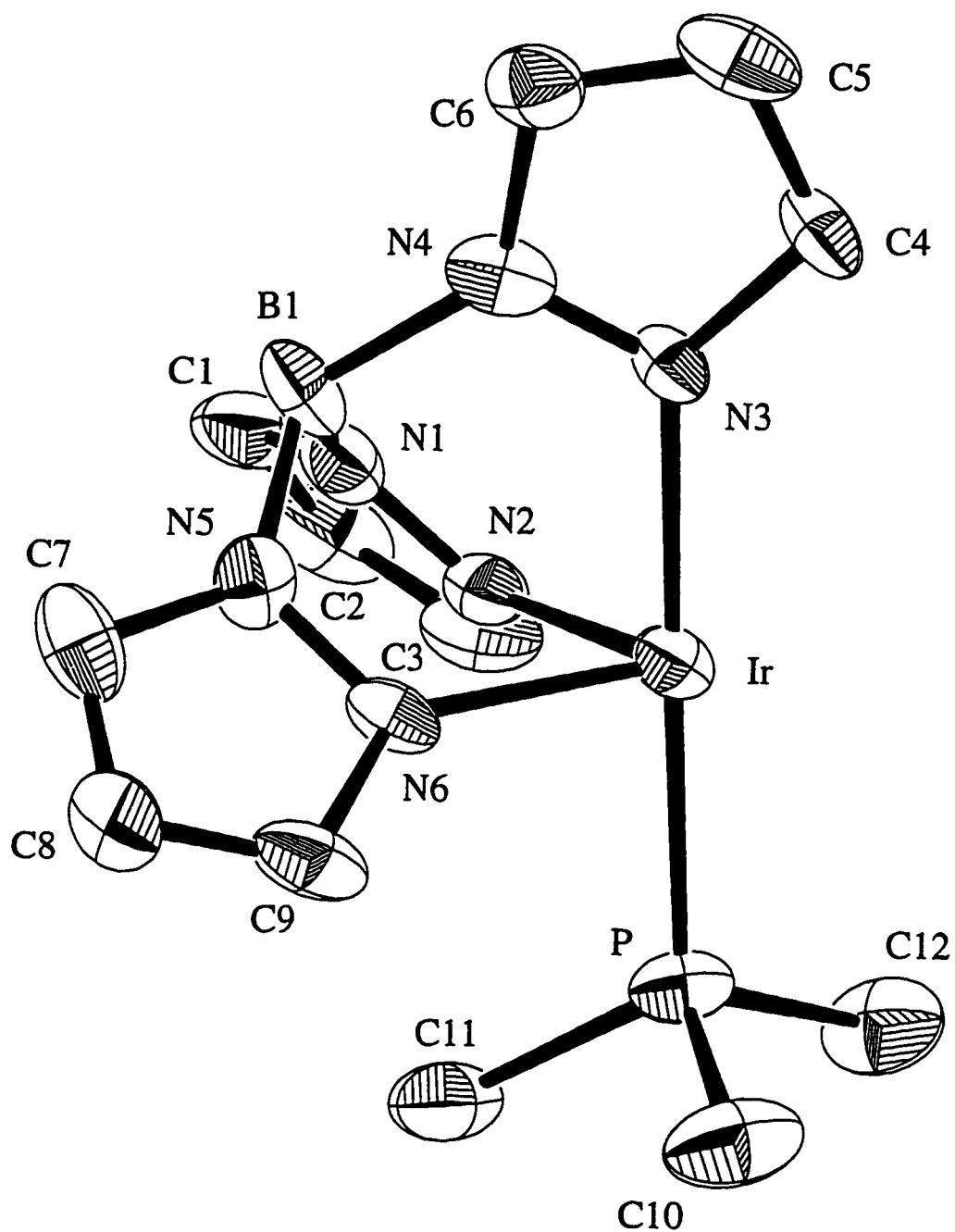


Figure 3.5 ORTEP drawing (50% probability ellipsoids) for [TpIr(PMe₃)(H₂)H]BF₄. Hydrogen atoms have been omitted for clarity.

Discussion

Synthesis. In contrast to the well developed synthetic routes used to prepare $\text{Cp}^*\text{Ir}(\text{PR}_3)\text{H}_2$ and $\text{CpIr}(\text{PR}_3)\text{H}_2$ complexes, similar approaches to prepare the corresponding Tp complexes are unsuccessful. The immediate precursor to $\text{Cp}^*\text{Ir}(\text{PR}_3)\text{H}_2$ is the corresponding dichloride complex. These are easily obtained upon reaction of $[\text{Cp}^*\text{IrCl}_2]_2$ with a range of phosphine donor ligands.¹⁴ Attempts by Powell and co-workers to prepare $\text{Tp}^{\text{R}2}\text{Ir}(\text{L})\text{Cl}_2$ complexes from $[\text{Tp}^{\text{R}2}\text{IrCl}_2]_2$ were reported to fail except in the case of $\text{L} = \text{AsPhMe}_2$.¹⁵ The diiodide complexes, $\text{CpIr}(\text{PR}_3)\text{I}_2$ employed in the Cp chemistry are prepared in a one pot reaction from $\text{CpIr}(\text{C}_2\text{H}_4)_2$.⁶ Both ethylene ligands are displaced upon addition of one equiv. of I_2 to afford an iodide bridged oligomer, $[\text{CpIrI}_2]_n$, to which one equiv. of phosphine is added in a second step to yield $\text{CpIr}(\text{PR}_3)\text{I}_2$. In contrast, we have found that $\text{TpIr}(\text{C}_2\text{H}_4)_2$ reacts with I_2 to yield, $[\text{TpIr}(\text{C}_2\text{H}_4)_2\text{I}]\text{I}$, which in turn reacts with PPh_3 to give $[\text{TpIr}(\text{PPh}_3)(\text{C}_2\text{H}_4)\text{I}]\text{I}$ (Chapter 2). The ethylene ligand in this complex is not easily displaced.

We find that the $\text{TpIr}(\text{PR}_3)\text{H}_2$ complexes are easily prepared from $[(\text{MeCN})_3\text{Ir}(\text{PR}_3)\text{H}_2]^+$, which is readily available by the reaction of acetonitrile with $[\text{Cp}^*\text{Ir}(\text{PR}_3)\text{H}_3]^+$ as reported by Petersen and Tilset.⁹ A more efficient approach involves reacting $\text{TpIr}(\text{C}_2\text{H}_4)_2$ sequentially with one equiv. of a phosphine ligand, then adding H_2 in a second step to give $\text{TpIr}(\text{PR}_3)\text{H}_2$. This approach is easily extended to include the related rhodium complexes. The details of this chemistry have been outlined in chapter 2. A preparation of complex **3** by thermolysis of $\text{Tp}^{\text{Me}2}\text{IrH}_4$ with PMe_3 has been briefly reported, but no details of characterization were given.¹⁶

Characterization of the Cationic Hydride Complexes. The cationic species resulting from protonation **1-4** give spectroscopic data consistent with new complexes containing a mirror plane of symmetry. A total of three hydride ligands (no structure implied) is indicated by the observation of a quartet in the ^{31}P NMR spectrum of **6** recorded with decoupling of the PMe_3 methyl protons. At all temperatures, only a single

hydride resonance is observed in the ^1H NMR spectrum which may result from a fluxional trihydride or a fluxional dihydrogen-hydride complex. These possibilities can be distinguished by a combination of $T_1(\text{min})$ measurements and analysis of the effect of partial substitution of the hydride ligands with deuterium or tritium.

$T_1(\text{min})$: Calculation of H-H Distances. The minimum of the longitudinal relaxation time ($T_1(\text{min})$) of the dihydrogen ligand has been shown to be a sensitive indicator of the H-H bond length.³ The short $T_1(\text{min})$ values observed for **6-9** are qualitatively consistent with the presence of a bound dihydrogen ligand in a dihydrogen-hydride structure. An accurate calculation of the H-H bond length requires that the mutual relaxation rate of the hydrogen atoms in the coordinated dihydrogen ligand ($R_{\text{d-d}}$) be known explicitly ($1/T_1 = \text{relaxation rate}, R^{17}$). The observed rate of dipolar relaxation for a dihydrogen ligand (R_{H_2}) is actually the sum of the mutual H-H dipolar relaxation ($R_{\text{d-d}}$) and the relaxation resulting from interactions with other dipoles in the molecule (R_0), thus $R_{\text{H}_2} = R_{\text{d-d}} + R_0$.⁴ Additionally, in the case of fluxional polyhydride complexes suspected to contain a dihydrogen ligand, the observed $T_1(\text{min})$ value is the population weighted average of all the hydride sites. For the dihydrogen-hydride complexes under study in this work, the observed relaxation rate is given by $R_{\text{obs}} = (2R_{\text{H}_2} + R_{\text{H}})/3$ where R_{H_2} and R_{H} are the relaxation rates of the dihydrogen and hydride ligands. The relaxation rate of the terminal hydride ligand (R_{H}) can be estimated from the $T_1(\text{min})$ value of the parent dihydride complexes such as **1**. Similarly R_0 can also be estimated from this measurement. Calculation of $R_{\text{d-d}}$ for the dihydrogen ligand of **6** is shown in scheme 3.2.

$$R_{\text{obs}}(\mathbf{6}) = (R_{\text{H}} + 2R_{\text{H2}})/3$$

$$= (R_{\text{H}} + 2(R_{\text{d-d}} + R_{\text{O}}))/3 \quad \text{if } R_{\text{H}} \text{ and } R_{\text{O}} \approx R_{\text{obs}}(\mathbf{1}), \text{ then:}$$

$$R_{\text{obs}}(\mathbf{6}) = (2R_{\text{d-d}} + 3R_{\text{obs}}(\mathbf{1}))/3$$

and

$$R_{\text{d-d}} = 3(R_{\text{obs}}(\mathbf{6}) - R_{\text{obs}}(\mathbf{1}))/2$$

$$R_{\text{d-d}} = 68.7 \text{ s}^{-1}$$

Scheme 3.2

Similar calculations have been carried out for **7** and **9**. The H-H bond length can now be calculated using eqs 1.5 and 1.6 (see chapter 1) in the limits of slow and fast hydrogen rotation (Table 3.5). We find that the H-H bond length of the dihydrogen ligand of **6** is bracketed by distances of 1.11 and 0.88 Å. We can estimate the true H-H bond length after first considering the results obtained upon partial substitution of the hydride positions with deuterium or tritium.

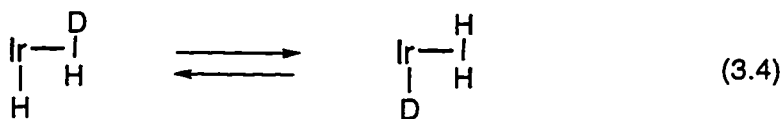
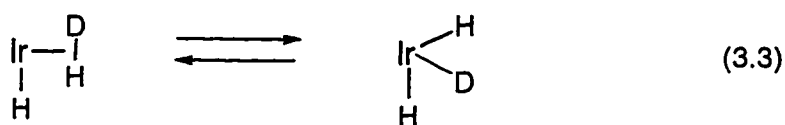
Table 3.5 Calculated H-H Bond Lengths from T_1 (min) data in the limit of slow and fast rotational motion.

Complex	H-H (Å) slow rotation	H-H (Å) fast rotation
[TpIr(PMe ₃)(H ₂)H] ⁺ (6)	1.11	0.88
[TpIr(PPh ₃)(H ₂)H] ⁺ (7)	1.12	0.89
[TpRh(PPh ₃)(H ₂)H] ⁺ (9)	0.92	0.73

Isotopic Perturbation of Equilibrium. We propose that the large temperature dependent isotope shifts observed for the new iridium dihydrogen-hydride complexes is a manifestation of isotopic perturbation of equilibria.¹⁸ These observations are novel in polyhydride complexes. Generally only small (0-70 ppb) temperature independent upfield isotope shifts are observed upon partial substitution of deuterium atoms in the

hydride positions of dihydrogen and polyhydride complexes.^{6,7,19-23} A few scattered reports of downfield isotope shifts in both these classes of molecules have also appeared.^{4,16,24-34} In some cases the observed isotope shifts have been rationalized by invoking isotopic perturbation of equilibria,^{8,26,33} however a detailed study of this phenomenon has not been reported.

Two types of equilibrium situations may be perturbed upon substitution of the hydride positions of **6-8** with deuterium or tritium. The observed isotope shifts may result from perturbation of an equilibrium between a dihydrogen-hydride complex and a trihydride complex (eq 3.3).^{26,35} Related to this equilibrium, but not considered here is the isotope effect on reversible binding of hydrogen to afford either dihydrogen complexes^{33,36} or dihydride complexes.³⁷⁻³⁹ This is not considered because exchange of the hydride positions with D₂ or T₂ gas occurs only slowly over several hours. A second possibility is that within a single dihydrogen-hydride ground state structure, the heavy hydrogen isotopes may concentrate in a particular hydride site (eq 3.4). These two possibilities can be distinguished by comparing the isotope shifts upon partial deuteration using both ¹H and ²H NMR spectroscopy. In our case, very broad lines were observed in the ²H NMR spectra, so we instead incorporated tritium in the hydride positions and

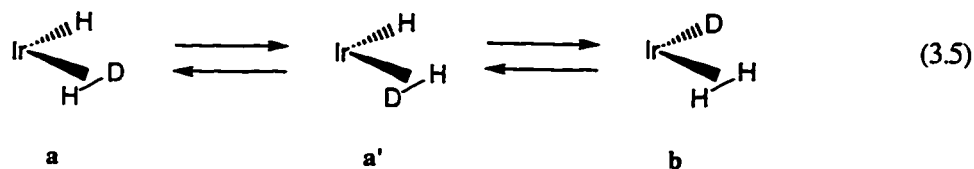


investigated this problem using ¹H and ³H NMR spectroscopy.⁴⁰ If the equilibrium in eq 3.3 is obtained, identical isotopomers will be observed at the same chemical shift in the ¹H and ³H NMR spectrum, but the H₃ and T₃ isotopomers will not coincide. If an

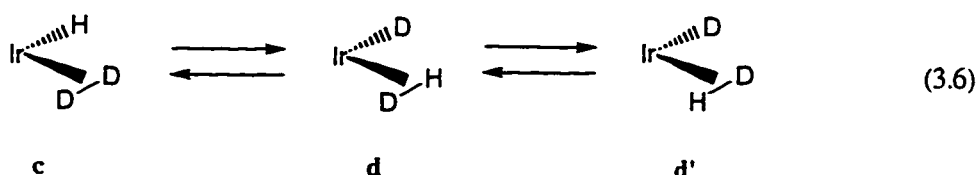
equilibrium between different sites in the same structure is perturbed (eq 3.4), then the H_3 and T_3 isotopomers will be observed at the same chemical shift, but the isotope shifts observed in the 1H NMR spectrum will be in the opposite direction to that observed in the 3H NMR spectrum. The spectra shown in Figure 3.4 and the data tabulated in Table 3.3 confirm that the isotope effect results from a nonstatistical site preference for deuterium (or tritium) in a single dihydrogen-hydride structure.

We now describe a procedure to analyze quantitatively the isotope shifts observed in the 1H NMR spectrum upon partial substitution of the hydride sites with deuterium. Our method is based on the procedure used by Calvert and Shapley⁴¹ in the study of agostic methyl groups. An identical procedure is followed to interpret the isotope shifts upon partial incorporation of tritium in the hydride positions. The observed chemical shifts and the J_{H-D} coupling data can be analyzed quantitatively to calculate the limiting chemical shifts of the dihydrogen ligand (δ_{H_2}) and the terminal hydride ligand (δ_H), $^1J_{H-D}$ for the dihydrogen ligand, and the energy difference between deuterium substitution of the dihydrogen site versus the hydride site. A set of five equations can be derived which relate the experimental observables to these unknown parameters.

The hydride chemical shift of the H_3 isotopomer is simply the statistical average of the dihydrogen site and the hydride site, thus $\delta_{H_3} = (2\delta_{H_2} + \delta_H)/3$. However, upon substitution of one deuterium atom in the hydride positions an equilibrium between three different species is obtained (eq 3.5). A similar mixture is obtained if two deuterium atoms are incorporated in the hydride positions (eq 3.6). In this analysis we assume that there is no preference between a and a' . We also assume that the chemical shift of the *exo* hydrogen atom in a is the same as the *endo* hydrogen atom in a' . The observed chemical shift of the H_2D isotopomer is given by eq 3.7, where a , a' , and b are the mol fractions of each species. Within this definition the sum of $a + a' + b = 1$. The Boltzmann factor, A_1 defined as $e^{-\Delta E/RT}$, may be introduced to account for an energy



(3.5)



(3.6)

difference between **a** (**a'**) and **b**. A_1 is equal to $b/a = b/a'$. Thus **a** and **a'** can be combined and the mol fractions can be rewritten in terms of the Boltzmann factor, A_1 . Substituting the relations $a = a' = 1/(2 + A_1)$ and $b = A_1/(2 + A_1)$ in eq 3.7 yields eq 3.8.

$$\delta_{(H_2D)} = a \left(\frac{\delta_{H_2} + \delta_H}{2} \right) + a' \left(\frac{\delta_{H_2} + \delta_H}{2} \right) + b(\delta_{H_2}) \quad (3.7)$$

$$\delta_{(H_2D)} = \frac{\delta_{H_2} + \delta_H + A_1 \delta_{H_2}}{2 + A_1} \quad (3.8)$$

In a similar fashion the observed J_{H-D} coupling constant is given by eq 3.9. If the two bond ${}^2J_{H-D}$ coupling between the dihydrogen ligand and the terminal hydride ligand is assumed to be zero and the **a** and **a'** terms are combined, then the equation can be rewritten in terms of the Boltzmann factor, A_1 and simplified to give eq 3.10.

$$J_{(H_2D)} = a \left(\frac{{}^1J_{H-D} + {}^2J_{H-D}}{2} \right) + a' \left(\frac{{}^1J_{H-D} + {}^2J_{H-D}}{2} \right) + b({}^2J_{H-D}) \quad (3.9)$$

$$J_{(H_2D)} = \frac{{}^1J_{H-D}}{2 + A_1} \quad (3.10)$$

In a similar fashion, expressions can be derived which relate the chemical shift and observed J_{H-D} coupling of the HD_2 isotopomer, written in terms of a second Boltzmann factor, A_2 . The five equations are listed in scheme 3.3. In addition to the approximations noted above, this analysis does not take into account intrinsic isotope effects on the chemical shift of the hydride resonances.

$$\delta_{(H_3)} = \frac{2\delta_{H_2} + \delta_H}{3}$$

$$\delta_{(H_2D)} = \frac{\delta_{H_2} + \delta_H + A_1\delta_{H_2}}{2 + A_1} \qquad J_{(H_2D)} = \frac{{}^1J_{H-D}}{2 + A_1}$$

$$\delta_{(HD_2)} = \frac{2A_2\delta_{H_2} + \delta_H}{2A_2 + 1} \qquad J_{(HD_2)} = \frac{{}^1J_{H-D}A_2}{2A_2 + 1}$$

Scheme 3.3

The results of this analysis for **6-8** are presented in Table 3.6. In the case of **6** the limiting spectroscopic parameters were also calculated at every temperature indicated in Figures 3.2 and 3.3. In this way the standard deviation in each calculated parameter was obtained: $\delta_{H_2} = -8.4 \pm 0.1$ ppm, $\delta_H = -14.4 \pm 0.3$ ppm, ${}^1J_{H-D} = 24.6 \pm 0.3$ Hz, $\Delta E_1 = -130 \pm 12$ cal/mol and $\Delta E_2 = -107 \pm 12$ cal/mol. However, comparison of the results calculated from the 1H and 3H NMR data for **7** and **8**, indicates that neglect of intrinsic isotope shifts is a significant source of error. Despite these shortcomings, the calculated parameters are in relatively good agreement. Larger ΔE values are observed for tritium than for deuterium substitution as expected. In both cases the heavy hydrogen isotope is found to concentrate in the terminal hydride position. Because the chemical shift of the dihydrogen ligand is downfield of the hydride signal, this leads to the significant

downfield shift in the ^1H NMR spectrum and the corresponding upfield shift in the ^3H NMR spectrum.

This site preference can be explained in terms of differences in zero point energy between the dihydrogen ligand and the hydride ligand. We are unable to attempt a full analysis because only a weak Ir-H stretch at 2199 cm^{-1} (6) or 2197 cm^{-1} (7) was observed. A total of six fundamental vibrations are expected for the dihydrogen ligand.⁴² In addition to the observed Ir-H stretch, two bending modes are expected for the hydride ligand. We can simplify the problem by considering only the H-H stretch and the Ir-H stretch. The approximate difference in energy between **a** and **b** (shown in eq 3.5) is then given by eq 3.11.^{43,44} The approximate difference in energy between **c** and **d** (shown in eq 3.6) is given by eq 3.12. If the H-H stretch for the iridium complexes can be assumed

$$\Delta E_1 = \frac{Nhc}{2} \{ (v_{\text{H-H}} - v_{\text{H-D}}) + (v_{\text{Ir-D}} - v_{\text{Ir-H}}) \} \quad (3.11)$$

$$\Delta E_2 = \frac{Nhc}{2} \{ (v_{\text{H-D}} - v_{\text{D-D}}) + (v_{\text{Ir-D}} - v_{\text{Ir-H}}) \} \quad (3.12)$$

to be *ca.* 2700 cm^{-1} by analogy to the value reported for $\text{W}(\text{PCy}_3)_2(\text{CO})_3(\text{H}_2)$,⁴⁵ then the H-D stretch should be reduced to *ca.* 2340 cm^{-1} by considering the differences in reduced mass ($v_{\text{H-H}}\sqrt{3}/2$). Similarly the D-D stretch should be reduced further to *ca.* 1910 cm^{-1} ($v_{\text{H-D}}\sqrt{2}/\sqrt{3}$). The Ir-D stretch can be estimated as 1555 cm^{-1} ($v_{\text{Ir-H}}/\sqrt{2}$).

Evaluating eqs 3.11 and 3.12, ΔE_1 and ΔE_2 are calculated as -400 and -300 cal/mol respectively. Despite the gross approximations employed in this analysis, the calculated energy differences are in rough agreement with the results of the IPR analysis (Table 3.6). Importantly ΔE_2 is predicted to be less negative than ΔE_1 as observed. A complete vibrational analysis of dihydrogen-hydride model complexes related to **6-8** using computational methods may help clarify this problem.

Table 3.6 Calculated Parameters via IPR Analysis of ^1H and ^3H NMR Spectra of **6-8** Acquired at 240 K.

complex:	6 ^a	6 (^3H) ^b	7 (^1H) ^c	7 (^3H) ^b	8 ^a	8 (^1H) ^c	8 (^3H) ^b
δ_{H_2} (ppm)	-8.3	-8.3	-7.2	-8.0	-9.1	-8.7	-9.2
δ_{H} (ppm)	-14.6	-14.4	-14.6	-13.2	-15.0	-15.9	-14.8
$^1J_{\text{H-D}}$ (Hz)	24.7				24.8		
$^1J_{\text{H-T}}$ (Hz)		177	176	180		178	183
ΔE_1 (cal/mol)	-125 ^d	-136 ^f	-143 ^f	-177 ^f	-153 ^d	-174 ^f	-203 ^f
ΔE_2 (cal/mol)	-103 ^e	-110 ^g	-143 ^g	-99 ^g	-118 ^e	-171 ^g	-132 ^g

^a ^1H NMR analysis of a partially deuterated sample. ^b ^3H NMR analysis of a partially tritiated sample. ^c ^1H NMR analysis of a partially tritiated sample. ^dEnergy difference between Tp(L)Ir(HD)H vs. $\text{Tp(L)Ir(H}_2\text{)D}$ (see eq 3.4). ^eEnergy difference between $\text{Tp(L)Ir(D}_2\text{)H}$ vs. Tp(L)Ir(HD)D (see eq 3.5). ^fEnergy difference between Tp(L)Ir(HT)H vs. $\text{Tp(L)Ir(H}_2\text{)T}$. ^gEnergy difference between $\text{Tp(L)Ir(T}_2\text{)H}$ vs. Tp(L)Ir(HT)T .

Structural Considerations. The above analysis establishes that a dihydrogen-hydride structure is adopted by complexes **6-9**. In contrast, the Cp (or Cp^{*}) analogs such as $[\text{CpIr(PR}_3\text{)H}_3]^+$ are trihydride complexes, with appropriately long T_1 (min) values of ca. 200-300 ms.^{6,46} Protonation of $\text{CpRh(PiPr}_3\text{)H}_2$ with HPF_6 is reported to yield a hydride bridged dimer, $[\{\text{CpRh(PiPr}_3\text{)}\}_2(\mu\text{-H}_3)]\text{PF}_6$ and H_2 .⁴⁷ Preliminary observations of a mononuclear rhodium trihydride complex, $[\text{Cp}^*\text{Rh(PMe}_3\text{)H}_3][\text{B(Ar)}_4]$ have been described by Hinkle.⁴⁸ A similar change in structure from trihydride to dihydrogen-hydride upon substitution of Tp for Cp ligands has been reported by Chaudret and coworkers in related ruthenium complexes.⁴⁹⁻⁵¹ The neutral $\text{CpRu(PR}_3\text{)H}_3$ complexes are characterized as classical trihydride complexes,⁵² however substitution of the Cp ligand for Tp^{Me_2} results in stable complexes of the form $\text{Tp}^{\text{Me}_2}\text{Ru(L)(H}_2\text{)H}$. In this case L can be a phosphine, nitrogen or sulfur donor ligand or even H_2 .

In most cases the Tp ligand is considered to be a more efficient donor than the Cp ligand.⁵³ This property would seem to favor a trihydride structure over the dihydrogen-hydride structure that is actually observed in this system. However, in the later transition metals such as iridium, the Tp ligand transfers less electron density to the metal center. This is reflected in the higher CO stretching frequency of TpIr(CO)H₂ (2020 cm⁻¹, CH₂Cl₂)⁵⁴ versus CpIr(CO)H₂ (2002 cm⁻¹, CH₂Cl₂)⁵⁵ and also TpIr(CO)(C₂H₄) (2000 cm⁻¹, cyclohexane)⁵⁶ versus CpIr(CO)(C₂H₄) (1980 cm⁻¹, cyclohexane).⁵⁷ The difference in relative donor ability is probably a function of orbital overlap between iridium and the Cp or Tp ligands. The soft iridium center is expected to form stronger, more covalent bonds with the soft Cp ligand. The bonding between iridium and the hard pyrazolyl nitrogen donors is presumably more ionic in character. Two additional factors may be even more important. The relative size of Cp versus Tp is reflected in their respective cone angles of 136° and 184°. All things being equal, the Tp ligand should favor complexes with a reduced coordination number. Additionally, Extended Hückel MO calculations have indicated that the Tp ligand promotes six-coordination to a greater extent than the Cp ligand by polarizing the metal orbitals into an octahedral array.⁵⁸ These conditions can be satisfied if two adjacent hydride ligands in the hypothetical [TpM(PR₃)H₃]⁺ (M = Rh and Ir) complexes formally “reductively couple” to form one dihydrogen ligand in their place.

Estimation of H-H Distances. As noted by Morris and co-workers, H-H bond distances inferred from T₁ data depends upon assumptions about the relative rate of dihydrogen rotation.⁵ In the case of iridium complexes **6** and **7** the observed T₁ (min) values of 21-22 ms are consistent with an H-H distance of 0.88 Å (fast rotation) or 1.11 Å (slow rotation). Further insight can be obtained by making use of the roughly linear

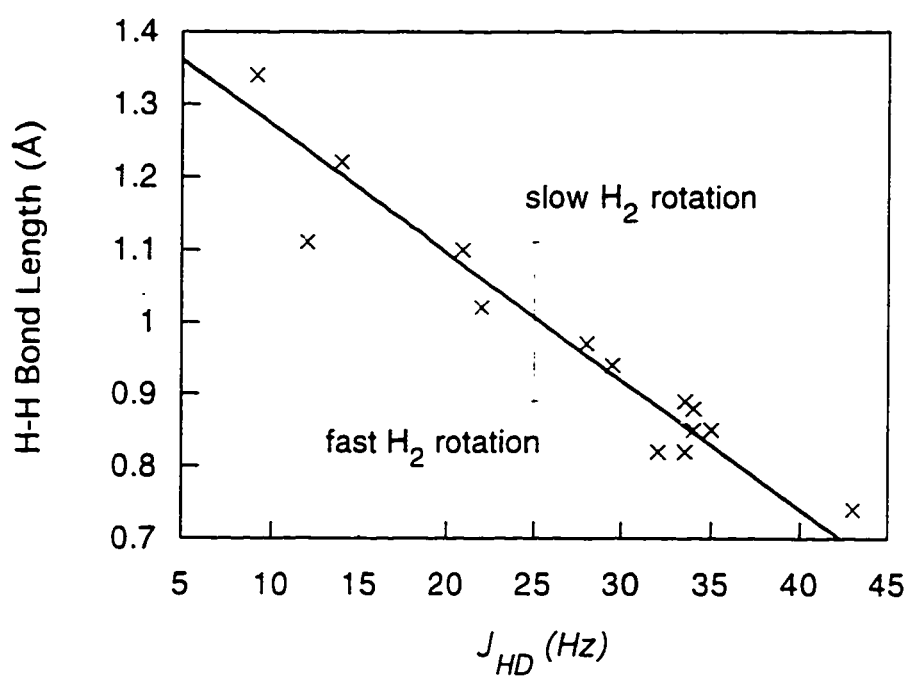


Figure 3.6 Plot of H-H bond length in angstroms versus J_{H-D} in hertz. The range of H-H bond lengths calculated from T_1 (min) data as a function of relative dihydrogen rotation is shown for 6.

inverse correlation between $^1J_{\text{H-D}}$ and the H-H bond length (determined by neutron diffraction or solid state NMR methods) as reported by Heinekey and Luther (Figure 3.6).⁵⁹ A similar analysis has been used to infer the relatively slow rotational motion of the dihydrogen ligand in $[\text{Cp}^*\text{Ru}(\text{dppm})(\text{H}_2)]\text{BF}_4$,⁶⁰ and the dicationic complex $[\text{Os}(\text{bpy})(\text{PPh}_3)_2(\text{CO})(\text{H}_2)](\text{OTf})_2$.⁵⁹ For the iridium complexes reported here, the H-D coupling in the bound dihydrogen ligand is *ca.* 25 Hz, which is consistent with an H-H distance of *ca.* 1 Å (Figure 3.6). These complexes may belong to the currently limited group of dihydrogen complexes such as $[\text{Os}(\text{H}_2)(\text{dppe})_2\text{X}]^+$ ($\text{X} = \text{Cl}$ and Br),⁶¹ in which dihydrogen rotational motion is comparable to the rate of molecular tumbling.

In the case of the rhodium complex **9**, the H-H bond length is calculated to be between 0.92 Å (slow rotation) and 0.73 Å (fast rotation). Since the H-H bond length of free hydrogen is 0.73 Å, the value calculated assuming fast rotation is probably not correct. The shortest H-H bond lengths which have been characterized by neutron diffraction are *ca.* 0.82 Å. Unfortunately the rhodium complex gave only a broad hydride resonance upon partial deuteration of the hydride positions, so a $J_{\text{H-D}}$ value is not available. Assuming that hydrogen rotation is relatively slow in complex **9**, as found for the iridium analogs, the longer H-H distance of *ca.* 0.92 Å results. Although a definitive value for the H-H distance in complex **9** cannot be obtained, it is clear that the H-H distance in the iridium complexes is significantly longer than for the corresponding rhodium complex.

Hydride Dynamics. Although a static low temperature limiting ^1H NMR spectrum was not obtained for complexes **6-9**, partial deuteration (tritiation) and the observation of IPR as detailed above allow the limiting chemical shifts δ_{H_2} and δ_{H} to be determined. From this data and the observation of a single hydride resonance for **6** at 127 K, the activation energy for exchange between the dihydrogen ligand and the hydride ligand can be calculated as $\Delta G^\ddagger \leq 5$ kcal/mol. It should be noted that these observations were made on a sample of complex **6** which was heavily deuterated in the hydride

positions. This rules out the possibility that exchange coupling could contribute to the observed spectrum as has been noted for other dynamic polyhydrides.⁶²

While our data offers no mechanistic insight, it is instructive to consider possible mechanisms for the rapid exchange of all three hydride nuclei. Two distinct dynamic processes are required. Rotation of the dihydrogen ligand around the M-H₂ bond axis must be rapid on the chemical shift timescale. This is quite reasonable, since reported barriers to hydrogen rotation are very low except in d² systems.^{63,64} A second process exchanges hydrogen nuclei between the dihydrogen and hydride ligands. Since our complexes are positively charged, it seems reasonable to speculate that an intramolecular proton transfer may be involved,^{65,66} although it has been reported that the hydride ligands of the closely related ruthenium complex Tp^{Me}₂Ru(PCy₃)(H₂)H also exchange rapidly on the NMR timescale.⁴⁹⁻⁵¹ In this case, heterolytic cleavage of the dihydrogen ligand is not facilitated by an overall positive charge.

Although rotation of the dihydrogen ligand is fast on the chemical shift timescale, inspection of Figure 3.6 indicates that the rate of dihydrogen rotational motion may be comparable to the rate of isotropic molecular tumbling. A possible consequence of hindered dihydrogen rotational motion is the observed distortion of the expected 1:1:1 and 1:2:3:2:1 coupling pattern for the respective hydride resonances of the H₂D and HD₂ isotopomers (Figure 3.1). As noted above, the hydride resonances of the partially deuterated isotopomers reveal a distortion of the H-D coupling pattern in which the outer lines are broadened and therefore reduced in intensity. This effect is commonly observed in organic molecules when the relaxation time (T₁) of the deuterium nucleus is comparable to J_{H-D}. Quadrupole nuclear relaxation is sensitive to the molecular correlation time (τ_c) and becomes significantly more efficient at low temperatures where τ_c is long.¹¹ In agreement with this explanation, we observe that distortion of the H-D coupling patterns becomes more severe at lower temperatures where τ_c is greatest. In

most cases rapid rotation of the H-D ligand can be expected to minimize this effect in dihydrogen complexes.

Chaudret and coworkers have recently reported the first examples of dihydrogen complexes in which hydrogen rotation is slow on the NMR timescale.^{63,64} The $[\text{Cp}_2\text{Nb}(\text{HD})(\text{PMe}_2\text{Ph})]^+$ complex reveals distinct proton resonances for the two rotamers of the H-D ligand separated by *ca.* 0.8 ppm (203 K). The H-D coupling pattern for the two resonances are distorted from the ideal 1:1:1 pattern, reminiscent of that observed for **6-8** (see Figure 3.1). Similar distortion of the H-D hydride resonance has not been reported for $[\text{Cp}^*\text{Ru}(\text{dppm})(\text{HD})]^{60}$, $[\text{Os}(\text{HD})(\text{dppe})_2\text{X}]^+$ (X = Cl and Br)⁶¹ or $[\text{Os}(\text{bpy})(\text{PPh}_3)_2(\text{HD})]^{2+}$,⁵⁹ where dihydrogen rotational motion is believed to be comparable to, or slower than molecular tumbling. In these cases the observed H-D coupling ($J_{\text{H-D}} = \text{ca.}$ 14-25 Hz) is not reduced by statistical averaging as for complexes **6-8** ($J_{\text{H-D}} = \text{ca.}$ 8 Hz). Therefore, a similar distortion will not be observed unless the rate of deuterium relaxation is approximately 2-3 times faster than in the iridium dihydrogen-hydride complexes **6-8**.

Comparison with Related Complexes. There are several examples of fluxional *cis*-dihydrogen-hydride complexes in the literature. Partial deuteration has been generally employed to establish the presence of the H₂ ligand, but large isotope effects such as those observed for **6-8** have not been reported. A modest upfield isotope shift has been reported by Field and coworkers in $[\text{Fe}\{\text{P}(\text{CH}_2\text{CH}_2\text{CH}_2\text{PMe}_2)_3\}(\text{H}_2)\text{H}]\text{BPh}_4$.⁶⁷ The fact that $J_{\text{H-D}}(\text{H}_2\text{D}) > J_{\text{H-D}}(\text{HD}_2)$ (10 and 9 Hz, respectively) in this iron complex is consistent with a slight preference for deuterium to concentrate in the dihydrogen ligand, opposite to the preference observed for **6-8**.

Distinct hydride resonances attributed to the H₃ and the H₂D isotopomers are observed for $[\text{Os}\{\text{P}(\text{CH}_2\text{CH}_2\text{PPh}_2)_3\}(\text{H}_2)\text{H}]\text{BPh}_4$ upon partial deuteration.³¹ The isotope shift $\delta(\text{H}_3) - \delta(\text{HD}_2)$ is claimed to be 300 ppb to lower field, however according to Table II of this paper the chemical shifts were measured in different solvents and cannot be

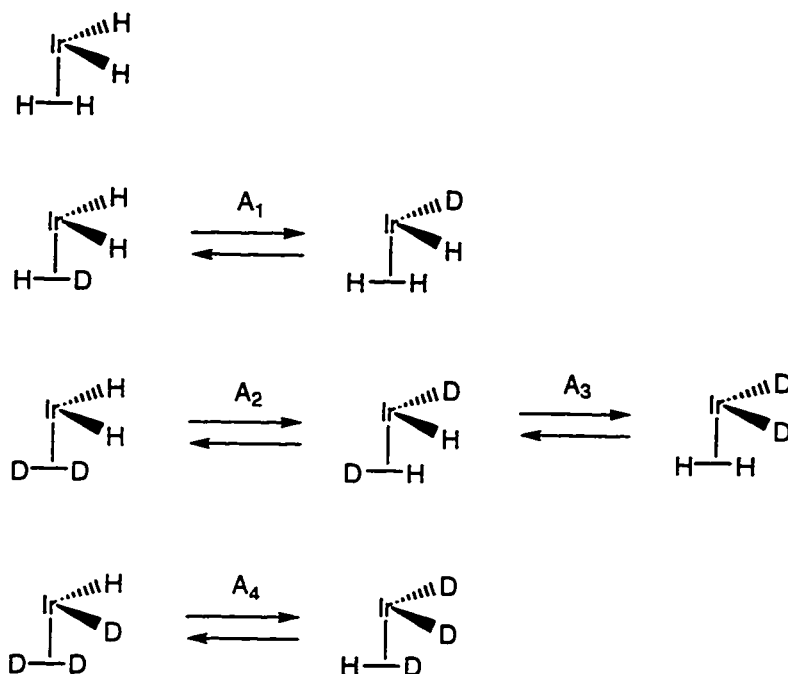
directly compared. Fortunately a ^1H NMR spectrum of the hydride region of a mixture of the H_3 and H_2D isotopomers was also included. Inspection of this figure indicates that the isotope shift is in fact *ca.* 83 ppb at 23 °C. The second isotope shift, $\delta(\text{H}_2\text{D}) - \delta(\text{HD}_2)$ is another 60 ppb to lower field. These observations are consistent with a modest preference for deuterium to concentrate in the hydride ligand, however the temperature dependence of the isotope shifts were not reported. At lower temperature the isotope shift may be similar to that observed for **6-8**. In fact, the observed H-D couplings in this complex are nearly identical to the H-D coupling constants for **6** and **8**, indicating that the dihydrogen ligand in each of these complexes is in a similar electronic environment. The zero point energy difference of H-H vs. H-D vs. D-D are probably similar between the osmium and iridium systems. Although vibrational data were not reported for the osmium complex, the Os-H and Ir-H stretches are probably similar, so that an IPR effect is expected.

Small downfield isotope shifts are also observed for *cis*- $\text{Ir}(\text{H}_2)\text{H}(\text{Cl})_2(\text{PiPr}_3)_2$.³³ The isotope shifts $\Delta_1 = \delta(\text{H}_3) - \delta(\text{H}_2\text{D})$ and $\Delta_2 = \delta(\text{H}_2\text{D}) - \delta(\text{HD}_2)$ are 40 and 30 ppb at 240 K. The H-D coupling was not clearly resolved but is estimated to be *ca.* 4 ± 1 Hz based on simulation of the experimental spectrum. The Ir-H stretch in this neutral iridium complex is nearly identical to the Ir-H stretch of **6** and **7**. Based on the observed $J_{\text{H-D}}$ coupling in $\text{Ir}(\text{H}_2)\text{H}(\text{Cl})_2(\text{PiPr}_3)_2$, the H-H bond is considerably more activated than in the cationic complexes **6-8**. Although the H-H stretch in $\text{Ir}(\text{H}_2)\text{H}(\text{Cl})_2(\text{PiPr}_3)_2$ is probably shifted to lower energy than in **6-8**, the $\text{Ir}(\text{H}_2)$ stretches are correspondingly shifted to higher energy, thereby minimizing a potential IPR effect. The absence of a large IPR effect could also result from a small chemical shift difference between the two sites.

Large temperature dependent downfield isotope shifts have been reported for $\text{Tp}^{\text{Me}_2}\text{IrH}_4$, along with substantial H-D coupling, which is suggestive of a dihydrogen-dihydride structure.¹⁶ The reported isotope shifts $\Delta_1 = \delta(\text{H}_4) - \delta(\text{H}_3\text{D})$, $\Delta_2 = \delta(\text{H}_3\text{D}) -$

$\delta(\text{H}_2\text{D}_2)$, $\Delta_3 = \delta(\text{H}_2\text{D}_2) - \delta(\text{HD}_3)$ are 171, 159, and 139 ppb at 25° C. At this temperature the averaged $J_{\text{H-D}}$ couplings are 2.5 (H_3D), 2.8 (H_2D_2), and 3.3 (HD_3) Hz. The isotope shifts increase to *ca.* 350, 330, and 285 ppb at -60 °C. However, this complex has a long T_1 (min) value of 400 ms (500 MHz), which led Poveda and co-workers to suggest a tetrahydride structure, related to that previously observed for Cp^*IrH_4 . The large isotope shifts were ascribed to an unusually large trans effect of the deuterium nucleus. Large isotope shifts are not observed for Cp^*IrH_4 . The proposed trans effect⁶⁸ does not explain the significant temperature dependence which is observed for the isotope shifts of $\text{Tp}^{\text{Me}_2}\text{IrH}_4$. An alternative explanation is that the structure is in fact a dihydrogen-dihydride complex with a stretched H-H bond. For example the corresponding rhodium complex $\text{Tp}^{\text{Me}_2}\text{Rh}(\text{H}_2)\text{H}_2$ has been formulated as a dihydrogen-dihydride species based on the observation of H-D coupling and short T_1 values for the hydride ligands.²⁷

If $\text{Tp}^{\text{Me}_2}\text{IrH}_4$ adopts a dihydrogen-dihydride structure, then the observed isotope shifts can be analyzed using the same methods we have described for 6-8. In this case, $\text{Tp}^{\text{Me}_2}\text{IrH}_4$ is an $\text{M}(\text{H}_2)\text{H}_2$, two site problem and appropriate equations which relate the observed chemical shifts and coupling constants to the limiting values are shown in scheme 3.6. In this analysis the two bond $^2J_{\text{H-D}}$ coupling between adjacent hydride ligands is assumed to be zero, which is probably not true. The analysis will then overestimate the true $^1J_{\text{H-D}}$ coupling of the dihydrogen ligand as well as the chemical shift difference between the dihydrogen and hydride ligands. The Boltzmann factors which relate the energy difference between deuterium substitution of the dihydrogen versus the hydride ligands will be underestimated if the $^2J_{\text{H-D}}$ is nonzero. The analysis also does not take into account the effect of intrinsic isotope shifts. The results calculated using the data reported at 25° C are: $\delta_{\text{H}_2} = -11.1$ ppm, $\delta_{\text{H}} = -18.3$ ppm, $^1J_{\text{H-D}} = 17.5$ Hz, $\Delta E_1 = -169$ cal/mol, $\Delta E_2 = -103$ cal/mol, $\Delta E_3 = -203$ cal/mol, and $\Delta E_4 = -155$ cal/mol.



$$\delta(H_4) = \frac{2\delta_{H_2} + 2\delta_H}{4}$$

$$\delta(H_3D) = \frac{\delta_{H_2} + 2A_1\delta_{H_2} + 2\delta_H + A_1\delta_H}{3 + 3A_1}$$

$$J(H_3D) = \frac{{}^1J_{H-D} + A_1{}^2J_{H-D}}{3 + 3A_1}$$

$$\delta(H_2D_2) = \frac{\delta_H + 2A_2\delta_{H_2} + 2A_2\delta_H + A_2A_3\delta_{H_2}}{1 + 4A_2 + A_2A_3}$$

$$J(H_2D_2) = \frac{A_2{}^1J_{H-D} + A_2{}^2J_{H-D}}{1 + 4A_2 + A_2A_3}$$

$$\delta(HD_3) = \frac{\delta_H + A_4\delta_{H_2}}{1 + A_4}$$

$$J(HD_3) = \frac{{}^2J_{H-D} + A_4{}^1J_{H-D}}{3 + 3A_4}$$

Scheme 3.4

The results of this analysis are similar to those calculated for **6-8**. The $^1J_{\text{H-D}}$ coupling constant calculated for the neutral $\text{Tp}^{\text{Me}_2}\text{IrH}_4$ complex is significantly smaller than in the cationic iridium complexes, indicating a longer H-H bond. Further structural information on this interesting complex would be very desirable. An analysis of the isotope shifts in the ^2H NMR spectrum similar to that undertaken using ^3H NMR spectroscopy in this work may be useful.

While large isotope effects are observed for $[\text{TpIr}(\text{PR}_3)(\text{H}_2)\text{H}]\text{BF}_4$ and $\text{Tp}^{\text{Me}_2}\text{IrH}_4$, the corresponding rhodium complexes reveal virtually none (e.g. $[(\text{TpRh}(\text{PPh}_3)(\text{H}_2)\text{H})\text{B}(\text{Ar})_4]$) or only small isotope shifts (e.g. $\text{Tp}^{\text{Me}_2}\text{Rh}(\text{H}_2)\text{H}_2$). This observation follows from a less activated H_2 ligand and a weaker M-H bond in the second row complexes. In this circumstance the zero point energy differences between the dihydrogen and the hydride ligands are expected to approximately cancel.

Conclusion

Protonation of $\text{TpM}(\text{PR}_3)\text{H}_2$ ($\text{M} = \text{Rh}$ and Ir) complexes affords highly dynamic dihydrogen-hydride complexes which reveal only a single hydride resonance at all accessible temperatures in the ^1H NMR spectrum. Short $T_1(\text{min})$ values of 21-22 ms (Ir) and 7 ms (Rh) indicate an H-H bond length of 0.88-1.11 Å in the iridium complexes and 0.73-0.92 Å in the rhodium complex depending on the relative rate of the dihydrogen rotational motion. In the case of the iridium complexes, partial substitution of the hydride positions with deuterium or tritium results in large temperature dependent isotope shifts, which result from a preference for the heavy hydrogen isotope to occupy the hydride site. Analysis of this effect gives the limiting chemical shifts of the dihydrogen and hydride ligands as well as the $^1J_{\text{H-D}}$ coupling constant (*ca.* 25 Hz). An H-D coupling constant of this magnitude is consistent with an H-H bond length of *ca.* 1 Å for the iridium complexes.

Experimental

The general experimental methods have been described in the experimental section of chapter 2. The procedures employed to safely store and manipulate tritium gas have been outlined previously.⁴⁸

Synthesis of Complexes.

$[(C_5Me_5)Ir(PMe_3)H_3]SO_3CF_3$. To a 300 mL glass bomb fitted with a Kontes valve was added $(C_5Me_5)Ir(PMe_3)Cl_2$ ⁶⁹ (2.01 g, 4.24 mmol), $AgSO_3CF_3$ (2.37 g, 9.2 mmol) and a teflon coated stir bar. CH_2Cl_2 (50 mL) was vacuum transferred into the flask and the head space backfilled with H_2 (1000 torr). The flask was covered with aluminum foil and allowed to stir overnight to yield a pale orange solution containing white precipitate. The insoluble $AgCl$ was filtered off. The volume of the filtrate was reduced under vacuum and then layered with Et_2O to afford colorless crystals upon standing at $-30\text{ }^\circ C$ for 3 days. These were washed with Et_2O (3 x 5 mL) and dried under vacuum. Yield 2.06 g (88%). The product was characterized by comparison of its 1H NMR spectrum to the literature.⁷⁰

$[(C_5Me_5)Ir(PPh_3)H_3]BF_4$. This complex was prepared from $(C_5Me_5)Ir(PPh_3)Cl_2$ ¹⁴ by a procedure identical to that employed to prepare $[(C_5Me_5)Ir(PMe_3)H_3]SO_3CF_3$. $AgBF_4$ was substituted for $AgSO_3CF_3$. Yield 60%; characterized by 1H NMR spectroscopy.⁹

$TpIr(PMe_3)H_2$. A colorless solution of $[(C_5Me_5)Ir(PMe_3)H_3]SO_3CF_3$ (146 mg, 0.263 mmol) in CH_3CN (15 mL) was stirred under argon at room temperature for 2-3 days. In the glove box, $NaTp$ (66 mg, 0.280 mmol) was added and then stirred at room temperature for an additional 2 days. The volatiles were stripped under vacuum and the resulting residue taken up in a minimum of toluene. Working in the air, the complex was isolated following chromatography on alumina, eluting with toluene (column measured 10 mm x 230 mm). Fractions containing the desired complex were identified by TLC and combined. The toluene was removed by rotary evaporation and the residue

crystallized by adding wet MeOH. The resulting white powder was dried under vacuum to yield 70 mg (55%) of analytically pure product. ^1H NMR (CD_2Cl_2): 7.70, 7.63 (d, 2 H each, 3,5-pz_{eq}); 7.67, 7.59 (m, 1 H each, 3,5-pz_{ax}); 6.18 (t, 2 H, 4-pz_{eq}); 6.08 (m, 1 H, 4-pz_{ax}); 1.63 (d, $J_{\text{P-H}} = 10.0$ Hz, 9 H, PMe_3); -21.3 (d, $J_{\text{P-H}} = 25.0$ Hz, 2 H, Ir-*H*). $^{13}\text{C}\{^1\text{H}\}$ NMR (CD_2Cl_2): 146.2, 134.0 (s, 1 C, 3,5-pz_{ax}); 144.0, 138.8 (s, 2 C, 3,5-pz_{eq}); 105.8 (s, 1 C, 4-pz_{ax}); 105.6 (s, 2 C, 4-pz_{eq}); 21.7 (d, $J_{\text{P-C}} = 39.4$ Hz). $^{31}\text{P}\{\text{Me } ^1\text{H}\}$ NMR (CD_2Cl_2): -45.6 (t, $J_{\text{P-H}} = 25$ Hz). ^1H NMR (C_6D_6): 7.93, 7.34 (br s and m respectively, 1 H each, 3,5-pz_{ax}); 7.57, 7.53 (d, 2 H each, 3,5-pz_{eq}); 5.94 (t, 2 H, 4-pz_{eq}); 5.68 (m, 1 H, 4-pz_{ax}); 1.32 (d, $J_{\text{P-H}} = 9.9$ Hz, PMe_3); -20.56 (d, $J_{\text{P-H}} = 25.5$ Hz, 2 H, Ir-*H*). $^{13}\text{C}\{^1\text{H}\}$ NMR (C_6D_6): 146.4, 133.3 (s, 1 C each, 3,5-pz_{ax}); 144.1, 134.4 (s, 2 C, 3,5-pz_{eq}); 105.7 (s, 1 C, 4-pz_{ax}); 105.4 (s, 2 C, 4-pz_{eq}); 21.5 (d, $J_{\text{P-C}} = 38.8$ Hz, PMe_3). $^{31}\text{P}\{\text{Me } ^1\text{H}\}$ NMR (C_6D_6): -46.55 (t, $J_{\text{P-H}} = 24.3$ Hz). IR: 2482 ($\nu_{\text{B-H}}$); 2143 ($\nu_{\text{Ir-H}}$). MS: m/z 484 (M^+). Anal. Calcd for $\text{C}_{12}\text{H}_{21}\text{BIrN}_6\text{P}$: C, 29.83; H, 4.38; N, 17.39. Found: C, 29.51; H, 4.83; N, 17.26.

$\text{TpIr}(\text{PPh}_3)\text{H}_2$ (2). Prepared as above, starting from $[(\text{C}_5\text{Me}_5)\text{Ir}(\text{PPh}_3)\text{H}_3]\text{BF}_4$. Yield: 60%. Alternatively complex **2** was prepared from $\text{TpIr}(\text{C}_2\text{H}_4)_2$ following the procedure outlined in chapter 2. Characterization data is given in the experimental section of chapter 2.

$\text{Tp}^{\text{Me}_2}\text{Ir}(\text{PMe}_3)\text{H}_2$ This complex was prepared on an 1.5 mmol scale by a procedure identical to that described for the Tp analog. Yield 74%. ^1H NMR (CD_2Cl_2): 5.84 (s, 2 H, 4-pz_{eq}); 5.70 (s, 1 H, 4-pz_{ax}); 2.41, 2.26 (s, 6 H each, 3,5-Me₂pz_{eq}); 2.26, 2.09 (s, 3 H each, 3,5-Me₂pz_{ax}); 1.63 (d, $J_{\text{P-H}} = 9.6$ Hz, 9 H, PMe_3); -22.11 (d, $J_{\text{P-H}} = 26.7$ Hz, 2 H, Ir-*H*). $^{13}\text{C}\{^1\text{H}\}$ NMR (CD_2Cl_2): 150.8, 144.7 (3,5-pz_{eq}); 150.0, 143.5 (3,5-pz_{ax}); 106.0 (4-pz_{eq}); 104.7 (4-pz_{ax}); 24.2 (d, $J_{\text{P-C}} = 38.2$ Hz, PMe_3); 17.35, 13.0 (3,5-Me₂pz_{eq}); 17.75, 12.7 (3,5-Me₂pz_{ax}). $^{31}\text{P}\{^1\text{H}\}$ NMR (CD_2Cl_2): -53.0 (s). ^1H NMR (C_6D_6): 5.76 (s, 2 H, 4-pz_{eq}); 5.47 (s, 1 H 4-pz_{ax}); 2.41, 2.10 (s, 3 H each, 3,5-Me₂pz_{ax}); 2.30, 2.27 (s, 6 H, 3,5-Me₂pz_{eq}); 1.41 (d, $J_{\text{P-H}} = 9.6$ Hz, 9 H, PMe_3); -21.21

(d, $J_{P-H} = 26.1$ Hz, 2 H, Ir-*H*). $^{13}C\{^1H\}$ NMR (C_6D_6): 150.5, 144.1 (3,5-*pz*_{eq}); 149.8, 142.4 (3,5-*pz*_{ax}); 106.0 (4-*pz*_{eq}); 104.9 (4-*pz*_{ax}); 23.6 (d, $J_{P-C} = 37.3$ Hz, PMe_3); 17.5, 12.9 (3,5- Me_2 -*pz*_{eq}); 17.6, 12.6 (3,5- Me_2 -*pz*_{ax}). $^{31}P\{Me^1H\}$ NMR (C_6D_6): -52.0 (t, $J_{P-H} = 24.7$ Hz). IR: 2511 (ν_{B-H}); 2138 (ν_{Ir-H}). Anal. Calcd for $C_{18}H_{33}BIrN_6P$: C, 38.10; H, 5.86; N, 14.81. Found: C, 38.67; H, 5.94; N, 14.55.

[TpIr(PMe₃)(H₂)H]BF₄. To a 50 mL schlenk flask containing a solution of TpIr(PMe₃)H₂ (24 mg, 0.050 mmol) in Et₂O (5 mL) at -78 °C was added HBF₄•Et₂O (85%, 10 mL, 0.07 mmol) dropwise. This was allowed to gradually warm to room temperature as fine white microcrystals precipitated from solution. The product was filtered off and washed with Et₂O (2 mL) and dried under vacuum. Yield 25 mg (87%). 1H NMR (CD_2Cl_2): 7.87, 7.85 (d, 2 H each, 3,5-*pz*_{eq}); 7.69, 7.67 (br s, 1 H each, 3,5-*pz*_{ax}); 6.43 (t, 2 H, 4-*pz*_{ax}); 6.21 (m, 1 H, 4-*pz*_{ax}); 1.78 (d, $J_{P-H} = 11$ Hz, 9 H, PMe_3); -10.40 (d, $J_{P-H} = 11$ Hz, 3 H, Ir-*H*). $^{13}C\{^1H\}$ NMR (CD_2Cl_2): 146.1, 135.8 (3,5-*pz*_{ax}); 144.9, 136.8 (3,5-*pz*_{eq}); 107.8 (4-*pz*_{eq}); 107.3 (4-*pz*_{ax}); 17.9 (d, $J_{P-C} = 42.9$ Hz, PMe_3). $^{31}P\{Me^1H\}$ NMR (CD_2Cl_2): -42.7 (q, $J_{P-H} = 9.8$ Hz). 1H NMR ($CDCl_2F$): 7.87, 7.79 (d, 2 H each, 3,5-*pz*_{eq}); 7.68, 7.59 (br s, 1 H each, 3,5-*pz*_{ax}); 6.40 (t, 2 H, 4-*pz*_{eq}); 6.13 (m, 1 H, 4-*pz*_{ax}); 1.76 (d, $J_{P-H} = 11.6$ Hz, 9 H, PMe_3); -10.42 (d, $J_{P-H} = 10.5$ Hz, 3 H, Ir-*H*). IR: 2499 (ν_{B-H}); 2199 (ν_{Ir-H}). Anal Calcd for $C_{12}H_{22}B_2F_4IrPN_6$: C, 25.24; H, 3.88; N, 14.72. Found: C, 25.45; H, 4.03; N, 14.40.

[Tp^{Me2}Ir(PMe₃)(H₂)H][B(3,5-(CF₃)₂C₆H₃)₄]. A typical sample was prepared by vacuum transfer of CD_2Cl_2 (0.4 mL) into an NMR tube (sealed to a Kontes valve vacuum line adaptor) containing Tp^{Me2}Ir(PMe₃)H₂ (12.8 mg, 0.023 mmol) and $[H(Et_2O)_2][B(3,5-(CF_3)_2C_6H_3)_4]^{71}$ (23 mg, 0.023 mmol) and then flame sealed under vacuum. 1H NMR (CD_2Cl_2): 7.73 (br, 8 H, *o*- $C_6H_3(CF_3)_2$); 7.58 (s, 4 H, *p*- $C_6H_3(CF_3)_2$); 6.08 (s, 2 H, 4-*pz*_{eq}); 5.75 (s, 1 H, 4-*pz*_{ax}); 2.46, 2.35 (s, 6 H each, 3,5-*pz*_{eq}); 2.25, 2.06 (s, 3 H each, 3,5-*pz*_{ax}); 1.63 (d, $J_{P-H} = 10.7$ Hz, 9 H, PMe_3); -11.0 (v br, 3 H, Ir-*H*). $^{31}P\{^1H\}$ NMR (CD_2Cl_2): -49.2 (s).

[TpIr(PPh₃)(H₂)H]BF₄. Methylene chloride was added dropwise to a suspension of TpIr(PPh₃)H₂ in Et₂O until a homogeneous solution was obtained. To this solution was added one equiv. of HBF₄•Et₂O, which was then reduced in volume under vacuum and stored at -30 °C overnight to afford a colorless powder which was filtered off, washed with Et₂O and dried under vacuum. This material did not yield a satisfactory elemental analysis. We note that a color change was observed from white to pale pink when this complex was exposed to vacuum and suspect that decomposition following loss of H₂ may explain the unsatisfactory analytical data. ¹H NMR (CD₂Cl₂): 7.83, 6.79 (d, 2 H each, 3,5-pz_{eq}); 7.76, 7.70 (m, 1 H each, 3,5-pz_{ax}); 7.58 (m, 3 H, *p*-C₆H₆); 7.44, 7.16 (m, 6 H each, *o*- and *m*-C₆H₆); 6.25 (m, 1 H, 4-pz_{ax}); 6.09 (t, 2 H, 4-pz_{eq}); -9.77 (br, 3 H, Ir-H). ³¹P{¹H} NMR (CD₂Cl₂): 1.1 (s). IR: 2502 (ν_{B-H}); 2197 (ν_{Ir-H}). Anal. Calcd for C₂₇H₂₈B₂F₄IrN₆P: C, 42.83; H, 3.73; N, 11.1. Found: C, 40.00; H, 4.25; N, 9.20.

[TpRh(PPh₃)(H₂)H][B(3,5-(CF₃)₂C₆H₃)₄]. A typical sample was prepared by vacuum transfer of CD₂Cl₂ into an NMR tube (fitted with a Kontes valve vacuum line adaptor) containing TpRh(PPh₃)H₂ (2.6 mg, 0.0045 mmol) and [H(Et₂O)₂][B(3,5-(CF₃)₂C₆H₃)₄] (5 mg, 0.0049 mmol) and then flame sealed under vacuum. The sample was warmed to -78 °C and stored at this temperature until immediately before being transferred to a precooled NMR probe (< 250 K). ¹H NMR (CD₂Cl₂): 7.80, 6.57 (d, 2 H each, 3,5-pz_{eq}); 7.72 (br, 8 H, *o*-C₆H₃(CF₃)₂); 7.57 (br, shoulder on *p*-C₆H₃(CF₃)₂ resonance); 7.54 (br, 3 H, *p*-C₆H₃(CF₃)₂); 7.41, 7.09 (m, 6 H each, *o*- and *m*-C₆H₅PPh₂); 6.22 (br m, 1 H, 4-pz_{ax}); 6.02 (t, 2 H, 4-pz_{eq}); -7.95 (br, 3 H, Rh-H).

X-ray Structure of [TpIr(PMe₃)(H₂)H]BF₄•CH₂Cl₂. Clear colorless crystals suitable for x-ray diffraction were obtained by slow diffusion of Et₂O into a CH₂Cl₂ solution of [TpIr(PMe₃)(H₂)H]BF₄ contained in a 5 mm glass tube. Diffraction measurements were made on a crystal fragment of dimensions 0.3 x 0.3 x 0.35 mm in a nitrogen stream at 183 K on an Enraf-Nonius CAD4 diffractometer using graphite-

monochromated MoK α radiation ($\lambda = 0.71073 \text{ \AA}$). An orientation matrix was determined from 24 centered peaks in the range of $28^\circ \leq 2\Theta \leq 34^\circ$. Monoclinic symmetry (space group P2₁/n) was indicated based on systematic absences. The cell parameters $a = 10.560(2) \text{ \AA}$, $b = 13.500(3) \text{ \AA}$, $c = 15.880(3) \text{ \AA}$, $\beta = 92.54(3)^\circ$, $V = 2261.6(11) \text{ \AA}^3$ ($Z = 4$) with a calculated density of 1.918 g/cm^3 . There were 3960 unique reflections collected, with $2\Theta < 50^\circ$, of those reflections 3196 with $I \geq 4\sigma I$ were adjudged observed. Reduction of the data was carried out with XCAD4 and further work was carried out using Siemens version of SHELX.

The structure was solved by direct methods, which agreed with the results of a Patterson function, and the iridium atom located reduced the R factor to 22%. The rest of the atoms were found from difference maps. The full refinement proceeded to a final R of 4.5% and a R_w of 5.9%, with a GOF of 1.9. The weighting scheme required a correction factor of 0.0015. Tables of crystal data and parameters, atomic coordinates, and anisotropic thermal parameters are included below.

Table 3.7 Crystal Data and Parameters for $6 \cdot \text{CH}_2\text{Cl}_2$.

Empirical formula	$\text{C}_{13}\text{H}_{21}\text{B}_2\text{Cl}_2\text{F}_4\text{IrN}_6\text{P}$
Color; Habit	Clear Fragment
Crystal size (mm)	0.2 0.25 0.3
Crystal System	Monoclinic
Space group	$\text{P}2_1/\text{n}$
Unit cell dimensions	$a = 10.560(2) \text{ \AA}$ $b = 13.500(3) \text{ \AA}$ $c = 15.880(3) \text{ \AA}$ $\beta = 92.54(3)^\circ$
Volume	$2261.6(11) \text{ \AA}^3$
Z	4
Formula weight	653.0
Density (calc)	1.918 mg/m^3
Adsorption Coefficient	6.255 mm^{-1}
F(000)	1252
Radiation	$\text{MoK}\alpha$ ($\lambda = 0.71073 \text{ \AA}$)
Temperature (K)	183
Monochromator	Highly oriented graphite crystal
2Θ Range	2.0 to 50.0°
Scan Type	ω
Scan Speed	Variables; 1.5 to $5.5^\circ/\text{min}$ in ω
Scan Range (ω)	$0.8 + 0.35(\tan \omega)^\circ$
Reflections Collected	4955
Independent reflections	3960 ($R_{\text{int}} = 3.64\%$)
Observed Reflections	3196 ($F > 4.0 \sigma(F)$)
Number of Parameters Refined	269
Final R Indices (obs. data)	$R = 4.45\%$, $wR = 5.88\%$
R Indices (all data)	$R = 5.66\%$, $wR = 8.77\%$
Goodness of Fit	1.89

Table 3.8. Atomic coordinates ($\times 10^5$) and equivalent isotropic displacement coefficients ($\text{\AA}^2 \times 10^4$)

atom	x	y	z	U(eq)
Ir	5863(3)	24551(2)	12554(2)	199(2)
P	602(24)	38062(19)	20274(17)	248(8)
C(10)	12433(111)	42031(88)	27793(74)	421(40)
C(11)	-3243(105)	48903(72)	14023(67)	343(35)
C(12)	-12836(93)	36194(83)	26622(73)	370(37)
B(1)	10355(111)	22093(82)	-7222(84)	263(36)
N(1)	-3434(90)	25567(48)	-5907(60)	243(27)
N(2)	-7296(79)	27505(59)	2042(53)	242(25)
C(1)	-12813(108)	27532(77)	-11532(71)	321(34)
C(2)	-23431(97)	30742(74)	-7426(74)	3589(36)
C(3)	-19570(87)	30501(72)	1143(70)	301(33)
N(3)	11402(66)	12009(51)	5754(51)	188(24)
N(4)	12712(67)	12388(55)	-2417(54)	250(26)
C(4)	14382(90)	2712(65)	8316(69)	266(31)
C(5)	17676(88)	-2710(71)	1416(73)	321(34)
C(6)	16464(89)	3530(71)	-5359(69)	275(31)
N(5)	18966(68)	30169(59)	-2913(50)	226(24)
N(6)	18640(65)	32214(54)	5491(52)	212(24)
C(7)	28065(90)	35833(70)	-6343(72)	324(34)
C(8)	33596(92)	41617(77)	195(67)	321(34)
C(9)	27865(91)	39202(70)	7394(71)	304(33)
B(2)	-4360(116)	-1591(92)	29974(79)	326(38)
F(1)	3484(66)	5414(52)	33917(50)	582(27)
F(2)	-13272(60)	3237(48)	25022(42)	4444(22)
F(3)	331(68)	-7845(55)	25140(46)	566(26)
F(4)	-9986(67)	-7246(51)	36121(42)	485(23)
Cl(1)	-37105(35)	15346(25)	16954(23)	596(12)
Cl(2)	-53624(45)	13849(36)	2047(38)	1095(23)
Cl(3)	-49532(142)	20230(91)	11125(92)	547(49)

Equivalent isotropic U defined as one third of the trace of the orthogonalized U_{ij} tensor.

Table 3.9. Anisotropic displacement coefficients ($\text{\AA}^2 \times 10^4$)

atom	U_{11}	U_{22}	U_{33}	U_{12}	U_{13}	U_{23}
Ir	209(3)	154(3)	234(3)	-3(1)	12(2)	16(1)
P	253(13)	244(14)	245(14)	19(10)	-6(11)	-66(11)
C(10)	446(68)	440(68)	371(69)	67(52)	-57(56)	-141(55)
C(11)	439(63)	268(55)	320(63)	77(46)	-16(52)	-66(47)
C(12)	257(55)	434(66)	432(69)	26(45)	171(51)	-99(54)
B(1)	244(60)	181(53)	365(72)	-4(45)	0(54)	117(51)
N(1)	269(46)	188(46)	271(50)	-38(29)	-15(39)	42(32)
N(2)	334(47)	153(36)	238(45)	26(35)	25(37)	1(35)
C(1)	443(67)	204(47)	304(61)	11(48)	-104(52)	-24(47)
C(2)	288(55)	256(55)	513(73)	4(43)	-179(52)	31(50)
C(3)	195(48)	262(52)	444(69)	3(39)	-11(47)	-71(46)
N(3)	148(37)	142(38)	282(48)	26(29)	92(33)	41(33)
N(4)	155(39)	215(42)	379(53)	54(31)	-5(36)	-33(36)
C(4)	279(52)	149(46)	376(63)	30(38)	91(46)	93(42)
C(5)	246(52)	173(48)	547(74)	54(38)	46(50)	-18(48)
C(6)	232(50)	270(52)	331(59)	-57(39)	83(44)	-35(45)
N(5)	174(38)	278(44)	221(43)	13(32)	-23(33)	58(35)
N(6)	135(37)	171(38)	330(49)	-74(29)	-2(34)	-14(33)
C(7)	239(51)	290(56)	446(68)	71(42)	67(48)	183(50)
C(8)	257(54)	360(60)	349(63)	-240(44)	40(47)	16(49)
C(9)	287(54)	195(47)	424(67)	-49(40)	-60(49)	-35(45)
B(2)	372(67)	346(67)	252(65)	-54(53)	-88(54)	103(52)
F(1)	514(43)	540(46)	673(52)	-143(34)	-188(38)	-94(39)
F(2)	453(37)	499(40)	366(38)	-22(30)	-120(31)	136(32)
F(3)	596(44)	614(47)	505(45)	61(35)	220(37)	-83(38)
F(4)	567(40)	514(43)	385(38)	25(33)	148(32)	200(33)
Cl(1)	770(24)	439(19)	577(22)	10(16)	-5(18)	124(16)
Cl(2)	840(32)	906(34)	1481(49)	174(25)	-593(33)	-435(33)
C(13)	662(87)	341(69)	656(97)	64(62)	220(74)	-112(64)

The anisotropic displacement exponent takes the form:

$$-2\pi^2 (h^2 a^2 U_{11} + \dots + 2hka^*b^*U_{12})$$

Notes to Chapter 3.

- (1) Kubas, G. J.; Ryan, R. R.; Swanson, B. I.; Vergamini, P. J.; Wasserman, H. J. *J. Am. Chem. Soc.* **1984**, *106*, 451-452.
- (2) Heinekey, D. M.; Oldham, W. J., Jr. *Chem. Rev.* **1993**, *93*, 913-926.
- (3) Hamilton, D. G.; Crabtree, R. H. *J. Am. Chem. Soc.* **1988**, *110*, 4126-4133.
- (4) Desrosiers, P. J.; Cai, L.; Lin, Z.; Richards, R.; Halpern, J. *J. Am. Chem. Soc.* **1991**, *113*, 4173-4184.
- (5) Bautista, M. T.; Earl, K. A.; Maltby, P. A.; Morris, R. H.; Schweitzer, C. T.; Sella, A. *J. Am. Chem. Soc.* **1988**, *110*, 7031-7036.
- (6) Heinekey, D. M.; Millar, J. M.; Koetzle, T. F.; Payne, N. G.; Zilm, K. W. *J. Am. Chem. Soc.* **1990**, *112*, 909-919.
- (7) Heinekey, D. M.; Hinkle, A. S.; Close, J. D. *J. Am. Chem. Soc.* **1996**, *118*, 5353-5361.
- (8) Heinekey, D. M.; Oldham, W. J., Jr. *J. Am. Chem. Soc.* **1994**, *116*, 3137-3138.
- (9) Peterson, A.; Tilset, M. *Organometallics* **1993**, *12*, 3064-3068.
- (10) Sanders, J. K. M.; Hunter, B. K. *Modern NMR Spectroscopy*; Oxford University Press: Oxford, 1989.
- (11) Akitt, J. W. *NMR and Chemistry*; 3rd ed.; Chapman & Hall: London, 1992.
- (12) Fernández, M. J.; Rodríguez, M. J.; Oro, L. A.; Lahoz, F. J. *J. Chem. Soc., Dalton Trans.* **1989**, 2073-2079.
- (13) Bovens, M.; Gerfin, T.; Gramlich, V.; Petter, W.; Venanzi, L. M.; Haward, M. T.; Jackson, S. A.; Eisenstein, O. *New. J. Chem.* **1992**, *16*, 337-345.
- (14) Kang, J. W.; Moseley, K.; Maitlis, P. M. *J. Am. Chem. Soc.* **1969**, *91*, 5970-5977.
- (15) May, S.; Reinsalu, P.; Powell, J. *Inorg. Chem.* **1980**, *19*, 1582-1589.
- (16) Paneque, M.; Poveda, M. L.; Toboada, S. *J. Am. Chem. Soc.* **1994**, *116*, 4519-4520.

- (17) The rate of relaxation (R) is used in preference to the relaxation time (T_1) because rates are additive.
- (18) Saunders, M.; Kates, M. R. *J. Am. Chem. Soc.* **1977**, *99*, 8070-8071.
- (19) Hamilton, D. G.; Luo, X. L.; Crabtree, R. H. *Inorg. Chem.* **1989**, *28*, 3198-3203.
- (20) Luo, X. L.; Crabtree, R. H. *J. Am. Chem. Soc.* **1990**, *112*, 4813-4821.
- (21) Luo, X.; Michos, D.; Crabtree, R. H. *Organometallics* **1992**, *11*, 237-241.
- (22) Baird, G. J.; Davies, S. G.; Moon, S. D.; Simpson, S. J.; Jones, R. H. *J. Chem. Soc., Dalton Trans.* **1985**, 1479-1486.
- (23) Casey, C. P.; Tanke, R. S.; Hazin, P. N.; Kemnitz, C. R.; McMahon, R. J. *Inorg. Chem.* **1992**, *31*, 5474-5479.
- (24) Heinekey, D. M.; Payne, N. G.; Sofield, C. D. *Organometallics* **1989**, *8*, 1824-1826.
- (25) Antoniutti, S.; Albertin, G.; Amendola, P.; Bordignon, E. *J. Chem. Soc., Chem. Comm.* **1989**, 229-230.
- (26) Earl, K. A.; Jia, G.; Maltby, P. A.; Morris, R. H. *J. Am. Chem. Soc.* **1991**, *113*, 3027-3039.
- (27) Nanz, D.; Philipsborn, W. v.; Bucher, U. E.; Venanzi, L. M. *Magnetic Resonance in Chemistry* **1991**, *29*, S38-44.
- (28) Michos, D.; Luo, X.; Crabtree, R. H. *Inorg. Chem.* **1992**, *31*, 4245-4250.
- (29) Collman, J. P.; Wagenknecht, P. S.; Hutchison, J. E.; Lewis, N. S.; Lopez, M. A.; Guillard, R.; L'Her, M.; Bothner-By, A. A.; Mishra, P. K. *J. Am. Chem. Soc.* **1992**, *114*, 5654-5664.
- (30) Miller, R. L.; Toreki, R.; LaPointe, R. E.; Wolczanski, P. T.; Van Duyne, G. D.; Roe, D. C. *J. Am. Chem. Soc.* **1993**, *115*, 5570-5588.
- (31) Bianchini, C.; Linn, K.; Masi, D.; Peruzzini, M.; Polo, A.; Vacca, A.; Zanobini, F. *Inorg. Chem.* **1993**, *32*, 2366-2376.

- (32) Heinekey, D. M.; Liegeois, A.; van Roon, M. *J. Am. Chem. Soc.* **1994**, *116*, 8388-8389.
- (33) Albinati, A.; Bakhmutov, V. I.; Caulton, K. G.; Clot, E.; Eckert, J.; Eisenstein, O.; Gusev, D. G.; Grushin, V. V.; Hauger, B. E.; Klooster, W. T.; Koetzle, T. F.; McMullan, R. K.; O'Loughlin, T. J.; Pélissier, M.; Ricci, J. S.; Sigalas, M. P.; Vymenits, A. B. *J. Am. Chem. Soc.* **1993**, *115*, 7300-7312.
- (34) Bullock, R. M.; Song, J.; Szalda, D. J. *Organometallics* **1996**, *15*, 2504-2516.
- (35) Luo, X.; Crabtree, R. H. *J. Am. Chem. Soc.* **1990**, *112*, 6912-6918.
- (36) Gusev, D. G.; Bakhmutov, V. I.; Gushin, V. V.; Vol'pin, M. E. *Inorg. Chim. Acta.* **1990**, *177*, 115.
- (37) Hostetler, M. J.; Bergman, R. G. *J. Am. Chem. Soc.* **1992**, *114*, 7629-7636.
- (38) Rabinovich, D.; Parkin, G. *J. Am. Chem. Soc.* **1993**, *115*, 353-354.
- (39) Abu-Hasanayn, F.; Krogh-Jespersen, K.; Goldman, A. S. *J. Am. Chem. Soc.* **1993**, *115*, 8019-8023.
- (40) Tritium incorporation in these complexes was carried out by Amber Hinkle using T₂ gas. General incorporation procedures have been outlined in reference 48.
- (41) Calvert, R. B.; Shapley, J. R. *J. Am. Chem. Soc.* **1978**, *100*, 7726-7727.
- (42) Kubas, G. J. *Acc. Chem. Res.* **1988**, *21*, 120-128.
- (43) Bullock In *Transition Metal Hydrides*; A. Dedieu, Ed.; VCH Publishers, Inc.: New York, 1992; pp 263-307.
- (44) Lowry, T. H.; Richardson, K. *Mechanism and Theory in Organic Chemistry*; Harper and Row: New York, 1976.
- (45) Kubas, G. J.; Ryan, R. R. *Polyhedron* **1986**, *5*, 473-485.
- (46) Heinekey, D. M.; Payne, N. G.; Schulte, G. K. *J. Am. Chem. Soc.* **1988**, *110*, 2303-2305.
- (47) Werner, H.; Wolf, J.; Höhn, A. *J. Organometal. Chem.* **1985**, *287*, 395-407.
- (48) Hinkle, A. S. Ph.D. Thesis, University of Washington, 1995.

- (49) Halcrow, M. A.; Chaudret, B.; Trofimenko, S. *J. Chem. Soc., Chem. Commun.* **1993**, 465-467.
- (50) Moreno, B.; Sabo-Etienne, S.; Chaudret, B.; Rodriguez-Fernandez, A.; Jalon, F.; Trofimenko, S. *J. Am. Chem. Soc.* **1994**, *116*, 2635-2636.
- (51) Moreno, B.; Sabo-Etienne, S.; Chaudret, B.; Rodriguez, A.; Jalon, F.; Trofimenko, S. *J. Am. Chem. Soc.* **1995**, *117*, 7441-7451.
- (52) Arliguie, T.; Border, C.; Chaudret, B. *Organometallics* **1989**, *8*, 1308.
- (53) Trofimenko, S. *Chem. Rev.* **1993**, *93*, 943-980.
- (54) Fernandez, M. J.; Rodriguez, M. J.; Oro, L. A. *J. Organometal. Chem.* **1992**, *438*, 337-342.
- (55) Shapley, J. R.; Adair, P. C.; Lawson, J. R.; Pierpont, C. G. *Inorg. Chem.* **1982**, *21*, 1702-1704.
- (56) Ciriano, M. A.; Fernández, M. J.; Modrego, J.; Rodríguez, M. J.; Oro, L. A. *J. Organometal. Chem.* **1993**, *443*, 249-252.
- (57) Szajek, L. P.; Lawson, R. J.; Shapley, J. R. *Organometallics* **1991**, *10*, 357-361.
- (58) Curtis, M. D.; Shiu, K.; Butler, W. M.; Huffman, J. C. *J. Am. Chem. Soc.* **1986**, *108*, 3335-3343.
- (59) Heinekey, D. M.; Luther, T. A. *Inorg. Chem.* **1996**, *35*, in press.
- (60) Klooster, W. T.; Koetzle, T. F.; Jia, G.; Fong, T. P.; Morris, R. H.; Albinati, A. *J. Am. Chem. Soc.* **1994**, *116*, 7677-7681.
- (61) Maltby, P. A.; Schlaf, M.; Steinbeck, M.; Lough, A. J.; Morris, R. H.; Klooster, W. T.; Koetzle, T. F.; Srivastava, R. C. *J. Am. Chem. Soc.* **1996**, *118*, 5396-5407.
- (62) Heinekey, D. M.; Payne, N. G.; Sofield, C. D. *Organometallics* **1990**, *9*, 2643-2645.
- (63) Jalón, F. A.; Otero, A.; Manzano, B. R.; Villaseñor, E.; Chaudret, B. *J. Am. Chem. Soc.* **1995**, *117*, 10123-10124.

- (64) Sabo-Etienne, S.; Chaudret, B.; el Makarim, H. A.; Barthelat, J.; Daudey, J.; Ulrich, S.; Limbach, H.; Moïse, C. *J. Am. Chem. Soc.* **1995**, *117*, 11602-11603.
- (65) Maseras, F.; Duran, M.; Lledós, A.; Bertrán, J. *J. Am. Chem. Soc.* **1992**, *114*, 2922-2928.
- (66) Luo, X. L.; Crabtree, R. H. *J. Chem. Soc., Chem. Commun.* **1990**, 189-190.
- (67) Bampos, N.; Field, L. D. *Inorg. Chem.* **1990**, *29*, 587-588.
- (68) Crabtree, R. H.; Habib, A. *Inorg. Chem.* **1986**, *25*, 3698-3699.
- (69) Isobe, K.; Bailey, P. M.; Maitlis, P. M. *J. Chem. Soc., Dalton Trans.* **1981**, 2003-2008.
- (70) Gilbert, T. M.; Bergman, R. G. *J. Am. Chem. Soc.* **1985**, *107*, 3502-3507.
- (71) Brookhart, M.; Grant, B.; Volpe, A. F., Jr. *Organometallics* **1992**, *11*, 3920-3922.

CHAPTER 4

CYCLOMETALLATION OF A PYRAZOLYL ARM IN HYDRIDOTRIS-(1-PYRAZOLYL)BORATE AND TRIS(1-PYRAZOLYL)METHANE COMPLEXES OF IRIDIUM

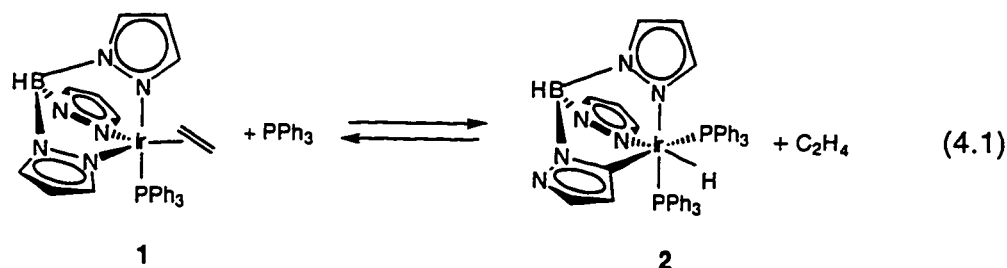
The synthesis and reactions of hydridotris(1-pyrazolyl)borate ($\text{Tp}^{\text{R}2}$, R = H or Me) complexes¹ of rhodium and iridium have recently been the focus of much interest due to their role in C-H bond activation reactions.²⁻⁸ Specifically, the $\text{Tp}^{\text{Me}2}$ complexes have received the most attention, due in part to the observation that methyl substituents in the 3- and 5-positions stabilize against thermal decomposition. For example, $\text{TpIr}(\text{C}_2\text{H}_4)_2$ (**1**) is reported to decompose at 70 °C to a complex mixture of products,⁹ whereas $\text{Tp}^{\text{Me}2}\text{Ir}(\text{C}_2\text{H}_4)_2$ cleanly isomerizes at 60 °C, first to the vinyl hydride complex, $\text{Tp}^{\text{Me}2}\text{Ir}(\text{C}_2\text{H}_4)(\text{CH}=\text{CH}_2)\text{H}$ ¹⁰ and then to other products^{11,12} depending on experimental conditions. The $\text{TpIr}(\text{C}_2\text{H}_4)(\text{CH}=\text{H}_2)\text{H}$ complex is not intrinsically unstable, evidenced by the fact that it can be formed in high yield under photochemical conditions. The difference in thermal reactivity is curious if one considers that the unsubstituted Tp ligand may actually afford greater steric protection of the metal center because it is more likely to adopt a tridentate structure (e.g. $\eta^3\text{-TpIr}(\text{CO})(\text{C}_2\text{H}_4)$ ¹³ vs. $\eta^2\text{-Tp}^{\text{Me}2}\text{M}(\text{CO})(\text{C}_2\text{H}_4)$ ^{3,5}). However, even when the ground state structure is trigonal bipyramidal (tbp), four coordinate square planar (sp) species are thermally accessible.¹⁴⁻¹⁷

In this chapter we report observations of a previously unknown cyclometallation reaction of the Tp ligand. This reaction leads to formal oxidation of the iridium center by formation of an iridium (III) alkyl hydride complex *via* activation of a C-H bond of a pyrazolyl ring. Related chemistry is presented for a similar cyclometallation reaction of cationic tris(1-pyrazolyl)methane (Tpm) complexes of iridium. The cyclometallated complexes display limited thermal stability. We suggest that the improved stability of

3,5-substituted Tp^{Me_2} complexes may be due to protection against pyrazolyl cyclometallation reactions provided by the methyl substituents.

Results

Cyclometallation of Tris(1-pyrazolyl)borate. Methylene chloride solutions of $\text{TpIr}(\text{PPh}_3)(\text{C}_2\text{H}_4)$ (**1**) and a six-fold excess of PPh_3 react to form equilibrium mixtures of **1** and the cyclometallated complex, $(\text{N}, \text{C}^5, \text{N-Tp})\text{Ir}(\text{PPh}_3)_2\text{H}$ (**2**) and free ethylene upon standing for 20 h (eq 4.1). These reactions were conducted under vacuum in sealed



NMR tubes. The relative concentration of each species was determined at equilibrium by integration of the appropriate resonances in the ^1H NMR spectra. No intermediates were detected. The equilibrium constant for eq 4.1 was calculated as $[\mathbf{2}][\text{C}_2\text{H}_4]/[\mathbf{1}][\text{PPh}_3]$ and equals 0.1 at room temperature ($\Delta G^\circ = 1.4$ kcal/mol). Because a significant fraction of the displaced ethylene diffuses into the headspace, the observed ratio of **2** : **1** is *ca.* 10 to 1. Addition of ethylene (one atmosphere) results in the regeneration of **1** at the expense of **2** over several hours. In a separate experiment, addition of H_2 to a similar equilibrium mixture gives $\text{TpIr}(\text{PPh}_3)\text{H}_2$, free PPh_3 and free ethylene upon standing overnight. Complete conversion to **2** was accomplished on a preparative scale by reaction of **1** with a six-fold excess of PPh_3 in CH_2Cl_2 solutions while periodically purging the system with argon. Clean formation of **2** requires excess PPh_3 , providing isolated samples

unfortunately contaminated with residual PPh_3 . Solutions of **2** decompose in solution within 4-5 days at ambient temperature.

Characterization of **2** was accomplished by ^1H and ^{31}P NMR, IR, and FABMS analysis. Selected ^1H NMR NOE experiments were also undertaken to completely assign the eight pyrazolyl resonances of the (N, C⁵, N-Tp) ligand. These experiments indicate that a cyclometallated (N, C⁵, N-Tp) ligand is coordinated to the iridium center of **2** by way of nitrogen donors for two of the pyrazolyl arms and through the C⁵-carbon atom of the activated pyrazolyl arm. The complex contains two PPh_3 ligands, one of which is trans to the C⁵-pyrazolyl donor. The sixth site of the octahedron is occupied by a hydride ligand, which was identified in solution by a characteristic resonance at -18.95 ppm (dd, $J_{\text{P-H}} = 21.1$ and 11.7 Hz) in the ^1H NMR spectrum. In the solid state a weak IR absorption at 2179 cm^{-1} was attributed to $\nu_{\text{Ir-H}}$ while a band at 2473 cm^{-1} was assigned to $\nu_{\text{B-H}}$ of the (N, C⁵, N-Tp) ligand. This value is unremarkable and implies that cyclometallation has little effect on the B-H vibrational mode. The observation also rules out the possibility that the hydride ligand of **2** results from oxidative addition of the B-H bond.¹⁸ The doublet of doublets pattern of the hydride resonance is consistent with *cis*-P-H coupling to two inequivalent phosphine ligands. This was confirmed by $^{31}\text{P}\{\text{aromatic } ^1\text{H}\}$ NMR experiments, which reveal resonances at 3.80 (t) and 1.02 (dd) ppm due to an AMX spin system ($J_{\text{P-P}} = 10$ Hz). The expected molecular ion peak at 930 amu was observed by FABMS. The 4-pz resonance of the cyclometallated pyrazolyl arm shifts significantly upfield from 5.93 ppm in **1** to 4.76 ppm in **2**. The new resonance at 4.76 ppm appears as an apparent triplet ($J = 1.4$ Hz) due to overlap of an H-H coupling and a *trans*-P-H coupling¹⁹ of the same magnitude (Figure 4.1). This assignment and those of the remaining pyrazolyl protons was established through a series of ^1H NMR NOE experiments. Irradiation of the hydride resonance at -18.95 ppm gives enhancement of **b** (4.76 ppm) and **f** (6.82 ppm) and of the ortho-phenyl protons (6.90 and 7.26 ppm). Irradiation of **b** in turn, gives an enhancement of **a** (6.79 ppm). The 3,5-pyrazolyl protons

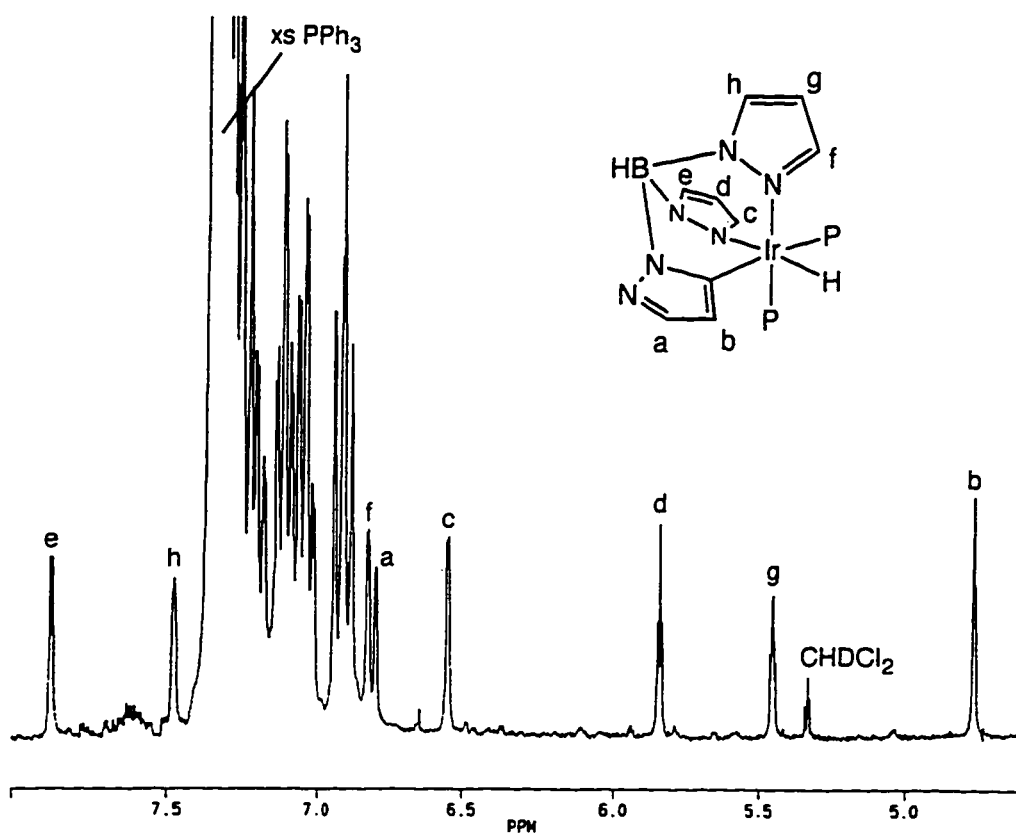
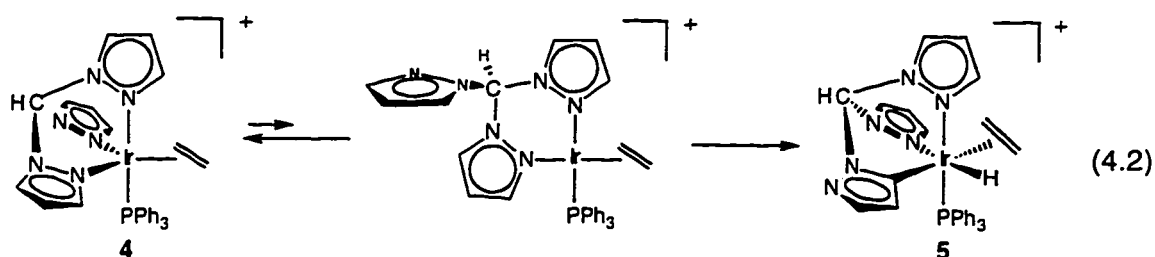


Figure 4.1 ^1H NMR spectrum of $(\text{N}, \text{C}^5, \text{N-Tp})\text{Ir}(\text{PPh}_3)_2\text{H}$ in CD_2Cl_2

of the pz-arm trans to the hydride ligand appear as simple doublets at 6.54 and 7.87 ppm, which were distinguished as **c** and **e** respectively, since irradiation of the ortho-phenyl resonance at 6.90 ppm gave an enhancement of **c** (6.54 ppm). A sharp triplet and a multiplet at 5.84 and 5.44 ppm are assigned to **d** and **g** respectively, based on the additional *trans*-P-H coupling of the latter resonance. Remaining is **h** at 7.48 ppm.

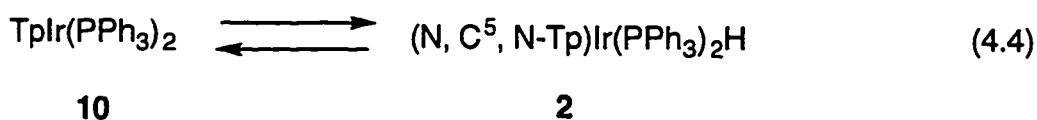
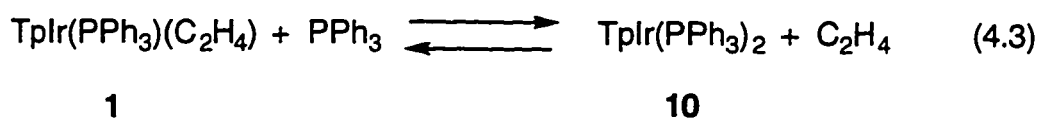
Cyclometallation of Tris(1-pyrazolyl)methane. We have undertaken a study of closely related Tpm complexes²⁰ in order to gain an understanding of the mechanism of pyrazolyl cyclometallation. Thus, the new [(Tpm)Ir(C₂H₄)₂]BF₄ (**3**) complex reacts at -78 °C with one equiv. of PPh₃ to form [(Tpm)Ir(PPh₃)(C₂H₄)]BF₄ (**4**) and free ethylene. Upon warming to -10° C, **4** is observed by ¹H NMR spectroscopy to isomerize (t_{1/2} = 5.5 h) to the cyclometallated, [(N, C⁵, N-Tpm)Ir(PPh₃)(C₂H₄)H]BF₄ (**5**) complex (eq 4.2).



Complex **5** is thermally unstable and slowly decomposes to a complex mixture of products. It was possible to collect spectroscopic data to support the (N, C⁵, N-Tpm) formulation because decomposition proceeds more slowly than cyclometallation. At temperatures less than -10 °C, the isomerization of **4** to **5** is unreasonably slow. While isomerization occurs more readily at slightly higher temperatures, decomposition also becomes a more significant factor. As was found in the case of **2**, cyclometallation causes a marked upfield shift of the 4-pz proton from 6.21 ppm in **4** to 4.94 ppm in **5**. The coupling pattern of the cyclometallated 4-pz resonance is now a simple doublet ($J = 1.6$ Hz), coupling to only one neighboring hydrogen. The hydride ligand is identified at -17.14 ppm (d, $J_{P-H} = 18.8$ Hz). No change in the course of this reaction is observed if

the reaction is carried out with an excess of PPh₃. Complex **4** can be trapped by H₂ (six atmospheres) at -20 °C to obtain [(Tp^m)Ir(PPh₃)H₂]BF₄ (**6**) and free ethylene. Likewise, SnBu₃H reacts immediately with **4** at -78 °C to form [(Tp^m)Ir(PPh₃)(SnBu₃)H]BF₄ (**7**), which is thermally stable.

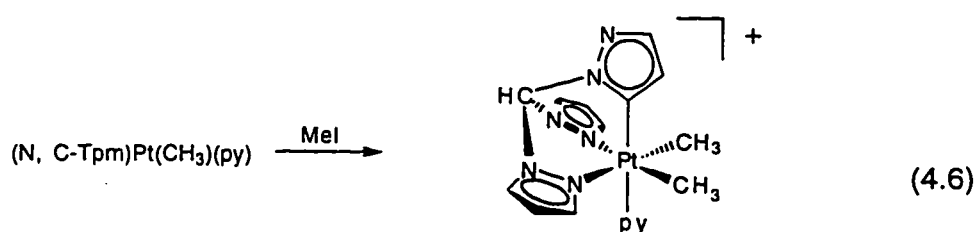
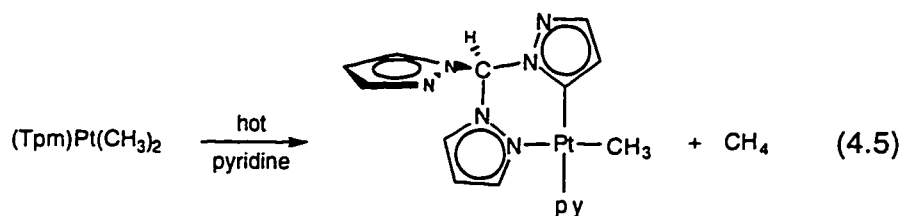
Mechanism of Pyrazolyl Cyclometallation. We have previously shown that **1** adopts a *tbp* structure in solution with PPh₃ coordinated in the axial site and ethylene positioned in the equatorial plane (chapter 2). A facile equilibrium with an unobserved *sp* intermediate was proposed based on kinetic data for the reaction of **1** with H₂. The spectroscopic data collected for **4** also supports a *tbp* structure (see experimental section). The isomerization of **4** to the cyclometallated complex **5** is convincing evidence that an equilibrium with a *sp* intermediate occurs (eq 4.2). We have found that **5** fails to react with excess PPh₃. In fact a number of reports in the literature have commented that iridium (III) alkene complexes stabilized by Tp^{R2} ligands are inert to substitution of the ethylene ligand under thermal conditions.^{9,21,22} Similarly we have found that the ethylene ligand is not displaced from [TpIr(PPh₃)(C₂H₄)H]BF₄ (**8**)²³ or TpIr(C₂H₄)(C₂H₅)Cl (**9**) upon addition of excess PPh₃. With this in mind we rule out (N, C⁵, N-Tp)Ir(PPh₃)(C₂H₄)H as a possible intermediate in the formation of **2**. Instead, we propose that **1** reacts with PPh₃ to form TpIr(PPh₃)₂ (**10**) which *then* rapidly cyclometallates (eqs 4.3 and 4.4). The structure of **10** is unknown, but this complex probably exists as a mixture of *tbp* and *sp* forms in solution.



Discussion

Cyclometallation represents an unprecedented mode of reactivity for the ubiquitous Tp ligand. In the case of low valent iridium complexes, this reaction is feasible due to the strong Ir-C and Ir-H bonds formed by oxidative addition of the pyrazolyl C-H bond.²⁴ These are the same attributes which make complexes of this type useful in alkane activation reactions and we suggest that cyclometallation may be a common reaction for Tp complexes of transition metals in the d^8 configuration.

We have also shown that cyclometallation of the Tpm ligand occurs readily. There is precedent for this reaction in platinum (II) complexes, but the driving force of methane elimination was apparently required. For example, $(\text{Tpm})\text{Pt}(\text{CH}_3)_2$ is reported to isomerize to $(\eta^2\text{-N, C}^5\text{-Tpm})\text{Pt}(\text{CH}_3)(\text{py})$ in hot pyridine (eq 4.5).²⁵ Oxidation of this complex with MeI then forms $[(\text{N, N, C}^5\text{-Tpm})\text{Pt}(\text{CH}_3)_2(\text{py})]\text{I}$ containing the tridentate



cyclometallated Tpm ligand (eq 4.6).²⁶ The pyridine ligand can be substituted with tertiary phosphine ligands to provide a family of related cationic platinum (IV) complexes. If $(\text{Tpm})\text{Pt}(\text{CH}_3)_2$ is reacted directly with MeI, then the neutral $(\text{N, N, C}^5\text{-Tpm})\text{Pt}(\text{CH}_3)_2\text{I}$ complex is obtained. Each of these platinum alkyl complexes is thermally robust. In contrast **2** and **5** retain both the alkyl and hydride ligands resulting

from pyrazolyl cyclometallation and are thermally quite unstable. In solution at room temperature, complexes **2** and **5** decompose within 4-5 days or within 5 minutes, respectively. The mechanism of decomposition is not understood, as we have been unable to identify any of the products formed upon decomposition. Trofimenko has previously suggested that methyl substituents in the 5-position stabilize Tp^{Me_2} complexes by steric protection of the B-H bond. However, our observations suggest another possibility is that methyl substituents discourage the pyrazolyl cyclometallation reaction. Further work is required to understand the subsequent decomposition pathways.

Conclusion

Solutions of $\text{TpIr}(\text{PPh}_3)(\text{C}_2\text{H}_4)$ (**1**) react with excess PPh_3 to form equilibrium mixtures of **1** and $(\text{N}, \text{C}^5, \text{N-Tp})\text{Ir}(\text{PPh}_3)_2\text{H}$ (**2**) and free ethylene ($K_{\text{eq}} = 0.1$). The closely related $[(\text{Tpm})\text{Ir}(\text{PPh}_3)(\text{C}_2\text{H}_4)]\text{BF}_4$ (**4**) complex isomerizes at $-10\text{ }^\circ\text{C}$ to form $[(\text{N}, \text{C}^5, \text{N-Tpm})\text{Ir}(\text{PPh}_3)(\text{C}_2\text{H}_4)\text{H}]\text{BF}_4$ (**5**) ($t_{1/2} = 5.5\text{ h}$). Based on the observation that **5** fails to react with excess PPh_3 , $\text{TpIr}(\text{PPh}_3)_2$ (**10**) is proposed as a key intermediate in the formation of **2**.

Experimental

General experimental methods and instrumentation are described in chapter 2. The pyrazolyl ligands, potassium hydridotris(1-pyrazolyl)borate (KTp)²⁷ and tris(1-pyrazolyl)methane (tpm)²⁸ were prepared by literature methods. The iridium starting material, $(\text{NH}_4)_2\text{IrCl}_6$ was recovered from laboratory iridium residues following published procedures.²⁹ $\text{TpIr}(\text{PPh}_3)(\text{C}_2\text{H}_4)$ (**1**) and $[\text{TpIr}(\text{PPh}_3)(\text{C}_2\text{H}_4)\text{H}]\text{BF}_4$ (**8**) were prepared as described in chapter 2.

Fast atom bombardment mass spectra (FABMS) were obtained using a VG 70 SEQ tandem hybrid instrument of EBqQ geometry, equipped with a standard saddle-field gun (Ion Tech Ltd., Middlesex, U. K.) producing a beam of xenon atoms at 8 keV and 1

mA. Solid samples were applied to the FAB target as suspensions in 3-nitrobenzylalcohol. All spectra were taken in the positive ion mode. Elemental analyses were performed by Canadian Microanalytical Services, Ltd., Vancouver, BC.

Synthesis of Complexes.

(N, C⁵, N-Tp)Ir(PPh₃)₂H (2). To a 100 mL schlenk flask containing TpIr(C₂H₄)₂⁹ (14.2 mg, 0.31 mmol), PPh₃ (56.4 mg, 0.22 mmol) and a teflon coated stir bar was added CH₂Cl₂ via cannula. The colorless solution was stirred briefly, then degassed with three pump-purge cycles, backfilling with Ar. The flask was covered with aluminum foil to exclude light and was left to stir for 22 h, periodically repeating the pump-purge cycles. The solvent was then stripped under dynamic vacuum and the residue isolated in the glove box. Attempts to purify this material by recrystallization or chromatography on silica gel gave only decomposed iridium products and PPh₃. The trans relationships are reflected in the order of atom labels of the (N, C⁵, N-Tp) ligand. For example, one PPh₃ ligand is trans to a nitrogen donor and the other is trans to the C₅-pz arm. ¹H NMR (CD₂Cl₂): 7.86 (d, 1 H, 5-pz trans to H); 7.47 (m, 1 H, 5-pz trans to PPh₃); 6.81 (m, 1 H, 3-pz trans to PPh₃); 6.78 (m, 1 H, 3-pz of cyclometallated arm); 6.54 (d, 1 H, 3-pz trans to H); 5.83 (t, 1 H, 4-pz trans to H); 5.43 (m, 1 H, 4-pz trans to PPh₃); 4.76 (t, 1 H, 4-pz of cyclometalated arm); 7.37-7.30 (excess PPh₃); 7.26, 6.90 (m, 6 H each, o-C₆H₅PPh₂); 7.20-7.07 (complex m, 12 H, aromatic); -18.95 (dd, J_{P-H} = 11.7 and 21.1 Hz, 1 H, Ir-H). ³¹P{aromatic ¹H} NMR: 3.80 (t, J_{P-P} = 10 Hz, J_{H-P} = 10 Hz); 1.02 (dd, J_{P-P} = 10 Hz, J_{H-P} = 20 Hz). IR: 2473 (ν_{B-H}); 2179 (ν_{Ir-H}). FABMS: *m/z* 930 (M⁺).

[(tpm)Ir(C₂H₄)₂]BF₄ (3). A THF (10 mL) suspension of [Ir(COE)₂Cl]₂³⁰ (162 mg, 0.181 mmol) was degassed with three freeze-pump-thaw cycles, then the head space back-filled with 1 atm of C₂H₄, while maintaining the mixture at 0 °C. Additional C₂H₄ was added until the original orange slurry became a clear pale yellow solution over *ca.* 30 min. A second THF (5 mL) solution of tris(pyrazolyl)methane (Tpm) (79 mg, 0.37

mmol) was then cannula transferred into the first flask to obtain a yellow solution which was allowed to warm to room temperature and stir for 15 min. Subsequent addition of AgBF_4 (78 mg, 0.40 mmol) as a THF solution/slurry in three portions gave a colorless precipitate which was filtered off through a bed of celite. The volume of the filtrate was then reduced under vacuum and pentane added to afford a light yellow microcrystalline solid, which was filtered off and dried under vacuum. Yield 184 mg (93%). As determined by ^1H and $^{13}\text{C}\{^1\text{H}\}$ NMR spectroscopy, this material contained 0.25 equiv. of THF trapped in the crystal lattice, which could not be removed under vacuum. When studied by ^1H NMR spectroscopy, the ethylene resonance was observed to decoalesce at 245 K ($\Delta G_c^\ddagger = 11.3$ kcal/mol) to an AA'XX' spin system centered at 2.20 ppm. A good simulation of the experimental spectrum in the static limit was obtained with the following parameters: $\delta_A = 2.53$, $\delta_X = 1.86$, $J_{\text{cis}} = 9.2$ Hz, $J_{\text{trans}} = 11.5$ Hz, $J_{\text{gem}} = -2.2$ Hz. ^1H NMR (CD_2Cl_2 , 296 K): 9.39 (s, 1 H, HCpz₃); 8.44, 7.99 (d, 3 H each, 3,5-pz); 6.51 (t, 3 H, 4-pz); 2.29 (s, 8H, C₂H₄). $^{13}\text{C}\{^1\text{H}\}$ NMR (CD_2Cl_2 , 296 K): 142.2, 134.1 (s, 3,5-pz); 108.7 (s, 4-pz), 76.5 (s, HCpz₃); 31.6 (s, C₂H₄). Anal. Calcd for $\text{C}_{14}\text{H}_{18}\text{BF}_4\text{IrN}_6 \cdot (\text{C}_4\text{H}_8\text{O})_{0.25}$: C, 31.76; H, 3.55; N, 14.81 Found: C, 29.61; H, 3.39; N, 13.99.

$[(\text{tpm})\text{Ir}(\text{PPh}_3)(\text{C}_2\text{H}_4)]\text{BF}_4$ (4). This complex was prepared and observed by ^1H , $^{13}\text{C}\{^1\text{H}\}$, and ^{31}P NMR spectroscopy at low temperature. **4** was observed to decompose to a complex mixture of products within five minutes of warming to ambient temperature. A typical sample was prepared by vacuum transfer of CD_2Cl_2 (0.5 mL) into an NMR tube containing $[(\text{tpm})\text{Ir}(\text{C}_2\text{H}_4)_2]\text{BF}_4$ (4.2 mg, 0.0076 mmol) and PPh_3 (2.0 mg, 0.0076 mmol). The sample was then flame sealed under vacuum and warmed to -78 °C until being transferred to a precooled NMR probe. Hindered rotation about the Ir-P bond causes line broadening of the PPh_3 resonances at temperatures above 240 K. ^1H NMR (300 MHz, CD_2Cl_2 , 220 K): 9.24 (s, 1 H, HCpz₃); 8.39, 7.26 (d, 2 H each, 3,5-pz_{eq}); 8.34, 7.39 (d, 1 H each, 3,5-pz_{ax}); 7.52-7.43, 7.32 (m and br respectively, 10 H, PPh_3);

7.22 (t, $J = 7.7$ Hz, 1 H, *p*-C₆H₅); 6.99, 6.63 (t, $J = 8$ Hz, 2 H each, *o*- and *m*-C₆H₅); 6.42 (m, 1 H, 4-*pz*_{ax}); 6.20 (t, 2 H, 4-*pz*_{eq}); 1.09, 0.96 (m, 2 H each, C₂H₄). ¹³C{¹H} NMR (125.8 MHz, CD₂Cl₂, 250 K): 144.8, 133.1 (s, 3,5-*pz*_{eq}); 136.5, 133.6 (s, 3,5-*pz*_{ax}); 134.9 (br); 133.8 (d, $J_{P-H} = 10$ Hz); 132.9 (br); 130.9 (br); 129.5 (br); 128.7 (d, $J = 7$ Hz); 128.4 (br); 108.0 (s, 4-*pz*_{eq}); 107.7 (s, 4-*pz*_{ax}); 76.5 (s, HCp_z); 5.0 (s, C₂H₄). ³¹P{¹H} NMR (202.5 MHz, CD₂Cl₂, 250 K): 9.0 (s).

[(N, C⁵, N-tpm)Ir(PPh₃)(C₂H₄)H]BF₄ (5). This complex was prepared from a CD₂Cl₂ solution of **4**, generated at low temperature (-78° C) in a sealed NMR tube. Optimal conditions for observation of the isomerization of **4** to **5** were found at -10° C ($t_{1/2} = 5.5$ h). At temperatures less than -10° C, the isomerization reaction was unreasonably slow. While isomerization was observed to proceed more readily at slightly higher temperatures, decomposition also became a significant factor. Typically the sample was allowed to stand for about 6 h at -15 ° C in a salt/ice bath before being transferred to a precooled NMR probe and monitored by ¹H NMR spectroscopy. Once the isomerization was essentially complete, the sample was then further cooled to prolong its lifetime. ¹H NMR (CD₂Cl₂, 250K): 9.13 (s, 1 H, HCp_z); 8.66, 8.46, 7.51, 7.49, 7.13 (d, 1 H each, 3,5-*pz*); 7.41-7.30, 7.11, 7.00 (br, PPh₃); 6.35 (t, 1H, 4-*pz* trans to H); 6.32 (m, 1 H, 4-*pz* trans to PPh₃); 4.94 (d, 1 H, 4-*pz* of cyclometallated arm); 3.87, 3.23 (m, 2 H each, C₂H₄); -17.14 (d, $J_{P-H} = 18.8$ Hz, Ir-*H*). ¹³C{¹H} NMR (75.464 MHz, 250K): 146.2 (s, 3-*pz* of cyclometallated arm); 141.3 (s, 3-*pz* trans to H); 140.8 (br s, 3-*pz* trans to PPh₃); 134.0 (d, $J_{P-H} = 58$ Hz, *i*-C₆H₅PPh₂); 133.9, 128.8 (d, $J_{P-H} = 10$ Hz and 10.6 Hz respectively, *o*- and *m*-C₆H₅PPh₂); 131.9 (d, $J_{P-H} = 2$ Hz, *p*-C₆H₅PPh₂); 131.3, 131.1, 130.4, 129.2, 129.1 (uncertain whether these result from decomposition products and/or 5-*pz* of nitrogen bound and cyclometallated pyrazolyl groups); 116.1 (s, 4-*pz* of cyclometallated arm); 108.5 (s, 4-*pz* trans to H); 108.2 (br s, 4-*pz* trans to PPh₃); 80.5 (s, HCp_z); 67.8 (s, C₂H₄).

[(tpm)Ir(PPh₃)H₂]BF₄ (6). To a thick walled glass bomb charged with [(tpm)Ir(C₂H₄)₂] (44 mg, 0.08 mmol), PPh₃ (22.5 mg, 0.086 mmol) and a teflon coated stir bar was vacuum transferred CH₂Cl₂ (5 mL). The mixture was warmed to -78 °C and stirred for 15 min. The sample was then refrozen at -196 °C, the head space evacuated and then backfilled with 1500 torr of H₂, while the vessel was immersed in N₂(l). The mixture was then rewarmed to -78 °C stirred for 30 min, then gradually warmed to -20 °C and allowed to stir for 10 h. The estimated H₂ pressure at this temperature is *ca.* 6 atm. The clear colorless solution was transferred via cannula to a schlenk flask and concentrated under vacuum. Et₂O was layered over the CH₂Cl₂ solution and colorless crystals obtained upon standing for 2 days at -30 °C. These crystals analyze for 6•1/2(Et₂O). The Et₂O may however be removed under vacuum (days) to obtain a colorless powder. ¹H NMR (CD₂Cl₂): 9.38 (s, 1 H, HCpz₃); 8.39, 6.59 (d, 2 H each, 3,5-pz_{eq}); 8.34, 8.02 (m and br s respectively, 1 H each, 3,5-pz_{ax}); 7.48-7.30 (complex m, 15 H, PPh₃); 6.40 (m, 1 H, 4-pz_{ax}); 6.15 (t, 2 H, 4-pz_{eq}); -20.93 (d, J_{P-H} = 23.3 Hz, 2 H, Ir-H). Anal. Calcd for C₂₈H₂₇BF₄IrN₆P•(C₄H₁₀O)_{0.5}: C, 45.35; H, 4.06; N, 10.58. Found: C, 45.87; H, 3.91; N, 10.26.

[(tpm)Ir(PPh₃)(SnBu₃)H]BF₄ (7). This complex was prepared on a small scale in CD₂Cl₂ solution and characterized by ¹H and ³¹P NMR spectroscopy. To an NMR tube charged with [(tpm)Ir(C₂H₄)₂]BF₄ (2.2 mg, 0.004 mmol) and PPh₃ (1.1 mg, 0.004 mmol) was vacuum transferred CD₂Cl₂ (0.5 mL). The tube was warmed to -78 °C and agitated. Then against a flow of Ar, HSnBu₃ (3 μL, 0.01 mmol) was added by syringe. The sample was then refrozen at -196 °C and the head space evacuated and flame sealed under vacuum. The sample was then carefully warmed to -20 °C and allowed to stand for 60 min before warming to room temperature. ¹H NMR (CD₂Cl₂): 9.31 (s, 1 H, HCpz₃); 8.38, 8.37, 8.34, 8.10 (br s), 6.51, 6.19 (d, 1 H each, 3,5-pz); 7.60-7.53, 7.44-7.22 (complex m, PPh₃); 6.44 (m, 1 H, 4-pz trans to PPh₃); 6.13, 6.06 (t, 1 H each, 4-pz); 1.6-0.4 (m, SnBu); -20.98 (d with ^{117/119}Sn satellites, J_{P-H} = 21.9 Hz, J_{Sn-H} = 78.8 Hz,

Ir-*H*). $^{31}\text{P}\{\text{aromatic } ^1\text{H}\}$ NMR (CD_2Cl_2): 10.65 (d with $^{117/119}\text{Sn}$ satellites, $J_{\text{P-H}} = 21.7$ Hz, $J_{\text{Sn-P}} = 127$ Hz).

TpIr(C₂H₅)(C₂H₄)Cl (9). Against a flow of argon, conc. HCl (0.3 mL) was added to a slurry of TpIr(C₂H₄)₂⁹ (66 mg, 0.14 mmol) in MeOH (5 mL). The mixture was refluxed for three hours, then allowed to cool to room temperature to yield a white precipitate. The supernate was drawn off and the white solid dried under vacuum. Yield 35 mg (49 %). No reaction was observed between **8** and excess PPh₃ even when heated to 60 °C for several days. ^1H NMR (CD_2Cl_2): 7.95, 7.90, 7.72 (2 H, overlapping), 7.69, 7.10 (d, 1 H each, 3,5-pz); 6.35, 6.34, 6.21 (t, 1 H each, 4-pz); 4.11, 3.85 (m, 2 H each, C₂H₄); 2.46, 2.20 (m, 1 H each, CH₂CH₃); 0.87 (t, $J_{\text{H-H}} = 7.7$ Hz, 3 H, CH₂CH₃). Anal. Calcd for C₁₃H₁₉BClIrN₆: C, 31.37; H, 3.85; N, 16.89. Found: C, 31.55; H, 3.76; N, 16.48.

[(η^2 -Tp)Ir(PPh₃)₂(C₂H₄)H]BF₄. This complex was observed in solution and characterized on the basis of ^1H and ^{31}P NMR spectroscopy. Samples were prepared by vacuum transfer of CD_2Cl_2 into an NMR tube containing [TpIr(PPh₃)(C₂H₄)H]BF₄ (1.7 mg, 0.0022 mmol) and PPh₃ (0.7 mg, 0.0027 mmol), then flame sealed under vacuum. Upon warming to room temperature a clear colorless solution was obtained. Although a slight excess of PPh₃ was added (confirmed by ^1H and ^{31}P NMR), *ca.* 15% of [TpIr(PPh₃)(C₂H₄)H]BF₄ remained in solution ($K_{\text{eq}} = 30$). ^1H NMR (CD_2Cl_2): 7.85-7.79 (m, 3 H, PPh₃); 7.67-7.59 (m, 8 H, PPh₃); 7.36-7.27 (m, 14 H, coordinated and free PPh₃); 7.17-7.10 (m, 12 H, PPh₃); 6.94, 6.29 (d, 1 H each, 3,5-pz, remaining 3,5-pz resonances presumably obscured by PPh₃ resonances); 6.10 (m, 1 H, 4-pz trans to PPh₃); 6.08, 5.79 (t, 1 H each, 4-pz); 2.94, 2.27, 1.72, 1.40 (m, 1 H each, C₂H₄); -20.15 (dd, $J_{\text{P-H}}$ (trans) = 21.4 Hz, $J_{\text{P-H}}$ (cis) = 5 Hz, Ir-*H*). $^{31}\text{P}\{\text{aromatic } ^1\text{H}\}$ NMR (CD_2Cl_2): 19.29 (br s, PWHH = 13 Hz, 1 P); 8.30 (d, $J_{\text{P-H}} = 21$ Hz, 1 P).

Notes to Chapter 4.

- (1) Trofimenko, S. *Chem. Rev.* **1993**, *93*, 943-980.
- (2) Ghosh, C. K.; Graham, W. A. G. *J. Am. Chem. Soc.* **1987**, *109*, 4726-4727.
- (3) Ghosh, C. K.; Rodgers, D. P. S.; Graham, W. A. G. *J. Chem. Soc., Chem. Commun.* **1988**, 1511-1512.
- (4) Ghosh, C. K.; Graham, W. A. G. *J. Am. Chem. Soc.* **1989**, *111*, 375-375.
- (5) Ghosh, C. K.; Hoyano, J. K.; Krentz, R.; Graham, W. A. G. *J. Am. Chem. Soc.* **1989**, *111*, 5480-5481.
- (6) Jones, W. D.; Hessell, E. T. *J. Am. Chem. Soc.* **1992**, *114*, 6087-6095.
- (7) Pérez, P. J.; Poveda, M. L.; Carmona, E. *Angew. Chem. Int. Ed. Engl.* **1995**, *34*, 231-233.
- (8) Paneque, M.; Poveda, M. L.; Rey, L.; Taboada, S.; Carmona, E.; Ruiz, C. *J. Organometal. Chem.* **1995**, *504*, 147-149.
- (9) Tanke, R. S.; Crabtree, R. H. *Inorg. Chem.* **1989**, *28*, 3444-3447.
- (10) Pérez, P. J.; Poveda, M. L.; Carmona, E. *J. Chem. Soc., Chem. Commun.* **1992**, 8-9.
- (11) Boutry, O.; Gutiérrez, E.; Monge, A.; Nicasio, M. C.; Pérez, P. J.; Carmona, E. *J. Am. Chem. Soc.* **1992**, *114*, 7288-7290.
- (12) Gutiérrez, E.; Monge, A.; Nicasio, M. C.; Poveda, M. L.; Carmona, E. *J. Am. Chem. Soc.* **1994**, *116*, 791-792.
- (13) Ciriano, M. A.; Fernández, M. J.; Modrego, J.; Rodríguez, M. J.; Oro, L. A. *J. Organometal. Chem.* **1993**, *443*, 249-252.
- (14) Cocivera, M.; Desmond, T. J.; Ferguson, G.; Kaitner, B.; Lalor, F. J.; O'Sullivan, D. J. *Organometallics* **1982**, *1*, 1125-1132.
- (15) Cocivera, M.; Ferguson, G.; Kaitner, B.; Lalor, F. J.; O'Sullivan, D. J.; Parvez, M.; Ruhl, B. *Organometallics* **1982**, *1*, 1132-1139.

Notes to Chapter 4.

- (1) Trofimenko, S. *Chem. Rev.* **1993**, *93*, 943-980.
- (2) Ghosh, C. K.; Graham, W. A. G. *J. Am. Chem. Soc.* **1987**, *109*, 4726-4727.
- (3) Ghosh, C. K.; Rodgers, D. P. S.; Graham, W. A. G. *J. Chem. Soc., Chem. Commun.* **1988**, 1511-1512.
- (4) Ghosh, C. K.; Graham, W. A. G. *J. Am. Chem. Soc.* **1989**, *111*, 375-375.
- (5) Ghosh, C. K.; Hoyano, J. K.; Krentz, R.; Graham, W. A. G. *J. Am. Chem. Soc.* **1989**, *111*, 5480-5481.
- (6) Jones, W. D.; Hessel, E. T. *J. Am. Chem. Soc.* **1992**, *114*, 6087-6095.
- (7) Pérez, P. J.; Poveda, M. L.; Carmona, E. *Angew. Chem. Int. Ed. Engl.* **1995**, *34*, 231-233.
- (8) Paneque, M.; Poveda, M. L.; Rey, L.; Taboada, S.; Carmona, E.; Ruiz, C. J. *Organometal. Chem.* **1995**, *504*, 147-149.
- (9) Tanke, R. S.; Crabtree, R. H. *Inorg. Chem.* **1989**, *28*, 3444-3447.
- (10) Pérez, P. J.; Poveda, M. L.; Carmona, E. *J. Chem. Soc., Chem. Commun.* **1992**, 8-9.
- (11) Boutry, O.; Gutiérrez, E.; Monge, A.; Nicasio, M. C.; Pérez, P. J.; Carmona, E. *J. Am. Chem. Soc.* **1992**, *114*, 7288-7290.
- (12) Gutiérrez, E.; Monge, A.; Nicasio, M. C.; Poveda, M. L.; Carmona, E. *J. Am. Chem. Soc.* **1994**, *116*, 791-792.
- (13) Ciriano, M. A.; Fernández, M. J.; Modrego, J.; Rodríguez, M. J.; Oro, L. A. *J. Organometal. Chem.* **1993**, *443*, 249-252.
- (14) Cocivera, M.; Desmond, T. J.; Ferguson, G.; Kaitner, B.; Lalor, F. J.; O'Sullivan, D. J. *Organometallics* **1982**, *1*, 1125-1132.
- (15) Cocivera, M.; Ferguson, G.; Kaitner, B.; Lalor, F. J.; O'Sullivan, D. J.; Parvez, M.; Ruhl, B. *Organometallics* **1982**, *1*, 1132-1139.

- (16) Cocivera, M.; Ferguson, G.; Lalor, F. J.; Szczecinski, P. *Organometallics* **1982**, *1*, 1139-1142.
- (17) Bucher, U. E.; Currao, A.; Nesper, R.; Rügger, H.; Venanzi, L. M.; Younger, E. *Inorg. Chem.* **1995**, *34*, 66-74.
- (18) Substituted Tp complexes are known which contain an agostic B-H bond. See for example: (a) Zhang, X.; McDonald, R.; Takats, J. *New J. Chem.* **1995**, *19*, 573-585. (b) Calabrese, J. C.; Dimaille, P. J.; Thompson, J. S.; Trofimenko, S. *Inorg. Chem.* **1990**, *29*, 4427-4437.
- (19) All complexes of the [TpM(PR₃)] (M = Rh or Ir) fragment reveal a 1-2 Hz P-H coupling in the proton resonances of the pyrazolyl arm positioned trans to the PR₃ ligand. See chapter 2.
- (20) For a review of polypyrazolyl ligands including tris(1-pyrazolyl)methane, see: Trofimenko, S. *Prog. Inorg. Chem.* **1986**, *34*, 115-210.
- (21) Bovens, M.; Gerfin, T.; Gramlich, V.; Petter, W.; Venanzi, L. M.; Haward, M. T.; Jackson, S. A.; Eisenstein, O. *New. J. Chem.* **1992**, *16*, 337-345.
- (22) Ferrari, A.; Polo, E.; Rügger, H.; Sostero, S.; Venanzi, L. M. *Inorg. Chem.* **1996**, *35*, 1602-1608.
- (23) In this case the pyrazolyl arm trans to the hydride ligand is displaced to form an equilibrium mixture of **7** and $(\eta^2\text{-Tp})\text{Ir}(\text{PPh}_3)_2(\text{C}_2\text{H}_4)\text{H}\text{JBF}_4$ ($K_{\text{eq}} = 30$).
Characterization data for this complex is provided in the experimental section.
- (24) Martinho Simões, J. A.; Beauchamp, J. L. *Chem. Rev.* **1990**, *90*, 629-688.
- (25) Canty, A. J.; Minchin, N. J.; Patrick, J. M.; White, A. H. *J. Chem. Soc., Dalton Trans.* **1983**, 1253-1259.
- (26) *c.f.*: Canty, A. J.; Honeyman, R. T. *J. Organomet. Chem.* **1990**, *387*, 247-263 and references therein.
- (27) Trofimenko, S. *Inorg. Synth.* **1979**, *12*, 99.

BIBLIOGRAPHY

- Abragam, A. *Principles of Nuclear Magnetism*; Oxford University Press: Oxford, 1983.
- Abu-Hasanayn, F.; Krogh-Jespersen, K.; Goldman, A. S. *J. Am. Chem. Soc.* **1993**, *115*, 8019-8023.
- Akitt, J. W. *NMR and Chemistry* 3rd ed., Chapman and Hall: London, 1992.
- Albinati, A.; Bakhmutov, V. I.; Caulton, K. G.; Clot, E.; Eckert, J.; Eisenstein, O.; Gusev, D. G.; Grushin, V. V.; Hauger, B. E.; Klooster, W. T.; Koetzle, T. F.; McMullan, R. K.; O'Loughlin, T. J.; Pélissier, M.; Ricci, J. S.; Sigalas, M. P.; Vymenits, A. B. *J. Am. Chem. Soc.* **1993**, *115*, 7300-7312.
- Albright, T. A.; Hoffmann, R.; Thibeault, J. C.; Thorn, D. L. *J. Am. Chem. Soc.* **1979**, *101*, 3801-3812.
- Antoniutti, S.; Albertin, G.; Amendola, P.; Bordignon, E. *J. Chem. Soc., Chem. Comm.* **1989**, 229-230.
- Arliguie, T.; Border, C.; Chaudret, B. *Organometallics* **1989**, *8*, 1308.
- Aubart, M. A.; Chandler, B. D.; Gould, R. A. T.; Krogstad, D. A.; Schoondergang, M. F. J.; Pignolet, L. H. *Inorg. Chem.* **1994**, *33*, 3724-3734.
- Bacskay, G. B. *Chem. Phys. Lett.* **1996**, *242*, 507.
- Bacskay, G. B.; Bytheway, I.; Hush, N. S. *J. Am. Chem. Soc.* **1996**, *118*, 3753-3756.
- Baird, G. J.; Davies, S. G.; Moon, S. D.; Simpson, S. J.; Jones, R. H. *J. Chem. Soc., Dalton Trans.* **1985**, 1479-1486.
- Ball, R. G.; Ghosh, C. K.; Hoyano, J. K.; McMaster, A. D.; Graham, W. A. G. *J. Chem. Soc., Chem. Commun.* **1989**, 341-342.
- Bampos, N.; Field, L. D. *Inorg. Chem.* **1990**, *29*, 587-588.

- Batchelor, R. J.; Einstein, F. W. B.; Lowe, N. D.; Palm, B. A.; Yan, X.; Sutton, D. *Organometallics* **1994**, *13*, 2041-2052.
- Bautista, M. T.; Cappellani, E. P.; Drouin, S. D.; Morris, R. H.; Schweitzer, C. T.; Sella, A.; Zubkowski, J. *J. Am. Chem. Soc.* **1991**, *113*, 4876-4887.
- Bautista, M. T.; Earl, K. A.; Maltby, P. A.; Morris, R. H.; Schweitzer, C. T.; Sella, A. *J. Am. Chem. Soc.* **1988**, *110*, 7031-7036.
- Bell, T. W.; Huddleton, D. M.; McCamley, A.; Partridge, M. G.; Perutz, R. N.; Willner, H. *J. Am. Chem. Soc.* **1990**, *112*, 9212-9226.
- Berry, R. S. *J. Chem. Phys.* **1960**, *32*, 933-938.
- Bianchini, C.; Linn, K.; Masi, D.; Peruzzini, M.; Polo, A.; Vacca, A.; Zanobini, F. *Inorg. Chem.* **1993**, *32*, 2366-2376.
- Boutry, O.; Gutiérrez, E.; Monge, A.; Nicasio, M. C.; Pérez, P. J.; Carmona, E. *J. Am. Chem. Soc.* **1992**, *114*, 7288-7290.
- Bovens, M.; Gerfin, T.; Gramlich, V.; Petter, W.; Venanzi, L. M.; Haward, M. T.; Jackson, S. A.; Eisenstein, O. *New. J. Chem.* **1992**, *16*, 337-345.
- Brammer, L.; Howard, J. A. K.; Johnson, O.; Koetzle, T. F.; Spencer, J. L.; Stringer, A. M. *J. Chem. Soc., Chem. Commun.* **1991**, 241-243.
- Brookhart, M.; Grant, B.; Volpe, A. F., Jr. *Organometallics* **1992**, *11*, 3920-3922.
- Brookhart, M.; Green, M. L. H.; Wong, L. *Prog. Inorg. Chem.* **1988**, *36*, 1-124.
- Bucher, U. E.; Currao, A.; Nesper, R.; Rügger, H.; Venanzi, L. M.; Younger, E. *Inorg. Chem.* **1995**, *34*, 66-74.
- Bucher, U. E.; Fässler, T. F.; Hunziker, M.; Nesper, R.; Rügger, H.; Venanzi, L. M. *Gazz. Chim. Ital.* **1995**, *125*, 181-188.
- Bucher, U. E.; Lengweiler, T.; Nanz, D.; Philipsborn, W. v.; Venanzi, L. M. *Angew. Chem. Int. Ed. Engl.* **1990**, *29*, 548-549.

- Bullock In *Transition Metal Hydrides*; A. Dedieu, Ed.; VCH Publishers, Inc.: New York, 1992; pp 263-307.
- Bullock, R. M.; Song, J.; Szalda, D. J. *Organometallics* **1996**, *15*, 2504-2516.
- Calabrese, J. C.; Dimaille, P. J.; Thompson, J. S.; Trofimenko, S. *Inorg. Chem.* **1990**, *29*, 4427-4437.
- Calvert, R. B.; Shapley, J. R. *J. Am. Chem. Soc.* **1978**, *100*, 7726-7727.
- Canty, A. J.; Honeyman, R. T. *J. Organomet. Chem.* **1990**, *387*, 247-263 and references therein.
- Canty, A. J.; Minchin, N. J.; Patrick, J. M.; White, A. H. *J. Chem. Soc., Dalton Trans.* **1983**, 1253-1259.
- Casey, C. P.; Tanke, R. S.; Hazin, P. N.; Kemnitz, C. R.; McMahon, R. J. *Inorg. Chem.* **1992**, *31*, 5474-5479.
- Ciriano, M. A.; Fernández, M. J.; Modrego, J.; Rodríguez, M. J.; Oro, L. A. *J. Organometal. Chem.* **1993**, *443*, 249-252.
- Cocivera, M.; Desmond, T. J.; Ferguson, G.; Kaitner, B.; Lalor, F. J.; O'Sullivan, D. J. *Organometallics* **1982**, *1*, 1125-1132.
- Cocivera, M.; Ferguson, G.; Kaitner, B.; Lalor, F. J.; O'Sullivan, D. J.; Parvez, M.; Ruhl, B. *Organometallics* **1982**, *1*, 1132-1139.
- Cocivera, M.; Ferguson, G.; Lalor, F. J.; Szczecinski, P. *Organometallics* **1982**, *1*, 1139-1142.
- Collman, J. P.; Hegedus, L. S.; Norton, J. R.; Finke, R. G. *Principles and Application of Organotransition Metal Chemistry*; University Science Books: Mill Valley, CA, 1987.
- Collman, J. P.; Wagenknecht, P. S.; Hutchison, J. E.; Lewis, N. S.; Lopez, M. A.; Guilard, R.; L'Her, M.; Bothner-By, A. A.; Mishra, P. K. *J. Am. Chem. Soc.* **1992**, *114*, 5654-5664.
- Costello, M. T.; Walton, R. A. *Inorg. Chem.* **1988**, *27*, 2563-2564.

- Crabtree, R. H. *The Organometallic Chemistry of the Transition Metals*; 2nd ed.; John Wiley & Sons: New York, 1994.
- Cramer, R. *Inorg. Synth.* **1973**, *15*, 14-16.
- Cramer, R. *J. Am. Chem. Soc.* **1972**, *94*, 5681-5685.
- Cramer, R.; Kline, J. B.; Roberts, J. D. *J. Am. Chem. Soc.* **1969**, *91*, 2519-2524.
- Cramer, R.; Seiwel, L. P. *J. Organometal. Chem.* **1975**, *92*, 245-252.
- Curtis, M. D.; Shiu, K.; Butler, W. M.; Huffman, J. C. *J. Am. Chem. Soc.* **1986**, *108*, 3335-3343.
- Dawkins, G. M.; Green, M.; Orpen, A. G.; Stone, F. G. A. *J. Chem. Soc., Chem. Comm.* **1982**, 41-43.
- Desrosiers, P. J.; Cai, L.; Lin, Z.; Richards, R.; Halpern, J. *J. Am. Chem. Soc.* **1991**, *113*, 4173-4184.
- Earl, K. A.; Jia, G.; Maltby, P. A.; Morris, R. H. *J. Am. Chem. Soc.* **1991**, *113*, 3027-3039.
- Eckert, J. *Spectrochim. Acta* **1992**, *48A*, 363-378.
- Eisenberg, R. *Acc. Chem. Res.* **1991**, *24*, 110-116.
- Emsley, J. *The Elements*; Oxford University Press: New York, 1989.
- Evans, D. F. *Chem. Ind. (London)* **1961**, 1960.
- Fernandez, M. J.; Rodriguez, M. J.; Oro, L. A. *Polyhedron* **1991**, *10*, 1595-1598.
- Fernández, M. J.; Rodriguez, M. J.; Oro, L. A.; Lahoz, F. J. *J. Chem. Soc., Dalton Trans.* **1989**, 2073-2079.
- Ferrari, A.; Polo, E.; Rügger, H.; Sostero, S.; Venanzi, L. M. *Inorg. Chem.* **1996**, *35*, 1602-1608.
- Fogg, P. G. T.; Gerrand, W. *Solubility of Gases in Liquids*; John Wiley & Sons: New York, 1991.

- Ghosh, C. K.; Graham, W. A. G. *J. Am. Chem. Soc.* **1987**, *109*, 4726-4727.
- Ghosh, C. K.; Graham, W. A. G. *J. Am. Chem. Soc.* **1989**, *111*, 375-375.
- Ghosh, C. K.; Hoyano, J. K.; Krentz, R.; Graham, W. A. G. *J. Am. Chem. Soc.* **1989**, *111*, 5480-5481.
- Ghosh, C. K.; Rodgers, D. P. S.; Graham, W. A. G. *J. Chem. Soc., Chem. Commun.* **1988**, 1511-1512.
- Gilbert, T. M.; Bergman, R. G. *J. Am. Chem. Soc.* **1985**, *107*, 3502-3507.
- Gonzalez, A. A.; Zhang, K.; Nolan, S. P.; de la Vega, R. L.; Mukerjee, S. L.; Hoff, C. L. *Organometallics* **1988**, *7*, 2429-2435.
- Gordon, A. J.; Ford, R. A. *The Chemist's Companion*; John Wiley & Sons: New York, 1972, pp 303.
- Gusev, D. G.; Bakhmutov, V. I.; Gushin, V. V.; Vol'pin, M. E. *Inorg. Chim. Acta.* **1990**, *177*, 115.
- Gusev, D. G.; Kuznetsov, V. F.; Eremenko, I. L.; Berke, H. *J. Am. Chem. Soc.* **1993**, *115*, 5831-5832.
- Gusev, D. G.; Notheis, J. U.; Rambo, J. R.; Hauger, B. E.; Eisenstein, O.; Caulton, K. G. *J. Am. Chem. Soc.* **1994**, *116*, 7409-7410.
- Gutiérrez, E.; Hudson, S. A.; Monge, A.; Nicasio, M. C.; Paneque, M.; Carmona, E. *J. Chem. Soc., Dalton Trans.* **1992**, 2651-2653.
- Gutiérrez, E.; Monge, A.; Nicasio, M. C.; Poveda, M. L.; Carmona, E. *J. Am. Chem. Soc.* **1994**, *116*, 791-792.
- Halcrow, M. A.; Chaudret, B.; Trofimenko, S. *J. Chem. Soc., Chem. Commun.* **1993**, 465-467.
- Hamilton, D. G.; Crabtree, R. H. *J. Am. Chem. Soc.* **1988**, *110*, 4126-4133.
- Hamilton, D. G.; Luo, X. L.; Crabtree, R. H. *Inorg. Chem.* **1989**, *28*, 3198-3203.
- Hansen, P. E. *Annu. Rep. NMR Spectrosc.* **1983**, *15*, 105-234.

- Hartwig, J. F.; De Gala, S. R. *J. Am. Chem. Soc.* **1994**, *116*, 3661-3662.
- Hasegawa, T.; Li, Z.; Parkin, S.; Hope, H.; McMullan, R. K.; Koetzle, T. F.; Taube, H. *J. Am. Chem. Soc.* **1994**, *116*, 4352-4356.
- Hay, P. J. *Chem. Phys. Lett.* **1984**, *103*, 466-469.
- Hay, P. J. In *Transition Metal Hydrides*; A. Dedieu, Ed.; VCH Publishers, Inc: New York, 1992.
- Haynes, G. R.; Martin, R. L.; Hay, P. J. *J. Am. Chem. Soc.* **1992**, *114*, 28-36.
- Heinekey, D. M.; Hinkle, A. S.; Close, J. D. *J. Am. Chem. Soc.* **1996**, *118*, 5353-5361.
- Heinekey, D. M.; Liegeois, A.; van Roon, M. *J. Am. Chem. Soc.* **1994**, *116*, 8388-8389.
- Heinekey, D. M.; Luther, T. A. *Inorg. Chem.* **1996**, *35*, in press.
- Heinekey, D. M.; Millar, J. M.; Koetzle, T. F.; Payne, N. G.; Zilm, K. W. *J. Am. Chem. Soc.* **1990**, *112*, 909-919.
- Heinekey, D. M.; Oldham, W. J., Jr. *Chem. Rev.* **1993**, *93*, 913-926.
- Heinekey, D. M.; Oldham, W. J., Jr. *J. Am. Chem. Soc.* **1994**, *116*, 3137-3138.
- Heinekey, D. M.; Payne, N. G.; Sofield, C. D. *Organometallics* **1990**, *9*, 2643-2645.
- Heinekey, D. M.; Payne, N. G.; Sofield, C. D. *Organometallics* **1989**, *8*, 1824-1826.
- Heinekey, D. M.; Schomber, B. M.; Radzewich, C. E. *J. Am. Chem. Soc.* **1994**, *116*, 4515-4516.
- Hinkle, A. S. Ph.D. Dissertation Thesis, University of Washington, 1995.
- Hostetler, M. J.; Bergman, R. G. *J. Am. Chem. Soc.* **1992**, *114*, 7629-7636.
- Howard, J. A. K.; Mason, S. A.; Johnson, O.; Diamond, I. C.; Crennell, S.; Keller, P. A.; Spencer, J. L. *J. Chem. Soc., Chem. Commun.* **1988**, 1502-1503.

- Isobe, K.; Bailey, P. M.; Maitlis, P. M. *J. Chem. Soc., Dalton Trans.* **1981**, 2003-2008.
- Jalón, F. A.; Otero, A.; Manzano, B. R.; Villaseñor, E.; Chaudret, B. *J. Am. Chem. Soc.* **1995**, *117*, 10123-10124.
- James, B. R. *Homogeneous Hydrogenation*; John Wiley & Sons: New York, 1973.
- Jean, Y.; Eisenstein, O.; Volatron, F.; Maouche, B.; Sefta, F. *J. Am. Chem. Soc.* **1986**, *108*, 6587-6592.
- Johnson, C. E.; Eisenberg, R. *J. Am. Chem. Soc.* **1985**, *107*, 3148-3160.
- Jones, W. D.; Hessell, E. T. *Inorg. Chem.* **1991**, *30*, 778-783.
- Jones, W. D.; Hessell, E. T. *J. Am. Chem. Soc.* **1992**, *114*, 6087-6095.
- Julia, S.; del Mazo, J. M.; Avila, L.; Elguero, J. *Org. Prep. Proc. Int.* **1984**, *16*, 299.
- Kang, J. W.; Moseley, K.; Maitlis, P. M. *J. Am. Chem. Soc.* **1969**, *91*, 5970-5977.
- Kauffman, G. B.; Myers, R. D. *Inorg. Synth* **1978**, *18*, 131-133.
- Klooster, W. T.; Koetzle, T. F.; Jia, G.; Fong, T. P.; Morris, R. H.; Albinati, A. *J. Am. Chem. Soc.* **1994**, *116*, 7677-7681.
- Kubas, G. J. *Acc. Chem. Res.* **1988**, *21*, 120-128.
- Kubas, G. J.; Ryan, R. R. *Polyhedron* **1986**, *5*, 473-485.
- Kubas, G. J.; Ryan, R. R.; Swanson, B. I.; Vergamini, P. J.; Wasserman, H. J. *J. Am. Chem. Soc.* **1984**, *106*, 451-452.
- Lawson, R. J. Thesis, University of Illinois, 1978.
- Limbach, H. H.; Scherer, G.; Maurer, M.; Chaudret, B. *Angew. Chem., Int.* **1992**, *31*, 1369-1372.
- Lowry, T. H.; Richardson, K. *Mechanism and Theory in Organic Chemistry*; Harper and Row: New York, 1976.

- Lundquist, E. G.; Folting, K.; Streib, W. E.; Huffman, J. C.; Eisenstein, O.; Caulton, K. G. *J. Am. Chem. Soc.* **1990**, *112*, 855-863.
- Luo, X. L.; Crabtree, R. H. *J. Am. Chem. Soc.* **1990**, *112*, 4813-4821.
- Luo, X.; Crabtree, R. H. *J. Am. Chem. Soc.* **1990**, *112*, 6912-6918.
- Luo, X.; Michos, D.; Crabtree, R. H. *Organometallics* **1992**, *11*, 237-241.
- Maltby, P. A.; Schlaf, M.; Steinbeck, M.; Lough, A. J.; Morris, R. H.; Klooster, W. T.; Koetzle, T. F.; Srivastava, R. C. *J. Am. Chem. Soc.* **1996**, *118*, 5396-5407.
- Manzer, L. E.; Meakin, P. Z. *Inorg. Chem.* **1976**, *15*, 3117-3120.
- Martinho Simões, J. A.; Beauchamp, J. L. *Chem. Rev.* **1990**, *90*, 629-688.
- Maseras, F.; Duran, M.; Lledós, A.; Bertrán, J. *J. Am. Chem. Soc.* **1992**, *114*, 2922-2928.
- May, S.; Reinsalu, P.; Powell, J. *Inorg. Chem.* **1980**, *19*, 1582-1589.
- Meakin, P.; Trofimenko, S.; Jesson, J. P. *J. Am. Chem. Soc.* **1972**, *94*, 5677-5681.
- Michos, D.; Luo, X.; Crabtree, R. H. *Inorg. Chem.* **1992**, *31*, 4245-4250.
- Michos, D.; Luo, X.; Howard, J. A. K.; Crabtree, R. H. *Inorg. Chem.* **1992**, *31*, 3914-3916.
- Miller, R. L.; Toreki, R.; LaPointe, R. E.; Wolczanski, P. T.; Van Duyne, G. D.; Roe, D. C. *J. Am. Chem. Soc.* **1993**, *115*, 5570-5588.
- Moreno, B.; Sabo-Etienne, S.; Chaudret, B.; Rodriguez, A.; Jalon, F.; Trofimenko, S. *J. Am. Chem. Soc.* **1995**, *117*, 7441-7451.
- Moreno, B.; Sabo-Etienne, S.; Chaudret, B.; Rodriguez-Fernandez, A.; Jalon, F.; Trofimenko, S. *J. Am. Chem. Soc.* **1994**, *116*, 2635-2636.
- Nanz, D.; von Philipsborn, W.; Bucher, U. E.; Venanzi, L. M. *Magnetic Resonance in Chemistry* **1991**, *29*, S38-44.
- Neuner, B.; Schrock, R. R. *Organometallics* **1996**, *15*, 5-6.
- O'Sullivan, D. J.; Lalor, F. J. *J. Organometal. Chem.* **1974**, *65*, 47-C49.

- Onderdelinden, A. L. *Inorg. Synth* **1974**, *15*, 18.
- Paneque, M.; Poveda, M. L.; Rey, L.; Taboada, S.; Carmona, E.; Ruiz, C. J. *Organometal. Chem.* **1995**, *504*, 147-149.
- Paneque, M.; Poveda, M. L.; Toboada, S. *J. Am. Chem. Soc.* **1994**, *116*, 4519-4520.
- Paneque, M.; Taboada, S.; Carmona, E. *Organometallics* **1996**, *15*, 2678-2679.
- Paonessa, R. S.; Trogler, W. C. *J. Am. Chem. Soc.* **1982**, *104*, 1138-1140.
- Parshall, G. W.; Ittel, S. D. *Homogeneous Catalysis*; 2nd ed.; John Wiley & Sons, Inc.: New York, 1992.
- Pérez, P. J.; Poveda, M. L.; Carmona, E. *Angew. Chem. Int. Ed. Engl.* **1995**, *34*, 231-233.
- Pérez, P. J.; Poveda, M. L.; Carmona, E. *J. Chem. Soc., Chem. Commun.* **1992**, 8-9.
- Peterson, A.; Tilset, M. *Organometallics* **1993**, *12*, 3064-3068.
- Rabinovich, D.; Parkin, G. *J. Am. Chem. Soc.* **1993**, *115*, 353-354.
- Reger, D. L.; Tarquini, M. E. *Inorg. Chem.* **1983**, *22*, 1064-1068.
- Rheingold, A. L.; Ostrander, R. L.; Haggerty, B. S.; Trofimenko, S. *Inorg. Chem.* **1994**, *33*, 3666-3676.
- Rossi, A. R.; Hoffmann, R. *Inorg. Chem.* **1975**, *14*, 365-374.
- Sabo-Etienne, S.; Chaudret, B.; el Makarim, H. A.; Barthelat, J.; Daudey, J.; Ulrich, S.; Limbach, H.; Moïse, C. *J. Am. Chem. Soc.* **1995**, *117*, 11602-11603.
- Saillard, J.; Hoffmann, R. *J. Am. Chem. Soc.* **1984**, *106*, 2006-2026.
- Sanders, J. K. M.; Hunter, B. K. *Modern NMR Spectroscopy*; Oxford University Press: Oxford, 1989.
- Sandström, J. *Dynamic NMR Spectroscopy*; Academic Press: London, 1982.
- Saunders, M.; Kates, M. R. *J. Am. Chem. Soc.* **1977**, *99*, 8070-8071.
- Schuster-Woldan, H. G.; Basolo, F. *J. Am. Chem. Soc.* **1966**, *88*, 1657-1663.

- Segal, J. A.; Johnson, B. F. G. *J. Chem. Soc., Dalton Trans.* **1975**, 677-681.
- Shanan-Atidi, H.; Bar-Eli, K. H. *J. Phys. Chem.* **1970**, *74*, 961-963.
- Shapley, J. R.; Adair, P. C.; Lawson, J. R.; Pierpont, C. G. *Inorg. Chem.* **1982**, *21*, 1702-1704.
- Steyn, M. M. d. V.; Singleton, E.; Hietkamp, S.; Liles, D. C. *J. Chem. Soc., Dalton Trans.* **1990**, 2991-2997.
- Sun, Y.; Landau, R. N.; Wang, J.; Le Blonde, C.; Blackmond, D. G. *J. Am. Chem. Soc.* **1996**, *118*, 1348-1353.
- Szajek, L. P.; Lawson, R. J.; Shapley, J. R. *Organometallics* **1991**, *10*, 357-361.
- Tanke, R. S.; Crabtree, R. H. *Inorg. Chem.* **1989**, *28*, 3444-3447.
- Trofimenko, S. *Chem. Rev.* **1993**, *93*, 943-980.
- Trofimenko, S. *Inorg. Synth.* **1979**, *12*, 99.
- Trofimenko, S. *J. Am. Chem. Soc.* **1969**, *91*, 588-595.
- Trofimenko, S. *Prog. Inorg. Chem.* **1986**, *34*, 115-210.
- Ugi, I.; Marquarding, D.; Klusacek, H.; Gillespie, P. *Acc. Chem. Res.* **1971**, *4*, 288-296.
- Van Der Sluys, L. S.; Eckert, J.; Eisenstein, O.; Hall, J. H.; Huffman, J. C.; Jackson, S. A.; Koetzle, T. F.; Kubas, G. J.; Vergamini, P. J.; Caulton, K. G. *J. Am. Chem. Soc.* **1990**, *112*, 4831-4841.
- Vigalok, A.; Ben-David, Y.; Milstein, D. *Organometallics* **1996**, *15*, 1839-1844.
- Werner, H.; Wolf, J.; Höhn, A. *J. Organomet. Chem.* **1985**, *287*, 395-407.
- Young, C. L., Ed. *Solubility Data Series, Hydrogen and Deuterium*, Pergamon Press: New York, 1981; Vol. 5/6.
- Zhang, X.; McDonald, R.; Takats, J. *New J. Chem.* **1995**, *19*, 573-585.
- Zilm, K. W.; Millar, J. M. *Adv. Magn. Opt. Reson.* **1990**, *15*, 163-200.

Warren James Oldham, Jr. was born June 25, 1969 in Kingsville, Texas. He attended Central Washington University in Ellensburg, Washington and was awarded The Anonymous Scholarship in Literature and Science during his Junior and Senior years of study. He was also a member of the William O. Douglas Honors College while attending CWU and completed a four year study of Western Literature and graduated with a Bachelor of Science in Chemistry in June of 1991. In the Fall of the same year, he began graduate work in chemistry at the University of Washington. He was recognized as the 1993/94 Chevron Fellow for his work in organometallic chemistry under the guidance of Professor D. M. Heinekey. In July of 1996, he earned a Doctor of Philosophy in Inorganic Chemistry.